CHOPPER CONTROL OF DC SEPARATELY EXCITED MOTOR

A Thesis
Submitted In Partial Fulfilment of the Requirements
for the Degree of
MASTER OF TECHNOLOGY

By

P. K. SAXENA

to the
DEPARTMENT OF ELECTRICAL ENGINEERING
INDIAN INSTITUTE OF TECHNOLOGY, KANPUR
AUGUST, 1980

Dedicated

to

Mummy, Papa & Baba

EE-1980-M-SAX-CHO

CERTIFICATE

Certified that this work "Chopper Control of dc Separately Excited Motor" by P.K. Saxena is carried out under my supervision and is not submitted elsewhere for a degree.

(G.K. DUBEY)
Professor
Department of Electrical Engineering
Indian Institute of Technology
KANPUR

ACKNOWLEDGEMENTS

I express my deep sense of gratitude to Dr. G.K. Dubey for suggesting me this topic and also for his valuable guidance in the course of this project.

I am also indebted to Dr. A. Joshi for all the useful discussions I had with him.

Thanks to my friends - Bhat, Satpathi, Rao, Bala, Anand and Kellogg for their encouragement and helpful attitudes.

Thanks are also due to all the staff members of all the laboratoris whose help I had received directly or indirectly in carrying out this work.

I would also like to thank Mr. J.S. Rawat for his excellent typing.

Last but not the least, my thanks to Mr. C.M. Abraham for his help in 'symbol filling'.

P.K. SAXENA

TABLE OF CONTENTS

NOMENCLATURE

t_{oN}	-	on time of chopper
T	-	time period of chopper
L	-	armature inductance, H
R	-	armature resistance, ohms
E	-	motor back emf, V
i_a, i_o	-	instantaneous armature current, Amp
V	-	supply voltage, volts
I_{av}	-	average armature current, Amp
δ	-	duty ratio of chopper
K_v	-	back emf constant
K_T	-	torque constant
τ, τ_e	-	electrical time constant $(\frac{L}{R})$
w	-	speed in radians/sec
a_n, b_n	-	fourier constants
i_s	-	instantaneous value of supply current, Amp
n	-	number of harmonic
γT	-	instant at which i_a becomes zero
PR_{av}	-	average power regenerated, watts
$PR_{av(N)}$	-	normalized power regenerated
v_c	-	control voltage, volts
V_{cm}	-	maximum control voltage, volts
V_o	-	average output voltage of chopper, volts

Q - thyristors

D - diodes

R_i - resistor

L - inductor

C - capacitor

i_Q - instantaneous current through thyristor, Amp

i_D - instantaneous current through diode, Amp

V_{AK} - voltage across thyristor, volts

i_c - instantaneous current through capacitor, Amp

i_G - gate current of thyristor, Amp

t_c - commutation interval, sec.

V_L - voltage across inductor, volts

V_c - voltage across capacitor, volts

t_q - time available for turn off, sec.

t_{off} - turn off time, sec.

T_l - load torque, NM

T_m - motor torque, NM

V_a - instantaneous value of armature voltage, volts

V_R - rated armature voltage, volts

I_{st} - standstill armature current (V_R/R), Amp

w_o - motor no load ideal speed (V_R/K_v) rad/sec.

J - moment of inertia of motor and load

τ_m - mechanical time constant (Jw_o/I_{st})

T_{st} - standstill torque ($K_v I_{st}$), NM

B - normalized viscous friction constant (includes load on the motor)

V_{c1} - output voltage of current controller, volts

V_{c2} - output voltage of speed controller, volts

V_{ref} - speed reference voltage, volts

V_i - current transducer output voltage, volts

H_i - normalized gain of current transducer

H_w - normalized gain of speed transducer

$I_a(s)$ - $\mathcal{L}\left[i_a / I_{st}\right]$

$V_a(s)$ - $\mathcal{L}\left[v_a / V_R\right]$

$W(s)$ - $\mathcal{L}\left[w/w_o\right]$

$T_l(s)$ - $\mathcal{L}\left[T_l/T_{st}\right]$

e_{ss} - steady state error

$V_R(s)$ - $\mathcal{L}\left[V_{ref}/V_{cm}\right]$

CHAPTER I

INTRODUCTION

Variable dc voltage for speed control of dc separately excited motor using-thyristors can be obtained either by using converter or chopper. The chopper control has the following advantages over converter control:

i) Phase controlled converters suffer from poor p.f., particularly at large firing angles.

ii) Because the choppers can be operated at high frequency, ripple in armature is less. As a result of this losses in motor are less, motor commutation is better and therefore derating of the motor is less.

iii) Control circuitry is simple.

iv) Regeneration can be achieved by doing simple modifications in the circuit.

In view of this, a study of chopper control of dc separately excited motor was undertaken to investigate the following aspects:

(a) Comparative study of two quadrant choppers for control of dc separately excited motor for forward motoring and braking.

(b) Analysis, design and fabrication of a two quadrant chopper.

(c) Study of closed-loop speed control of chopper fed dc drive.

Comparative study of two quadrant choppers is reported in Chapter II. The performance has been compared for the following aspects:

i) Motor performance characteristics.
ii) Motor armature current ripple factor.
iii) Supply current harmonics.
iv) Regenerated power and efficiency of regeneration.
v) Steady state transfer characteristics.

Design, analysis and performance of two quadrant chopper forms the contents of Chapter III. A digital firing scheme for the control of dual chopper has been developed. A dual chopper was fabricated and its performance was investigated experimentally. This chopper had serious commutation problem for duty ratio

greater than 0.5. In view of this, control range was limited and the chopper was not suitable for closed loop operation.

A single quadrant chopper was therefore selected for closed loop operation. Initially, open loop performance of the dc motor fed by single quadrant chopper was investigated for steady-state and transients operation. These results have also been reported in Chapter III.

Closed-loop speed controlled dc motor drive using single quadrant chopper was designed and investigated, theoretically and experimentally. The results of this investigation are presented in Chapter IV.

CHAPTER II

COMPARATIVE STUDY OF TWO QUADRANT CHOPPERS

2.1 INTRODUCTION:

Two quadrant operation of dc motor, consisting of forward motoring and braking requires a chopper capable of giving positive voltage and current in either direction. This two quadrant operation of the motor can be realised in the following three ways.

1. One single-quadrant chopper is used and the connections of motor and chopper are changed with the help of relays and contactors or drum controller as shown in the Fig. 2.1.

2. A dual chopper consisting of two choppers connected as shown in Fig. 2.2 is used. One chopper is kept in operation at a time, chopper Q_1 for motoring and chopper Q_2 for braking.

3. A dual chopper similar to one shown in Fig. 2.2 is used but both the choppers Q_1 and Q_2 remain in operation simultaneously. Motoring operation is obtained when duty ratio of Q_1 is greater than that of Q_2 and braking operation as realized by making duty ratio of Q_2 greater than that of Q_1.

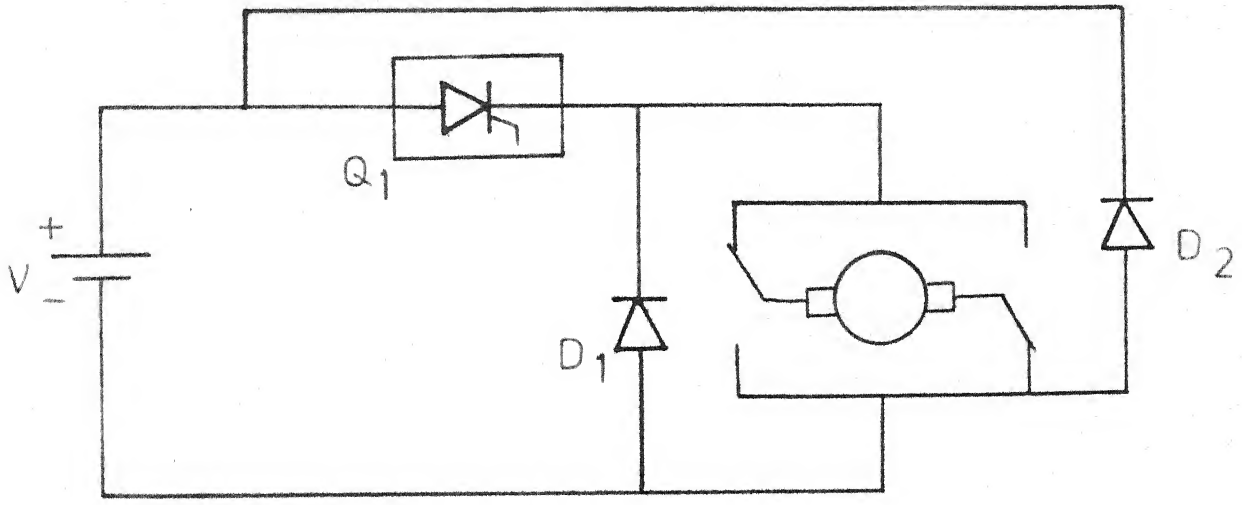

FIG.2.1(a) Circuit for Motoring.

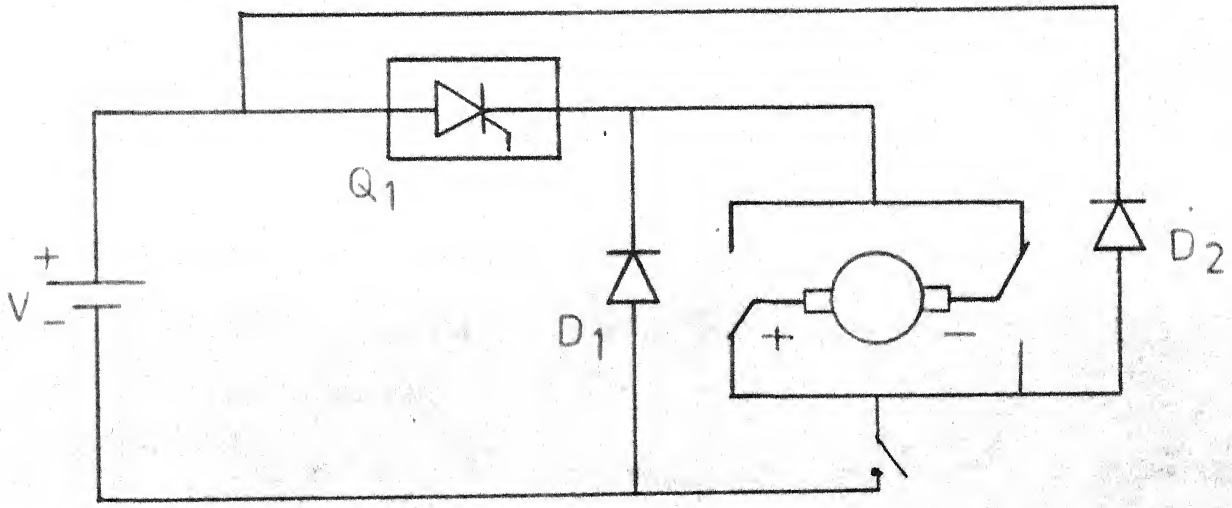

FIG.2.1(b)Circuit for Regenerative braking.

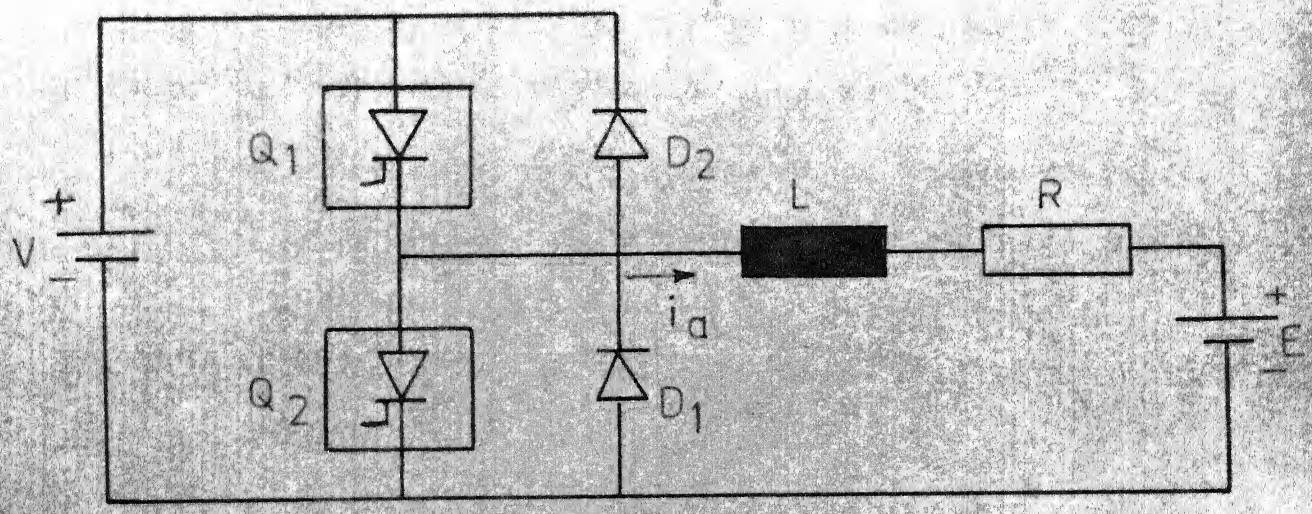

FIG.2.2 Dual chopper.

When the chopper of Fig. 2.2 operates as in (2) above, it can be termed as dual chopper with circulating current free operation. Similarly, when it operates as in (3) above it can be called dual chopper with circulating current operation.

The operations listed in (1) and (2) above will be similar except that the additional delay will be introduced in (1) when operation is changed from motoring to braking and vice versa. Furthermore, the cost in case (2) is expected to be higher than in (1). The two quadrant choppers capable of giving motoring and regenerative braking operations in forward direction can be classified as

I) dual chopper with circulating current free operation and,

II) dual chopper with circulating current operation.

The comparative study of these two kinds of dual choppers has been carried out in this chapter. This study is related to the following aspects.

(a) Nature of motor speed-torque characteristics, including the effect of discontinuous conduction.

(b) Motor armature current - ripple factor.

(c) Supply current harmonics.

(d) The regenerated power and efficiency of regeneration.

(e) Transfer characteristics

2.2 ANALYSIS FOR DUAL CHOPPER WITH CIRCULATING CURRENT FREE OPERATION:

The waveforms of motor voltage, motor current and line current are shown in Figs. 2.3 and 2.4 for the following cases.

(a) Motoring operation with non-circulating current chopper for continuous and discontinuous conduction.

(b) Regenerative braking operation with non-circulating current chopper for continuous as well as discontinuous conduction.

It is assumed that

(a) the thyristors and diodes are ideal switches

(b) the resistance and inductance of motor armature are constant, and

(c) the motor speed is fairly constant during a given steady-state condition. Since the mechanical time constant of the motor is very large compared to chopping period, the fluctuation in speed is in fact negligible.

2.2.1 Speed-Torque Characteristics for Motoring Operation:

A. Continuous Conduction:

In this mode of operation, there are two possible intervals viz. the duty interval and the freewheeling interval.

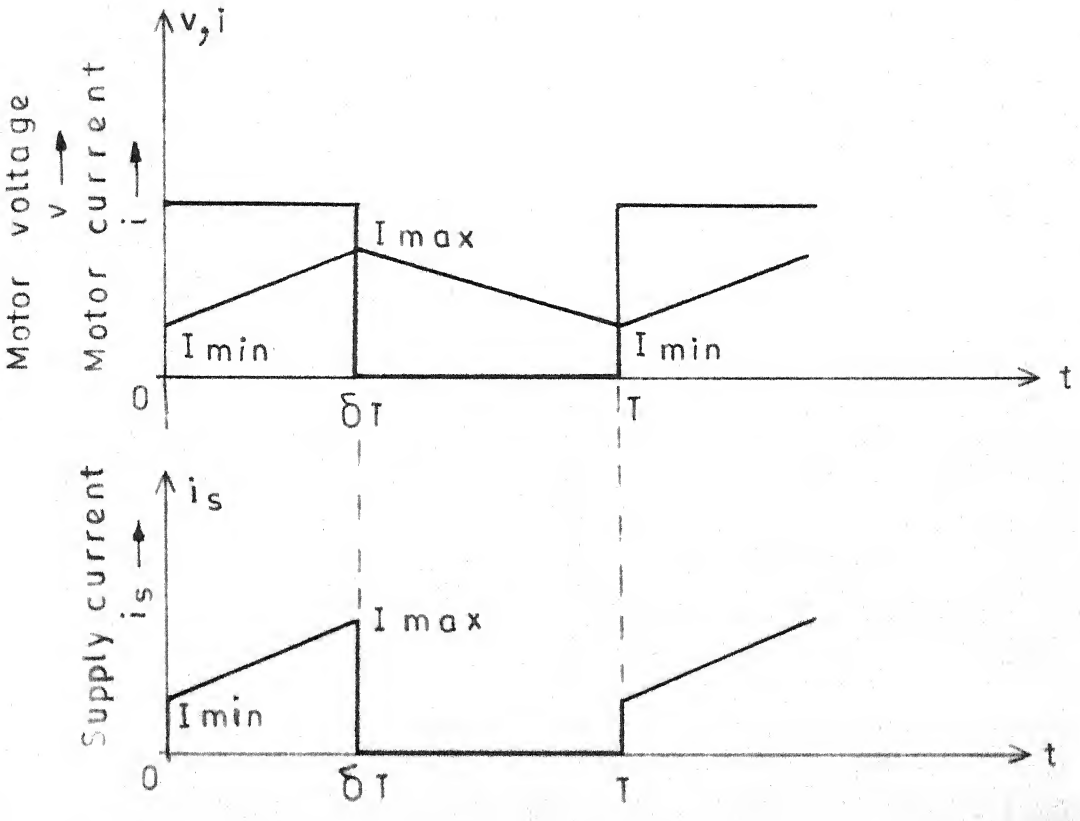

(a)

FIG.2.3 Motoring operation with non-circulating current chopper

(a) Continuous conduction

(b) Discontinuous conduction

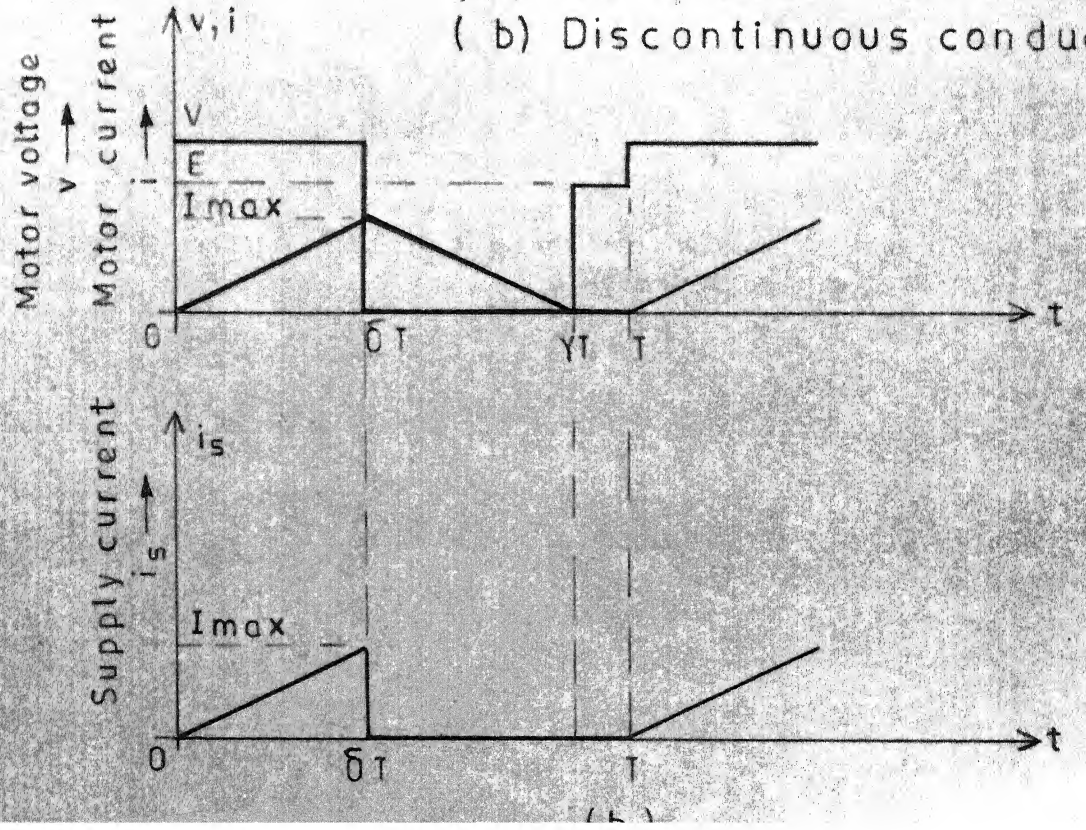

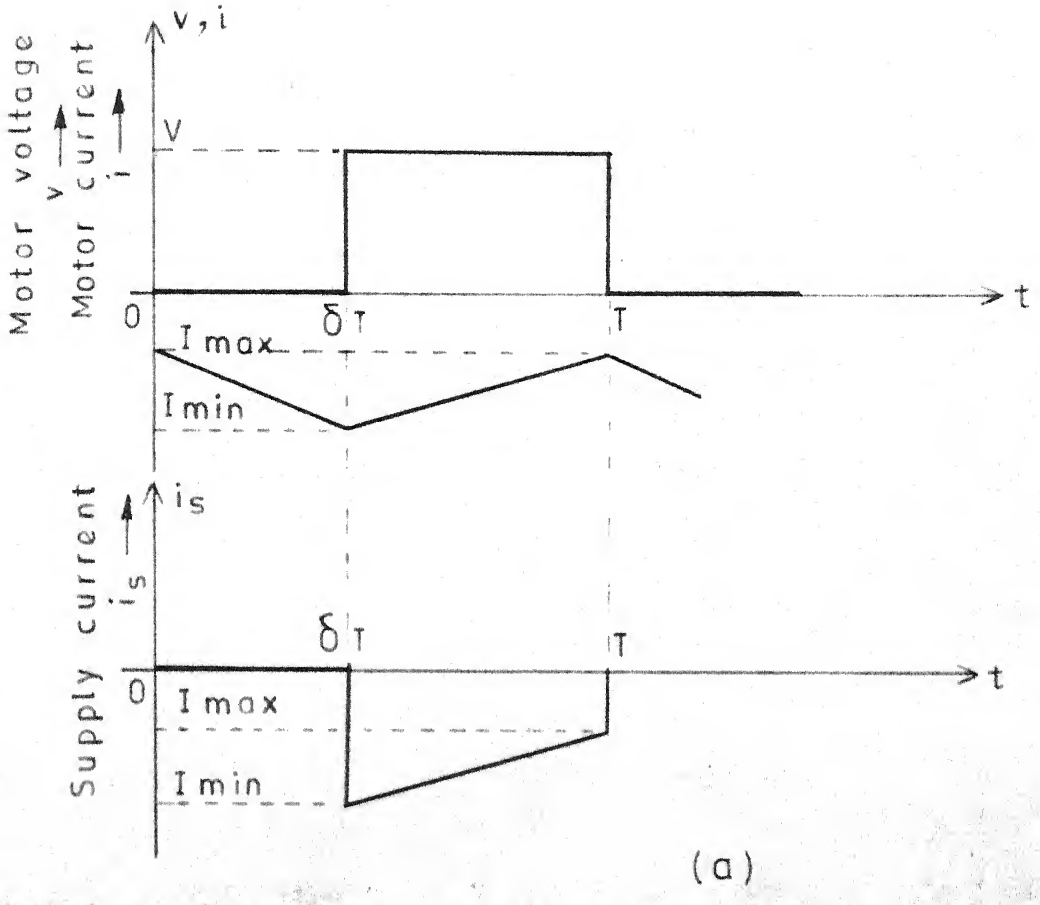

(a)

FIG.2.4 Regenerative braking operation with non-circulating current chopper
(a) Continuous conduction.
(b) Discontinuous conduction.

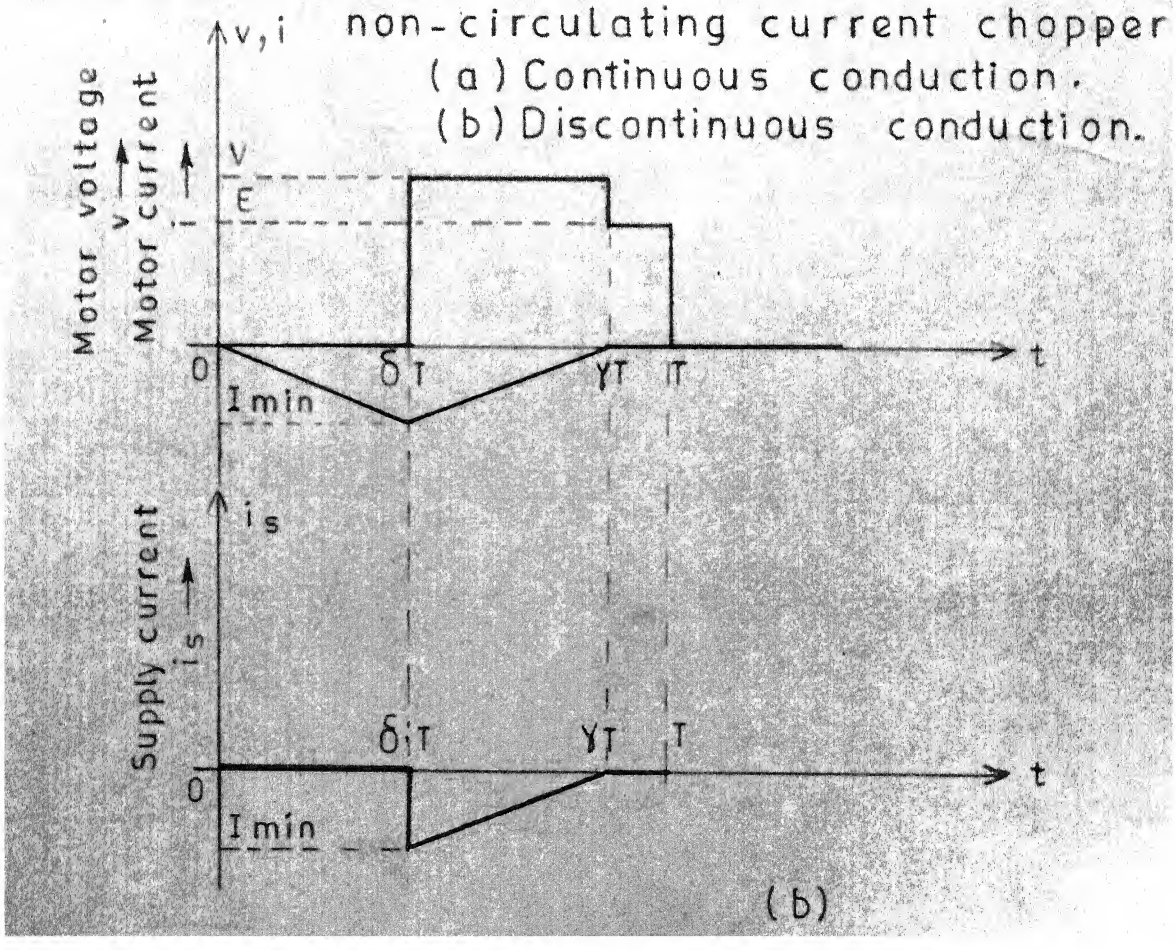

(b)

Considering the Fig. 2.5(a), one can write

Duty interval

$$L \frac{di_a}{dt} + Ri_a + E = V \quad \text{for} \quad 0 \leq t \leq t_{oN} \qquad (2.1)$$

Freewheeling interval

$$L \frac{di_a}{dt} + Ri_a + E = 0 \quad \text{for} \quad t_{oN} \leq t \leq T \qquad (2.2)$$

Taking average of eqns. (2.1) and (2.2) for the whole time period T, one gets

$$R\, I_{av} = \frac{1}{T} \int_0^{t_{oN}} V \, dt - E = \frac{t_{oN}}{T} V - E$$

In steady-state, average voltage drop across the inductor will be zero.

Now

$$I_{av} = \frac{\delta V - E}{R} = \frac{\delta V - K_v w}{R} \qquad (2.3)$$

and

$$T_{av} = K_T I_{av} = K_T \left[\frac{\delta V - K_v w}{R} \right] \qquad (2.4)$$

Now, for duty-interval,

$$\text{let } i_a \Big|_{t=o} = I_{min} \text{ , therefore from eqn. (2.1)}$$

$$i_a = \frac{V-E}{R} (1 - e^{-t/\tau}) + I_{min}\, e^{-t/\tau} \quad \text{for } 0 \leq t \leq \delta T \qquad (2.5)$$

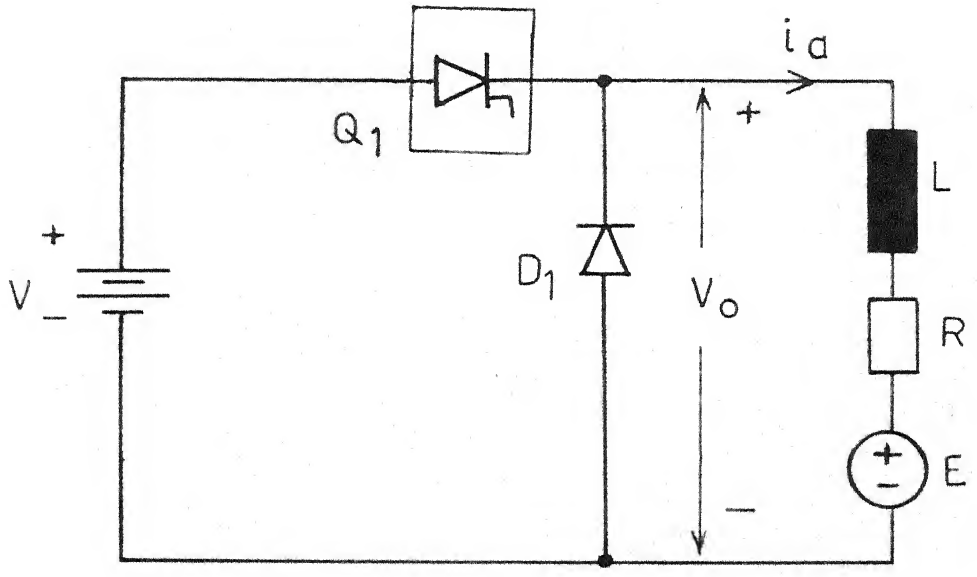

(a)

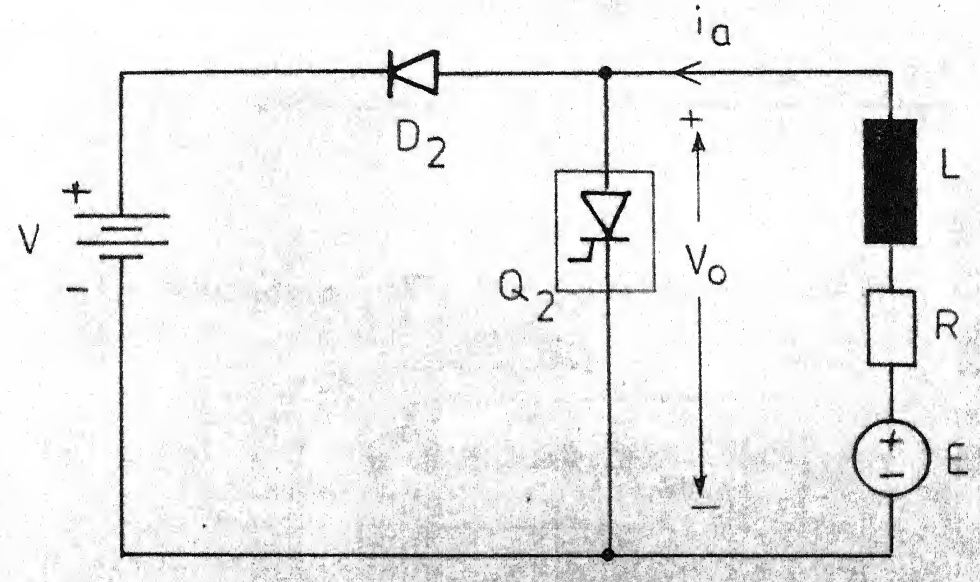

FIG. 2.5 Circuits for non-circulating current chopper under
(a) Motoring (b) Regenerative braking.

For freewheeling interval, let $i_a\Big|_{t=o} = I_{max}$, hence from eqn. (2.2)

$$i_a = -\frac{E}{R}(1-e^{-t/\tau}) + I_{max}\, e^{-t/\tau} \quad \text{for } \delta T \leq t \leq T \tag{2.6}$$

In the steady state, from eqns. (2.5) and (2.6)

$$I_{max} = \frac{V}{R}\left[\frac{1 - e^{-\delta T/\tau}}{1 - e^{-T/\tau}}\right] - \frac{E}{R} \tag{2.7}$$

$$I_{min} = \frac{V}{R}\left[\frac{e^{\delta T/\tau} - 1}{e^{T/\tau} - 1}\right] - \frac{E}{R} \tag{2.8}$$

The current fluctuations Δi_f is

$$\Delta i_f = \frac{I_{max} - I_{min}}{2} = \frac{V}{2R}\left[\frac{1 - e^{-\delta T/\tau}}{1 - e^{-T/\tau}} - \frac{e^{\delta T/\tau} - 1}{e^{T/\tau} - 1}\right] \tag{2.9}$$

Making use of straight line approximation [3]

$$I_{av} = \frac{I_{max} + I_{min}}{2} \tag{2.10}$$

$$I_{rms} = \sqrt{\frac{I_{max}^2 + I_{min}^2 + I_{max}\, I_{min}}{3}} \tag{2.11}$$

$$CRF = \frac{\sqrt{I_{rms}^2 - I_{av}^2}}{I_{av}}$$

$$\text{or} \quad CRF = \frac{I_{max} - I_{min}}{\sqrt{3}\,(I_{max} + I_{min})} \tag{2.12}$$

B. Discontinuous Conduction:

In this case, the chopper will operate in three modes known as the duty interval, the freewheeling interval and the zero current interval. Eqns. for different intervals are

Duty interval

$$L\frac{di_a}{dt} + Ri_a + E = V \quad \text{for } 0 \leq t \leq \delta T \qquad (2.13)$$

Freewheeling interval

$$L\frac{di_a}{dt} + Ri_a + E = 0 \quad \text{for } \delta T \leq t \leq \gamma T \qquad (2.14)$$

Taking the average of above two eqns. over the time period T, one gets

$$RI_{av} + \frac{\gamma T}{T} E = \delta V$$

$$\text{or } I_{av} = \frac{\delta V - \gamma K_v w}{R} \qquad (2.15)$$

and

$$T_{av} = K_T I_{av} = K_T \left[\frac{\delta V - \gamma K_v w}{R}\right] \qquad (2.16)$$

Since, for the duty interval $i_a\big|_{t=0} = 0$, then from eqn. (2.5)

$$i_a = \frac{V-E}{R}\left(1 - e^{-t/\tau}\right) \quad \text{for } 0 \leq t \leq \delta T \qquad (2.17)$$

For the freewheeling interval i_a is given by eqn. (2.6). Noting that I_{max} is the value of i_a at the end of duty interval, eqn. (2.6) takes the form of

$$i_a = -\frac{E}{R}(1-e^{-t/\tau}) + \frac{V-E}{R}(1-e^{-\delta T/\tau})\, e^{-t/\tau}$$

$$\text{for } \delta T \leq t \leq \gamma T \qquad (2.18)$$

Let i_a become 0 at time γT measured from the beginning of the duty interval. Then from the above eqn.

$$\gamma = \delta + \frac{\tau}{T} \ln\left[\frac{V}{E} + \left(1-\frac{V}{E}\right) e^{-\delta T/\tau}\right] \qquad (2.19)$$

The critical speed w_c, representing boundary between, continuous and discontinuous conditions, is obtained by letting $\gamma = 1$, in eqn. (2.19).

$$w_c = \frac{V}{K_v}\left[\frac{e^{\delta T/\tau}-1}{e^{T/\tau}-1}\right] \qquad (2.20)$$

Further, making use of straight line approximation [3]

$$I_{av} = \frac{1}{T}\left[\frac{I_{max}\,\delta T}{2} + \frac{I_{max}(\gamma-\delta)T}{2}\right]$$

$$\text{or} \quad I_{av} = \frac{1}{2}\gamma\, I_{max} \qquad (2.21)$$

$$\Delta i_f = \frac{I_{max}}{2} \qquad (2.22)$$

$$I_{rms} = \sqrt{\frac{1}{T}\left[\int_0^{\delta T}\left(\frac{t}{\delta T} I_{max}\right)^2 dt + \int_0^{(\gamma-\delta)T}\left(\frac{I_{max}\, t}{(\gamma-\delta)T}\right)^2 dt\right]}$$

$$\text{or} \quad I_{rms} = I_{max}\sqrt{\frac{\gamma}{3}} \qquad (2.23)$$

$$CRF = \frac{\sqrt{I_{rms}^2 - I_{av}^2}}{I_{av}} = \sqrt{\frac{4}{3\gamma} - 1} \qquad (2.24)$$

2.2.2 Speed-Torque Characteristics for Regenerative Braking:

A. Continuous Conduction:

Considering Fig. 2.5(b), the eqns. for freewheeling interval and duty interval are

Freewheeling interval

$$L\frac{di_a}{dt} + Ri_a - E = 0 \quad \text{for} \quad 0 \le t \le \delta T \qquad (2.25)$$

Duty interval

$$L\frac{di_a}{dt} + Ri_a - E = -V \quad \text{for} \quad \delta T \le t \le T \qquad (2.26)$$

Taking the average of eqns. (2.25) and (2.26) over the time period T, one gets,

$$RI_{av} - E = \frac{1}{T}\int_{\delta T}^{T} V\,dt = (1-\delta)V$$

Therefore,

$$I_{av} = \frac{K_v w - (1-\delta)V}{R} \qquad (2.27)$$

and

$$T_{av} = K_T I_{av} = K_T\left[\frac{K_v w-(1-\delta)V}{R}\right] \qquad (2.28)$$

Let $i_a|_{t=0} = I_{min}$ and $i_a|_{t=\delta T} = I_{max}$, therefore from eqns. (2.25) and (2.26)

$$i_a = \frac{E}{R}(1-e^{-t/\tau}) + I_{min}\, e^{-t/\tau} \quad \text{for} \quad 0 \le t \le \delta T \qquad (2.29)$$

and

$$i_a = \frac{E-V}{R}\left(1 - e^{-t/\tau}\right) + I_{max}\, e^{-t/\tau} \quad \text{for } \delta T \leq t \leq T \tag{2.30}$$

$$i_a(\delta T) = I_{max} = \frac{E}{R}\left(1 - e^{-\delta T/\tau}\right) + I_{min}\, e^{-\delta T/\tau} \tag{2.31}$$

$$i_a(T) = I_{min} = \frac{E-V}{R}\left(1 - e^{-(T-\delta T)/\tau}\right) + I_{max}\, e^{-(T-\delta T)/\tau} \tag{2.32}$$

Solving simultaneous eqns. (2.31) and (2.32), one gets

$$I_{max} = \frac{E}{R} - \frac{V}{R}\,\frac{\left(e^{(1-\delta)T/\tau} - 1\right)}{e^{T/\tau} - 1} \tag{2.33}$$

$$I_{min} = \frac{E}{R} - \frac{V}{R}\left(\frac{1 - e^{-(1-\delta)T/\tau}}{1 - e^{-T/\tau}}\right) \tag{2.34}$$

The current fluctuation Δi_f is given by

$$\Delta i_f = \frac{I_{max} - I_{min}}{2} \tag{2.35}$$

Using straight line approximation [3], I_{av}, I_{rms} and CRF will be given by eqns. (2.10), (2.11) and (2.12) respectively.

B. Discontinuous Conduction:

Following are the eqns. for different intervals

Freewheeling interval

$$L\frac{di_a}{dt} + Ri_a - E = 0 \quad \text{for } 0 \leq t \leq \delta T \tag{2.36}$$

Duty interval

$$L \frac{di_a}{dt} + Ri_a - E = -V \quad \text{for} \quad \delta T \leq t \leq \gamma T \tag{2.37}$$

Taking average of eqns. (2.36) and (2.37) over the time period T, one gets

$$RI_{av} - \gamma E = \frac{1}{T} \int_{\delta T}^{\gamma T} (-V)dt = -\frac{V}{T}(\gamma - \delta)T$$

Therefore,

$$I_{av} = \frac{\gamma E - V(\gamma - \delta)}{R} = \frac{\gamma \cdot K_v w - V(\gamma - \delta)}{R} \tag{2.38}$$

and

$$T_{av} = K_T I_{av} = K_T \left[\frac{\gamma \cdot K_v w - V(\gamma - \delta)}{R} \right] \tag{2.39}$$

Since $i_a|_{t=0} = 0$, then from eqn. (2.35)

$$i_a = \frac{E}{R}\left(1 - e^{-t/\tau}\right) \quad \text{for} \quad 0 \leq t \leq \delta T \tag{2.40}$$

Solution of eqn. (2.37) is

$$i_a = \frac{E-V}{R}\left(1 - e^{-t/\tau}\right) + I_{max}\, e^{-t/\tau} \quad \text{for} \quad \delta T \leq t \leq \gamma T \tag{2.41}$$

i_a becomes zero at time γT measured from the beginning of the cycle. Hence from eqn. (2.41)

$$\gamma = \delta + \frac{\tau}{T} \ln \left[\frac{E}{E-V}\, e^{-\delta T/\tau} - \frac{V}{E-V} \right] \tag{2.42}$$

I_{max} is the value of i_a at time δT. Hence eqn. (2.41) becomes

$$i_a = \frac{E-V}{R}(1 - e^{-t/\tau}) + \frac{E}{R}(1 - e^{-\delta T/\tau})\, e^{-t/\tau}$$

$$\text{for } \delta T \leq t \leq \gamma T \qquad (2.43)$$

The critical speed w_c is given by following eqn.

$$w_c = \frac{V}{K_v}\left(\frac{1 - e^{-(1-\delta)T/\tau}}{1 - e^{-T/\tau}}\right). \qquad (2.44)$$

Further, I_{av}, Δi_f, I_{rms} and CRF can be obtained by making use of eqns. (2.21) to (2.24) respectively.

2.2.3 Harmonics in Supply Current with Motoring Operation:

A. Continuous Conduction:

The waveform of supply current shown in Fig. 2.3(a) can be expressed mathematically as follows

$$i_s = \frac{V-E}{R}(1 - e^{-t/\tau}) + I_{min}\, e^{-t/\tau} \text{ for } 0 \leq t \leq \delta T$$

$$= 0 \qquad \text{for } \delta T \leq t \leq T \qquad (2.45)$$

where I_{min} is given by eqn. (2.8).

For finding harmonics in supply current, fourier analysis of eqn. (2.45) is done.

The dc current is

$$I_o = \frac{1}{T}\int_0^T i_s\, dt$$

or

$$I_o = \frac{V}{R}\left[(1 - \frac{E}{V})\delta + \frac{\tau}{T}\left(\frac{e^{\delta T/\tau} - e^{T/\tau}}{e^{T/\tau}-1}\right)\left(1 - e^{-\delta T/\tau}\right)\right] \quad (2.46)$$

The fourier constants are

$$a_n = \frac{2}{T}\int_0^T i_s \sin nwt\, dt$$

or

$$a_n = \frac{V}{R}\left[\frac{(1 - \frac{E}{V})(1-\cos(2n\pi\delta))}{n\pi} + \frac{2(e^{\delta T/\tau} - e^{T/\tau})}{e^{T/\tau} - 1}\right. \quad (2.47)$$

$$\left.\left\{\frac{(1-e^{-\delta T/\tau}\cos(2n\pi\delta))2\tau^2 n\pi - \tau^2 T\, e^{-\delta T/\tau}\sin(2n\pi\delta)}{T^2 + 4\tau^2 n^2\pi^2}\right\}\right]$$

and

$$b_n = \frac{2}{T}\int_0^T i_s \cos nwt\, dt$$

or

$$b_n = \frac{V}{R}\left[(1- \frac{E}{V})\frac{\sin(2n\pi\delta)}{n\pi} + \frac{2(e^{\delta T/\tau} - e^{T/\tau})}{e^{T/\tau} - 1}\right. \quad (2.48)$$

$$\left.\left\{\frac{2\tau^2 n\pi e^{-\delta T/\tau}\sin(2n\pi\delta) + \tau T(1-e^{-\delta T/\tau}\cos(2n\pi\delta))}{T^2 + 4\tau^2 n^2\pi^2}\right\}\right]$$

Therefore, the rms value of nth harmonic in supply current is

$$I_n = \sqrt{a_n^2 + b_n^2}\,/\,2 \quad (2.49)$$

B. Discontinuous Conduction

Following is the mathematical representation of supply current valid for this case and shown in Fig. 2.3(b).

$$i_s = \left(\frac{V-E}{R}\right)\left(1 - e^{-t/\tau}\right) \quad \text{for } 0 \leq t \leq \delta T$$
$$= 0 \quad \text{for } \delta T \leq t \leq T \tag{2.50}$$

After doing fourier analysis of above eqn. one gets the dc component of supply current I_o as

$$I_o = \frac{1}{T} \int_0^T i_s \, dt$$

or

$$I_o = \frac{V}{R}\left[\left(1 - \frac{E}{V}\right)\delta + \frac{\delta}{T}\left(\frac{E}{V} - 1\right)\left(1 - e^{-\delta T/\tau}\right)\right] \tag{2.51}$$

and the fourier constants are

$$a_n = \frac{2}{T} \int_0^T i_s \sin nwt \, dt$$

or

$$a_n = \frac{V}{R}\left[\left(1 - \frac{E}{V}\right)\left(\frac{1-\cos(2n\pi\delta)}{n\pi}\right) + 2\left(\frac{E}{V} - 1\right)\right.$$
$$\left.\frac{\left\{\left(1-e^{-\delta T/\tau}\cos(2n\pi\delta)\right) 2\tau^2 n\pi - \tau^2 T e^{-\delta T/\tau} \sin(2n\pi\delta)\right\}}{T^2 + 4\tau^2 n^2 \pi^2}\right] \tag{2.52}$$

$$b_n = \frac{2}{T} \int_0^T i_s \cos nwt \, dt$$

or

$$b_n = \frac{V}{R}\left[\left(1-\frac{E}{V}\right)\frac{\sin(2n\pi\delta)}{n\pi} + 2\left(\frac{E}{V}-1\right)\right.$$

$$\left.\left\{\frac{2\tau^2 n\pi e^{-\delta T/\tau}\sin(2n\pi\delta) + \tau T\left(1-e^{-\delta T/\tau}\cos(2n\pi\delta)\right)}{T^2 + 4\tau^2 n^2\pi^2}\right\}\right] \qquad (2.53)$$

Hence, the rms value of nth harmonic in supply current will be given by

$$I_n = \sqrt{a_n^2 + b_n^2}\,/\,2 \qquad (2.54)$$

2.2.4 Harmonics in Supply Current with Regenerative Braking :

A. Continuous Conduction:

The expression for supply current shown in Fig. 2.4(a) is

$$i_s = 0 \qquad \text{for } 0 \le t \le \delta T$$

$$= \frac{(E-V)}{R}\left(1-e^{-t/\tau}\right) + I_{max}\, e^{-t/\tau} \quad \text{for } \delta T \le t \le T \qquad (2.55)$$

where I_{max} is given by eqn. (2.31).

After doing fourier analysis of above eqn. one gets the dc component of supply current as

$$I_o = \frac{1}{T}\int_0^T i_s\, dt$$

or

$$I_o = \frac{V}{R}\left[\left(1-\frac{E}{V}\right)(1-\delta)+\frac{\tau}{T}\left(\frac{e^{(1-\delta)T/\tau}\, e^{T/\tau}}{e^{T/\tau}-1}\right)\left(1-e^{-(1-\delta)T/\tau}\right)\right] \tag{2.56}$$

Fourier constants are

$$a_n = \frac{2}{T}\int_0^T i_s \sin nwt \; dt$$

or

$$a_n = \frac{V}{R}\left[\left(1-\frac{E}{V}\right)\left(\frac{1-\cos(2n\pi(1-\delta))}{n\pi}\right)+2\left(\frac{e^{(1-\delta)T/\tau}-e^{T/\tau}}{e^{T/\tau}-1}\right)\right.$$

$$\left[1-e^{-(1-\delta)T/\tau}\cdot\cos(2n\pi(1-\delta))\right]\cdot 2\tau^2 n\pi$$

$$\left.\left\{\frac{-\tau^2 T\, e^{-(1-\delta)T/\tau}\sin(2n\pi(1-\delta))}{T^2+4\tau^2 n^2\pi^2}\right\}\right] \tag{2.57}$$

and

$$b_n = \frac{2}{T}\int_0^T i_s \cos nwt \; dt$$

or

$$b_n = \frac{V}{R}\left[\left(1-\frac{E}{V}\right)\frac{\sin(2n\pi(1-\delta))}{n\pi}+2\left(\frac{e^{(1-\delta)T/\tau}-e^{T/\tau}}{e^{T/\tau}-1}\right)\right.$$

$$\left.\left\{\frac{2\tau^2 n\pi e^{-(1-\delta)T/\tau}\sin(2n\pi(1-\delta))+\tau T\left(1-e^{-(1-\delta)T/\tau}\cdot\cos(2n\pi(1-\delta))\right)}{T^2+4\tau^2 n^2\pi^2}\right\}\right] \tag{2.58}$$

Hence, the rms value of nth harmonic of supply current will be

$$I_n = \sqrt{a_n^2 + b_n^2}\,/\,2 \tag{2.59}$$

B. Discontinuous Conduction:

The mathematical expression of supply current for this case shown in Fig. 2.4(b) is

$$i_s = 0 \qquad \text{for } 0 \leq t \leq \delta T \qquad (2.60)$$

$$= \left(\frac{E-V}{R}\right)\left(1-e^{-t/\tau}\right) + \frac{E}{R}\left(1-e^{-\delta T/\tau}\right)e^{-t/\tau}$$

$$\text{for } \delta T \leq t \leq \gamma T$$

Fourier analysis of above expression yields the dc component of supply current as

$$I_o = \frac{1}{T}\int_0^T i_s \, dt$$

or

$$I_o = \frac{V}{R}\left[\left(1-\frac{E}{V}\right)(1-\delta) + \frac{\tau}{T}\left(\frac{E}{V}e^{-\delta T/\tau} - 1\right)\left(1-e^{-(1-\delta)T/\tau}\right)\right] \qquad (2.61)$$

And the fourier constants are

$$a_n = \frac{2}{T}\int_0^T i_s \sin nwt \, dt$$

or

$$a_n = \frac{V}{R}\left[\left(1-\frac{E}{V}\right)\left(\frac{1-\cos(2n\pi(1-\delta))}{n\pi}\right) + 2\left(\frac{E}{V}e^{-\delta T/\tau} - 1\right)\right.$$

$$\left.\left(1-e^{-(1-\delta)T/\tau}.\cos(2n\pi(1-\delta))\right)\frac{2\tau^2 n\pi - \tau^2 T e^{-(1-\delta)T/\tau}\sin(2n\pi(1-\delta))}{T^2 + 4\tau^2 n^2 \pi^2}\right] \qquad (2.62)$$

$$b_n = \frac{2}{T}\int_0^T i_s \cos nwt \, dt$$

or

$$b_n = \frac{V}{R}\left[\frac{\left(1-\frac{E}{V}\right)\sin(2n\pi(1-\delta))}{n\pi} + 2\left(\frac{E}{V}e^{-\delta T/\tau} - 1\right)\right.$$

$$2\tau^2 n\pi e^{-(1-\delta)T/\tau}\sin(2n\pi(1-\delta)) + \tau T(1-e^{-(1-\delta)T/\tau}\left[\frac{\cos(2n\pi(1-\delta))}{T^2+4\tau^2n^2\pi^2}\right]\Big] \quad (2.63)$$

Therefore, the rms value of nth harmonic in supply current will be

$$I_n = \sqrt{a_n^2 + b_n^2}\,/\,2 \quad (2.64)$$

2.2.5 The Regenerated Power and Efficiency of Regeneration:

A. Continuous Conduction

The current supplied from the motor to the source is given by (please see Fig. 2.4(a))

$$i_o = 0 \qquad \text{for } 0 \le t \le \delta T \quad (2.65)$$

$$= \left(\frac{E-V}{R}\right)(1-e^{-t/\tau}) + \left[\frac{E}{R} - \frac{V}{R}\left(\frac{e^{(1-\delta)T/\tau}-1}{e^{T/\tau}-1}\right)\right]e^{-t/\tau}$$

$$\text{for } \delta T \le t \le T$$

Hence, the average power regenerated is

$$PR_{av} = \frac{1}{T}\int_0^{(1-\delta)T} (V\,i_o)\,dt$$

or

$$PR_{av} = \frac{V^2}{R}\left[\left(\frac{E}{V}-1\right)(1-\delta) + \frac{\tau}{T}\left(\frac{e^{T/\tau} - e^{(1-\delta)T/\tau} - e^{\delta T/\tau} + 1}{e^{T/\tau}-1}\right)\right] \quad (2.66)$$

The normalized power regenerated is given by

$$PR_{av(N)} = \frac{PR_{av}}{V^2/R} = \left(\frac{E}{V} - 1\right)(1-\delta) + \frac{\tau}{T}\left(\frac{e^{T/\tau} - e^{(1-\delta)T/\tau} - e^{\delta T/\tau} + 1}{e^{T/\tau} - 1}\right) \tag{2.67}$$

The average power generated by the motor can be calculated as

$$PG_{av} = \frac{1}{T}\int_0^T E\, i_o\, dt$$

or

$$PG_{av} = \frac{E}{T}\left[\int_0^T \left(\frac{E}{R}(1-e^{-t/\tau}) + I_{min}\, e^{-t/\tau}\right) dt + \int_0^{(1-\delta)T} \left(\frac{E-V}{R}\right)(1-e^{-t/\tau}) + I_{max}\, e^{-t/\tau}\, dt\right]$$

where I_{min} and I_{max} are given by eqns. (2.34) and (2.33) respectively.

After simplifying the above expression, one gets

$$PG_{av} = \frac{V^2}{R}\left[\left(\frac{E}{V}\right)^2 - \left(\frac{E}{V}\right)(1-\delta)\right] \tag{2.68}$$

Now, the normalized power generated by the motor is

$$PG_{av}(N) = \frac{PG_{av}}{V^2/R} = \left(\frac{E}{V}\right)^2 - \left(\frac{E}{V}\right)(1-\delta) \tag{2.69}$$

Hence, the efficiency of regeneration, η in %, is

$$\eta = \frac{PR_{av}(N)}{PG_{av(N)}} \times 100 \tag{2.70}$$

B. Discontinuous Conduction:

The mathematical expression for the current which flows from the motor to the source is (please see Fig. 2.4(b))

$$\begin{aligned} i_o &= 0 && \text{for } 0 \leq t \leq \delta T \\ &= \left(\frac{E-V}{R}\right)\left(1-e^{-t/\tau}\right)+\frac{E}{R}\left(1-e^{-\delta T/\tau}\right)e^{-t/\tau} \\ & && \text{for } \delta T \leq t \leq \gamma T \qquad (2.71) \\ &= 0 && \text{for } \gamma T \leq t \leq T \end{aligned}$$

Therefore, the average power regenerated is

$$PG_{av} = \frac{1}{T}\int_0^{(\gamma-\delta)T} (V\, i_o)\,dt$$

or

$$PG_{av} = \frac{V^2}{R}\left[\left(\frac{E}{V}-1\right)(\gamma-\delta)+\frac{\tau}{T}\left(1-\frac{E}{V}e^{-\delta T/\tau}\right)\left(1-e^{-(\gamma-\delta)T/\tau}\right)\right] \qquad (2.72)$$

The normalized power regenerated will be given by

$$PR_{av(N)} = \frac{PR_{av}}{V^2/R} = \left(\frac{E}{V}-1\right)(\gamma-\delta)+\frac{\tau}{T}\left(1-\frac{E}{V}e^{-\delta T/\tau}\right)\left(1-e^{-(\gamma-\delta)T/\tau}\right) \qquad (2.73)$$

Now, the average power generated by the motor can be found as

$$PG_{av} = \frac{1}{T}\int_0^T E\, i_o\, dt$$

or

$$PG_{av} = \frac{E}{T}\left[\int_0^{\delta T} \frac{E}{R}(1-e^{-t/\tau})\,dt + \int_0^{(\gamma-\delta)T} \left\{\left(\frac{E-V}{R}\right)\right.\right.$$

$$\left.\left.(1-e^{-t/\tau}) + \frac{E}{R}(1-e^{-\delta T/\tau})\,e^{-t/\tau}\right\}dt\right]$$

or

$$PG_{av} = \frac{V^2}{R} x\left[\left(\frac{E}{V}\right)\delta + \left(\frac{E}{V}\right)\gamma\left(\frac{E}{V}-1\right) + \frac{E}{V}\cdot\frac{\tau}{T}\left\{\frac{E}{V}\left(e^{-\gamma T/\tau}-1\right)\right.\right.$$

$$\left.\left. + 1 - e^{-(\gamma-\delta)T/\tau}\right\}\right] \qquad (2.74)$$

and the normalized power generated is

$$PG_{av(N)} = \frac{PG_{av}}{V^2/R} = \left(\frac{E}{V}\right)\delta + \gamma\frac{E}{V}\left(\frac{E}{V}-1\right) + \frac{E}{V}\cdot\frac{\tau}{T}$$

$$\left\{\frac{E}{V}\left(e^{-\gamma T/\tau}-1\right) + 1 - e^{-(\gamma-\delta)T/\tau}\right\} \qquad (2.75)$$

Hence, the efficiency of regeneration, η, in % , is

$$\eta = \frac{PR_{av(N)}}{PG_{av(N)}} x\ 100 \qquad (2.76)$$

2.2.6 <u>The Steady State Transfer Characteristics</u>:

Since choppers normally operate well above the drive cut-off frequency, hence their dynamical characteristics are not of much significance in drives design, In contrast, incremental gain which exhibits substantial variation with load, is a crucial factor in the design of a high performance system.

The steady state transfer function of a chopper defines the relationship between the mean output voltage delivered to the load by the chopper and the chopper control voltage [4].

1. Motoring Operation:

The circuit for this case is shown in Fig. 2.5(a).

A. Continuous Conduction:

The mean output voltage, V_o, is equal to the load emf plus the drop in the load resistance produced by the mean output current I_{av}.

$$V_o = E + RI_{av} \tag{2.77}$$

Putting value of I_{av} from eqn. (2.3), one gets

$$V_o = E + R\left(\frac{\delta V - E}{R}\right) = \delta V$$

Hence

$$\frac{V_o}{V} = \delta \tag{2.78}$$

Assuming that thyristor on time is linearly dependent on the control voltage, i.e.,

$$\delta = \frac{V_c}{V_{cm}} \tag{2.79}$$

Substituting the value of δ from eqn. (2.79) into eqn. (2.78), one gets the relationship between the mean output voltage and the control voltage as

$$\frac{V_o}{V} = \frac{V_c}{V_{cm}} \qquad (2.80)$$

or

$$\text{gain } G = \frac{d(\frac{V_o}{V})}{d(\frac{V_c}{V_{cm}})} = 1 \qquad (2.81)$$

B. Discontinuous Conduction:

From eqn. (2.15), the mean load current in this case is

$$I_{av} = \frac{\delta V - \gamma E}{R}$$

Therefore, from eqn. (2.77), the mean output voltage will be

$$V_o = E + \delta V - \gamma E$$

or

$$\frac{V_o}{V} = (1 - \gamma) \frac{E}{V} + \delta$$

Putting the value of δ from eqn. (2.19) into above eqn., one gets

$$\frac{V_o}{V} = (1 - \delta - \frac{\tau}{T} \ln [\frac{V}{E} + (1 - \frac{V}{E}) e^{-\delta T/\tau}]) \frac{E}{V} + \delta \qquad (2.82)$$

Replacing δ by $\frac{V_c}{V_{cm}}$ in above eqn., one gets the following eqn. from which the transfer characteristic of chopper can be obtained

$$\frac{V_o}{V} = \left(1 - \frac{V_c}{V_{cm}} - \frac{\tau}{T} \ln \left[\frac{V}{E} + \left(1 - \frac{V}{E}\right) e^{-\frac{V_c}{V_{cm}} \frac{T}{\tau}}\right]\right) \frac{E}{V} + \frac{V_c}{V_{cm}} \tag{2.83}$$

The gain of the system will be given by

$$G = \frac{d\left(\frac{V_o}{V}\right)}{d\left(\frac{V_c}{V_{cm}}\right)} = \frac{E}{V}\left[-1 + \frac{\left(1 - \frac{V}{E}\right) e^{-\frac{V_c}{V_{cm}} \frac{T}{\tau}}}{\frac{V}{E} + \left(1 - \frac{V}{E}\right) e^{-\frac{V_c}{V_{cm}} \frac{T}{\tau}}}\right] + 1 \tag{2.84}$$

2. Regenerative Braking

The circuit for regenerative braking is shown in Fig. 2.5(b).

A. Continuous Conduction:

Considering Figs. 2.4(a) and 2.5, the mean output voltage is

$$V_o = E - RI_{av} \tag{2.85}$$

Putting the value of I_{av} from eqn. (2.27), the above eqn. becomes

$$V_o = (1 - \delta)V \tag{2.86}$$

In order to correlate the characteristic with that of chopper for motoring operation, δ_1 is taken as $(1-\delta)$ which is the time during which the chopper would connect the load to the supply.

Therefore, from eqn. (2.86)

$$\frac{V_o}{V} = \delta_1 \qquad (2.87)$$

Since, from our previous assumption $\delta_1 = \frac{V_c}{V_{cm}}$, hence the eqn. (2.87) yields the relationship between the mean output voltage and control voltage

$$\frac{V_o}{V} = \frac{V_c}{V_{cm}} \qquad (2.88)$$

or

$$\text{gain} = G = \frac{d(\frac{V_o}{V})}{d(\frac{V_c}{V_{cm}})} = 1 \qquad (2.89)$$

B. Discontinuous Conduction:

Referring fig. 2.4(b), the mean output voltage, V_o, is

$$\frac{V_o}{V} = \delta_1 - \frac{\tau}{T} \ln \left[\frac{E-V}{E\, e^{-T/\tau} - V\, e^{-\delta_1 T/\tau}} \right] \left[1 - \frac{E}{V}\right] \qquad (2.90)$$

Therefore the relation between mean output voltage and control voltage is

$$\frac{V_o}{V} = \frac{V_c}{V_{cm}} - \frac{\tau}{T} \ln \left[\frac{\frac{E}{V} - 1}{\frac{E}{V} e^{-T/\tau} - e^{-V_c/V_{cm}\, T/\tau}}\right] \left[1 - \frac{E}{V}\right] \qquad (2.91)$$

or

$$\text{gain} \quad G = \frac{d(\frac{Vo}{V})}{d(\frac{V_c}{V_{cm}})} = 1 - \frac{(\frac{E}{V} - 1)\, e^{-\frac{V_c}{V_{cm}} \frac{T}{\tau}}}{(\frac{E}{V} e^{-T/\tau_e} - \frac{V_c}{V_{cm}} \frac{T}{\tau})} \qquad (2.92)$$

2.3 ANALYSIS FOR DUAL CHOPPER WITH CIRCULATING CURRENT OPERATION:

This kind of chopper is free from discontinuous conduction. The typical waveforms of motor voltage, motor current and line current for motoring and regenerative braking are shown in Fig. 2.6.

2.3.1 Speed-Torque Characteristics:

Considering the chopper circuit of Fig. 2.2, one can write the eqns. for duty and freewheeling intervals as

Duty interval

$$L \frac{di_a}{dt} + Ri_a + E = V \text{ for } 0 \leq t \leq t_{oN} \qquad (2.93)$$

Freewheeling interval

$$L \frac{di_a}{dt} + Ri_a + E = 0 \text{ for } t_{oN} \leq t \leq T \qquad (2.94)$$

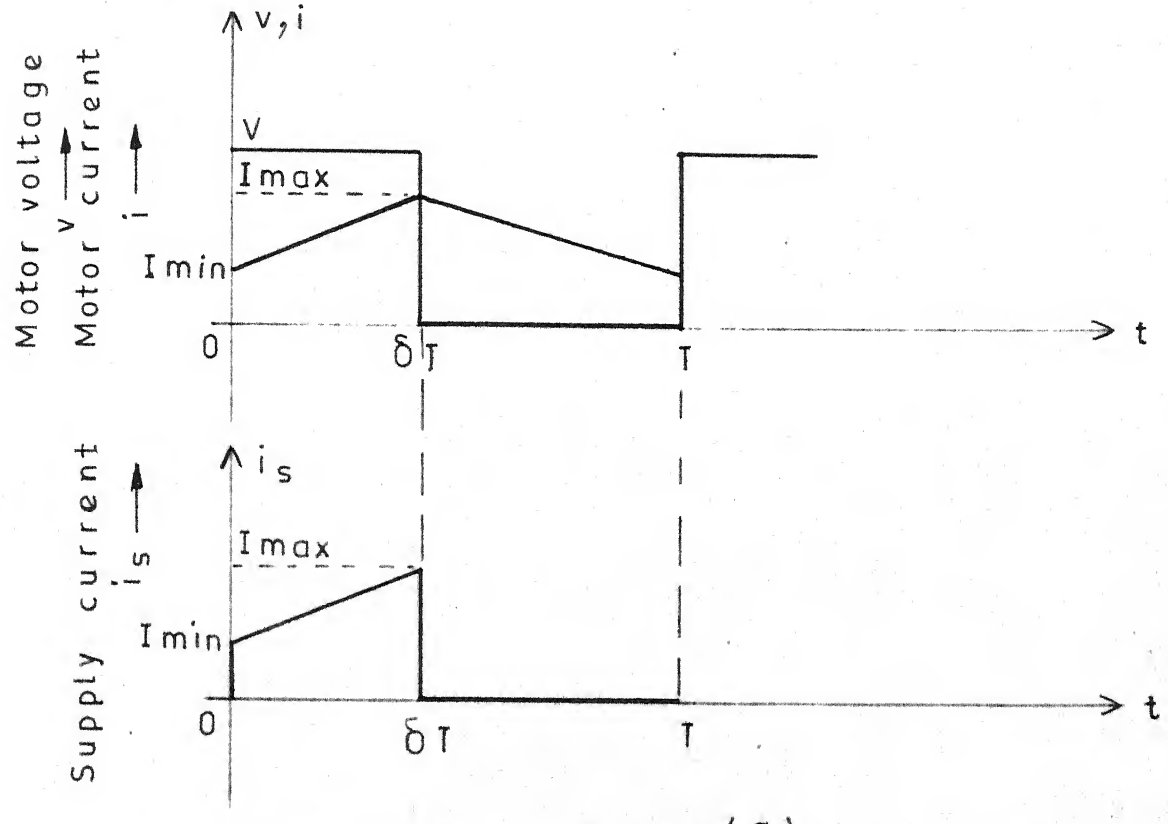

(a)

FIG.2.6 Circulating current chopper.
(a) Motoring.
(b) Regenerative braking

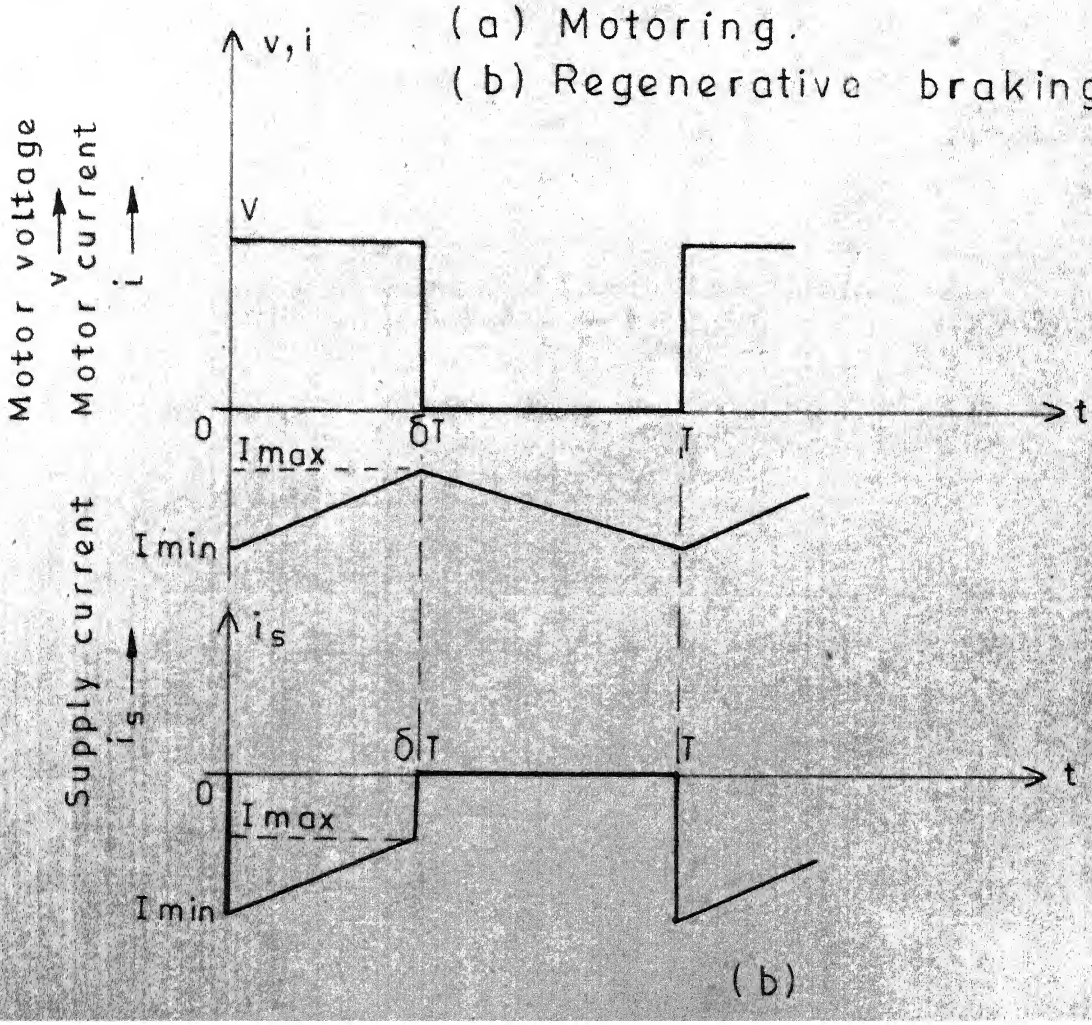

(b)

Taking the average of above two eqns. for the time period T, one gets

$$I_{av} = \frac{\delta V - E}{R} = \frac{\delta V - K_v w}{R} \qquad (2.95)$$

and

$$T_{av} = K_T I_{av} = K_T \left[\frac{\delta V - K_v w}{R} \right] \qquad (2.96)$$

The solutions of eqns. (2.93) and (2.94) are

$$i_a = \frac{V-E}{R} (1-e^{-t/\tau}) + I_{min} e^{-t/\tau} \qquad (2.97)$$

for $0 \leq t \leq t_{oN}$

and

$$i_a = -\frac{E}{R} (1-e^{-t/\tau}) + I_{max} e^{-t/\tau} \qquad (2.98)$$

for $t_{oN} \leq t \leq T$

where

$$I_{min} = \frac{V}{R} \left[\frac{e^{\delta T/\tau} - 1}{e^{T/\tau} - 1} \right] - \frac{E}{R} \qquad (2.99)$$

and

$$I_{max} = \frac{V}{R} \left[\frac{1 - e^{-\delta T/\tau}}{1 - e^{-T/\tau}} \right] - \frac{E}{R} \qquad (2.100)$$

The current fluctuation is

$$\Delta i_f = \frac{I_{max} - I_{min}}{2}$$

or

$$\Delta i_f = \frac{V}{2R} \left[\frac{1 - e^{-\delta T/\tau}}{1 - e^{-T/\tau}} - \frac{e^{\delta T/\tau} - 1}{e^{T/\tau} - 1} \right] \qquad (2.101)$$

Using straight line approximation [3]

$$I_{av} = \frac{I_{max} + I_{min}}{2} \qquad (2.102)$$

$$I_{rms} = \sqrt{\frac{I_{max}^2 + I_{min}^2 + I_{max} \cdot I_{min}}{3}} \qquad (2.103)$$

$$CRF = \frac{I_{max} - I_{min}}{\sqrt{3}\,(I_{max} + I_{min})} \qquad (2.104)$$

2.3.2 Harmonics in Supply Current:

The waveform for supply current is shown in Fig. 2.6. It can be expressed mathematically as

$$i_s = \frac{V-E}{R}(1-e^{-t/\tau}) + I_{min}\, e^{-t/\tau} \quad \text{for } 0 \le t \le \delta T \qquad (2.105)$$

$$= 0 \quad \text{for } \delta T \le t \le T$$

where I_{min} is given by eqn. (2.99),

Fourier analysis of above eqn. yields the dc current

$$I_o = \frac{V}{R}\left[(1-\frac{E}{V})\delta + \frac{\tau}{T}\left(\frac{e^{\delta T/\tau} - e^{T/\tau}}{e^{T/\tau} - 1}\right)(1-e^{-\delta T/\tau})\right] \qquad (2.106)$$

Fourier constants

$$a_n = \frac{V}{R}\left[\frac{(1-\frac{E}{V})(1-\cos(2n\pi\delta))}{n\pi} + \frac{2(e^{\delta T/\tau} - e^{T/\tau})}{e^{T/\tau} - 1}\right.$$

$$\left.\left\{\frac{(1-e^{-\delta T/\tau}\cdot\cos(2n\pi\delta))\,2\tau^2 n\pi - \tau T\, e^{-\delta T/\tau}\cdot\sin(2n\pi\delta)}{T^2 + 4\tau^2 n^2\pi^2}\right\}\right] \qquad (2.107)$$

$$b_n = \frac{V}{R}\left[\left(1-\frac{E}{V}\right)\frac{\sin(2n\pi\delta)}{n\pi} + \frac{2\left(e^{\delta T/\tau} - e^{T/\tau}\right)}{e^{T/\tau}-1}\right.$$

$$\left\{\frac{2\tau^2 n\pi e^{-\delta T/\tau}.\sin(2n\pi\delta)+\tau T\left(1-e^{-\delta T/\tau}.\cos(2n\pi\delta)\right)}{T^2+4\tau^2 n^2\pi^2}\right\}\Bigg] \qquad (2.108)$$

Hence, the rms value of nth harmonic of supply current is given by

$$I_n = \sqrt{a_n^2 + b_n^2}\ /\ 2 \qquad (2.109)$$

2.3.3 The Regenerated Power and Efficiency of Regeneration:

The current which flows from load to the source during regeneration is given by

$$i_o = \left(\frac{V-E}{R}\right)\left(1-e^{-t/\tau}\right) + \left[\frac{V}{R}\left[\frac{e^{\delta T/\tau}-1}{e^{T/\tau}-1}\right] - \frac{E}{R}\right] e^{-t/\tau} \qquad (2.110)$$

$$\text{for } 0 \le t \le \delta T$$

Therefore, the average power regenerated by the load can be calculated as

$$PR_{av} = \frac{1}{T}\int_0^T (V\, i_o)\, dt$$

or

$$PR_{av} = \frac{V^2}{R}\left[\left(1-\frac{E}{V}\right)\delta + \frac{\tau}{T}\left\{\frac{e^{\delta T/\tau} - e^{T/\tau} - 1 + e^{(1-\delta)T/\tau}}{e^{T/\tau}-1}\right\}\right] \qquad (2.11)$$

Hence, the normalized regenerated power is

$$PR_{av(N)} = \frac{PR_{av}}{V^2/R} = (1 - \frac{E}{V})\delta + \frac{\tau}{T}\left\{\frac{e^{\delta T/\tau} - e^{T/\tau} - 1 + e^{(1-\delta)T/\tau}}{e^{T/\tau} - 1}\right\} \quad (2.112)$$

Now, the average power generated by the load is

$$PG_{av} = \frac{1}{T}\int_0^T (E\, i_o)\, dt$$

or

$$PG_{av} = \frac{V^2}{R}\left[(\frac{E}{V})\delta - (\frac{E}{V})^2\right] \quad (2.113)$$

And, the normalized average power generated is

$$PG_{av(N)} = \frac{PG_{av}}{V^2/R} = (\frac{E}{V})\delta - (\frac{E}{V})^2 \quad (2.114)$$

Hence, the efficiency of regeneration, η, in %, is

$$\eta = \frac{PR_{av(N)}}{PG_{av(N)}} \times 100 \quad (2.115)$$

2.3.4 <u>The Steady-State Transfer Function:</u>

Since there is always continuous conduction in case of circulating current chopper, its transfer function comes out to be the same in motoring and generative braking regions.

Considering Fig. 2.6, the mean output voltage is given by

$$V_o = E + RI_{av}$$

or

$$V_o = E + R\left[\frac{\delta V - E}{R}\right] = \delta V$$

$$\frac{V_o}{V} = \delta \quad (2.116)$$

Now, since $\delta = \frac{V_c}{V_{cm}}$ from eqn. (2.79), one gets the relationship between the mean output voltage and the control voltage as

$$\frac{V_o}{V} = \frac{V_c}{V_{cm}} \qquad (2.117)$$

Hence, the gain of the chopper is

$$G = \frac{d\left(\frac{V_o}{V}\right)}{d\left(\frac{V_c}{V_{cm}}\right)} = 1 \qquad (2.118)$$

2.4 COMPARISON BETWEEN NON-CIRCULATING CURRENT CHOPPER AND CIRCULATING CURRENT CHOPPER:

For simplicity, non-circulating current chopper will be called as chopper A, and circulating current chopper as chopper B.

The comparison between chopper A and chopper B has been done in following respects.

1. Nature of motor speed-torque characteristics.
2. Motor armature current ripple factor.
3. Harmonics in supply current.
4. The regenerated power and efficiency of regeneration.
5. Transfer characteristics.

For this study, a motor, details of which are given in Appendix A, is chosen.

2.4.1 Nature of Motor Speed-Torque Characteristics:

The speed-torque characteristics of motor with choppers A and B are shown in Fig. 2.7. It reveals that chopper A suffers from the disadvantage of discontinuous conduction which is undesirable from the point of view of good regulation of speed. Also it has been reported in literature that discontinuous conduction slows down transient response of motor [3,4,5]. On the other hand, chopper B is having continuous conduction in both the quadrants i.e. I and II. In first quadrant, the characteristics of chopper A for various values of δ are converging to the point (0.0,1.0) and also they are converging to the point (0,0) in 2nd quadrant of operation. On contrary to this, characteristics of chopper B for all δ is a straight line which extends in both the quadrants. In case of regeneration down to zero speed, a continuous decrease in value of δ is required when operating with chopper B. While chopper A allows one to get regeneration down to zero speed at any value of δ though with small working torque. The change from one quadrant of operation to another is carried out through

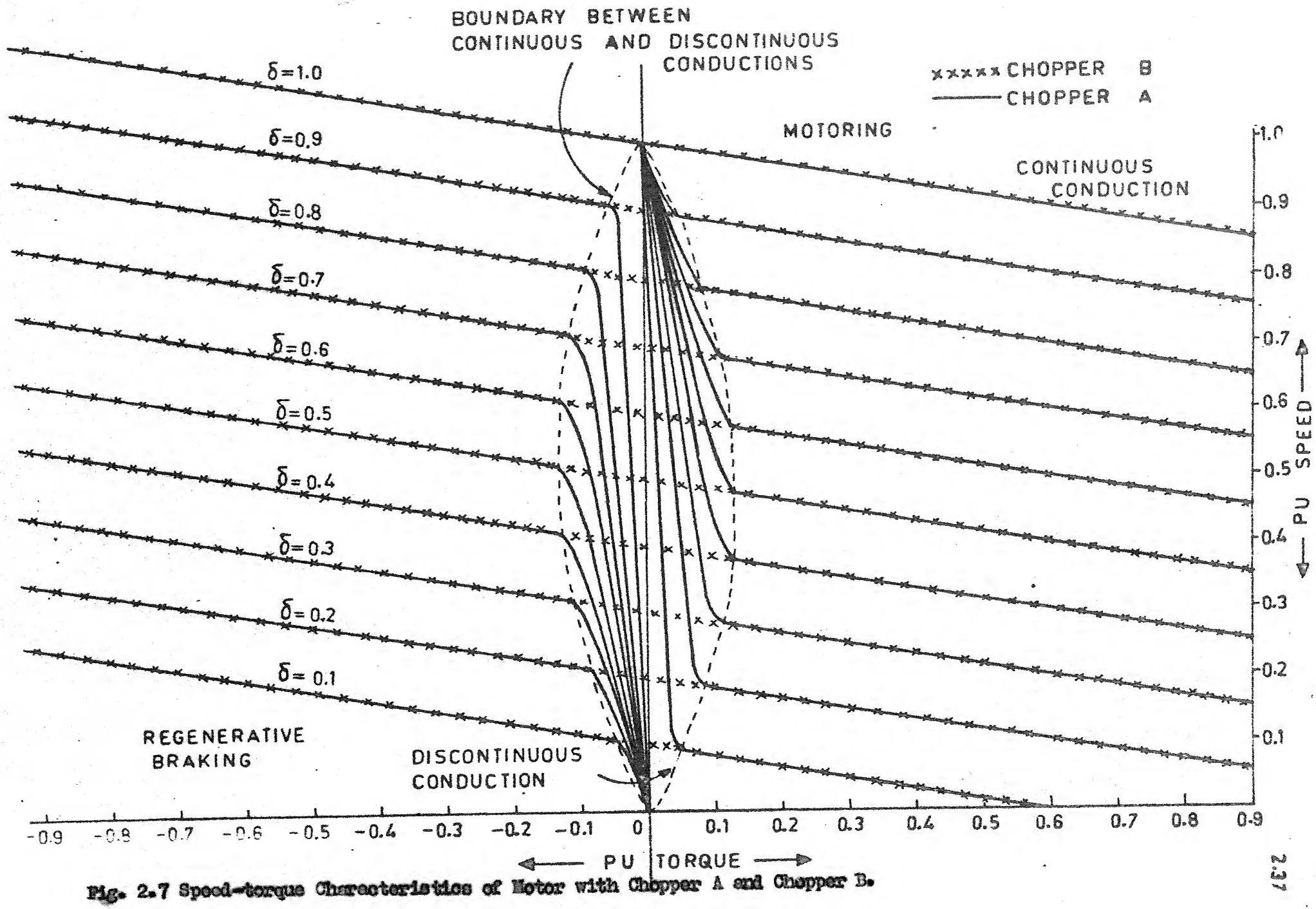

Fig. 2.7 Speed-torque Characteristics of Motor with Chopper A and Chopper B.

control circuit in chopper B while it requires a change of circuit in case of chopper A. The difference between the speed-torque characteristics of choppers A and B is only in the region shown with dotted lines. Otherwise they are same.

2.4.2 Motor Armature Current Ripple Factor:

The motor armature current ripple factor is a measure of increase in heating and commutation problems.

The maximum values of current ripple factor for choppers A and B have been listed in Table 2.1 for various values of δ.

Table 2.1

δ	Chopper A		Chopper B
	Motoring	Regen.Braking	
0.1	3.512	0.694	25.994
0.2	2.380	0.816	34.652
0.3	1.856	0.951	51.982
0.4	1.528	1.106	103.945
0.5	1.291	1.291	∞
0.6	1.106	1.528	103.925
0.7	0.951	1.856	51.977
0.8	0.816	2.380	34.656
0.9	0.694	3.512	25.992

The above table shows that chopper B has got very high value of maximum CRF in comparison to chopper A. The point of occurrence of maximum CRF in both the choppers lies on the boundary line between the two quadrants.

The average armature current vs. rms armature current curves for choppers A and B for two values of δ i.e., 0.5 and 0.8 have been shown in Fig. 2.8. These curves indicate that no load heating of motor in case of chopper B will be more.

2.4.3 Harmonics in Supply Current:

The dc component of supply current vs pu speed for choppers A and B has been shown in Fig. 2.9. It reveals that in discontinuous conduction region, for a particular value of δ a small amount of change in dc component of supply current results in large change in p.u. speed in case of chopper A while the same cause gives rise to comparatively a very small change in p.u. speed in case of chopper B.

First harmonic of supply current/dc component of supply current i.e., (a_1/a_0) vs. p.u. speed and second harmonic of supply current/dc component of supply current i.e. (a_2/a_0) vs. p.u. speed have been illustrated

δ	AV CURRENT	RMS CURRENT	SPEED IN R P M
0.1	0.001	0.035	150
0.2	0.002	0.062	300
0.3	0.002	0.081	450
0.4	0.001	0.092	600
0.5	0.000	0.096	750
0.6	-0.001	0.092	900
0.7	-0.002	0.081	1050
0.8	-0.002	0.062	1200
0.9	-0.001	0.035	1350

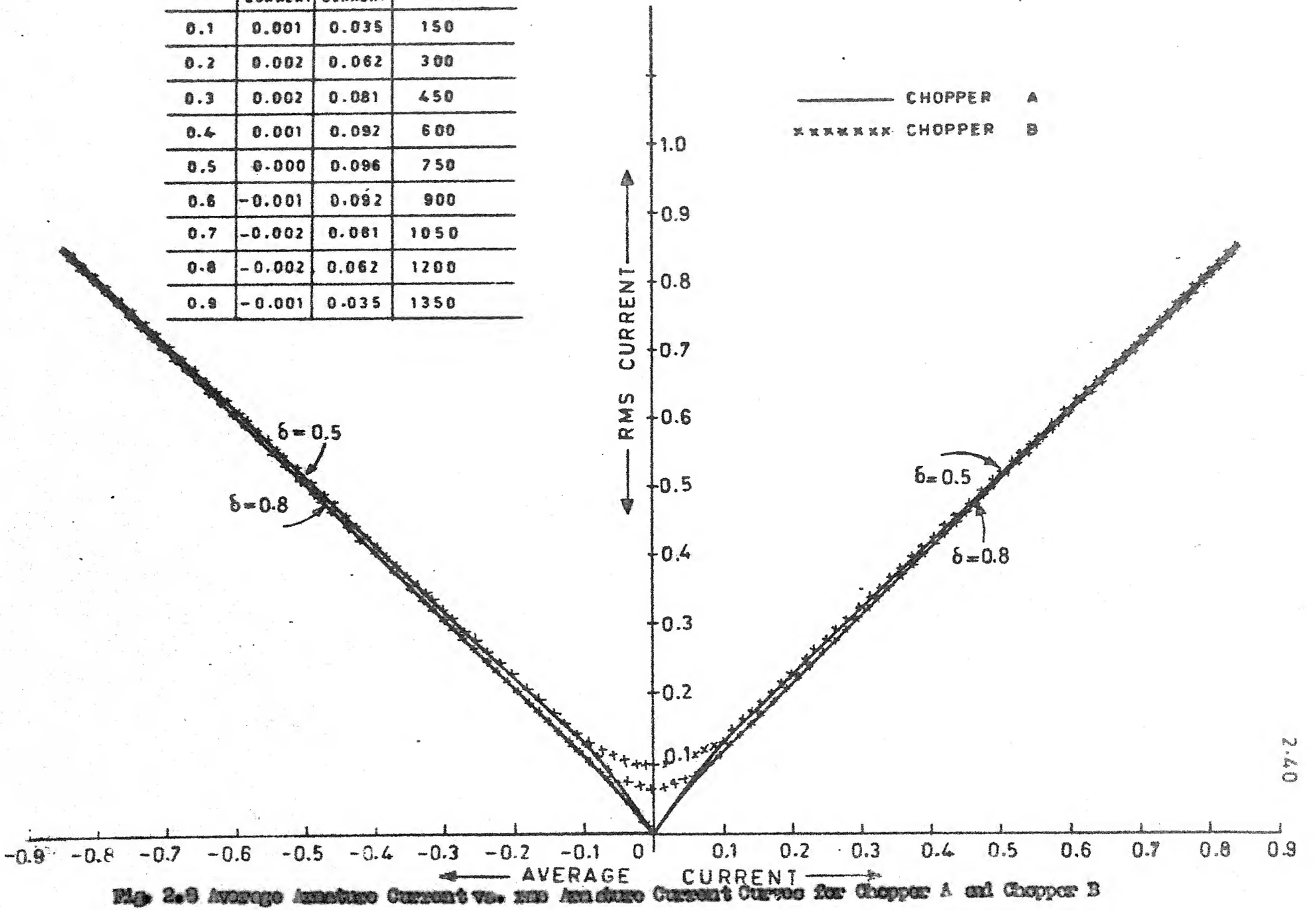

Fig. 2.9 Average Armature Current vs. and Armature Current Curves for Chopper A and Chopper B

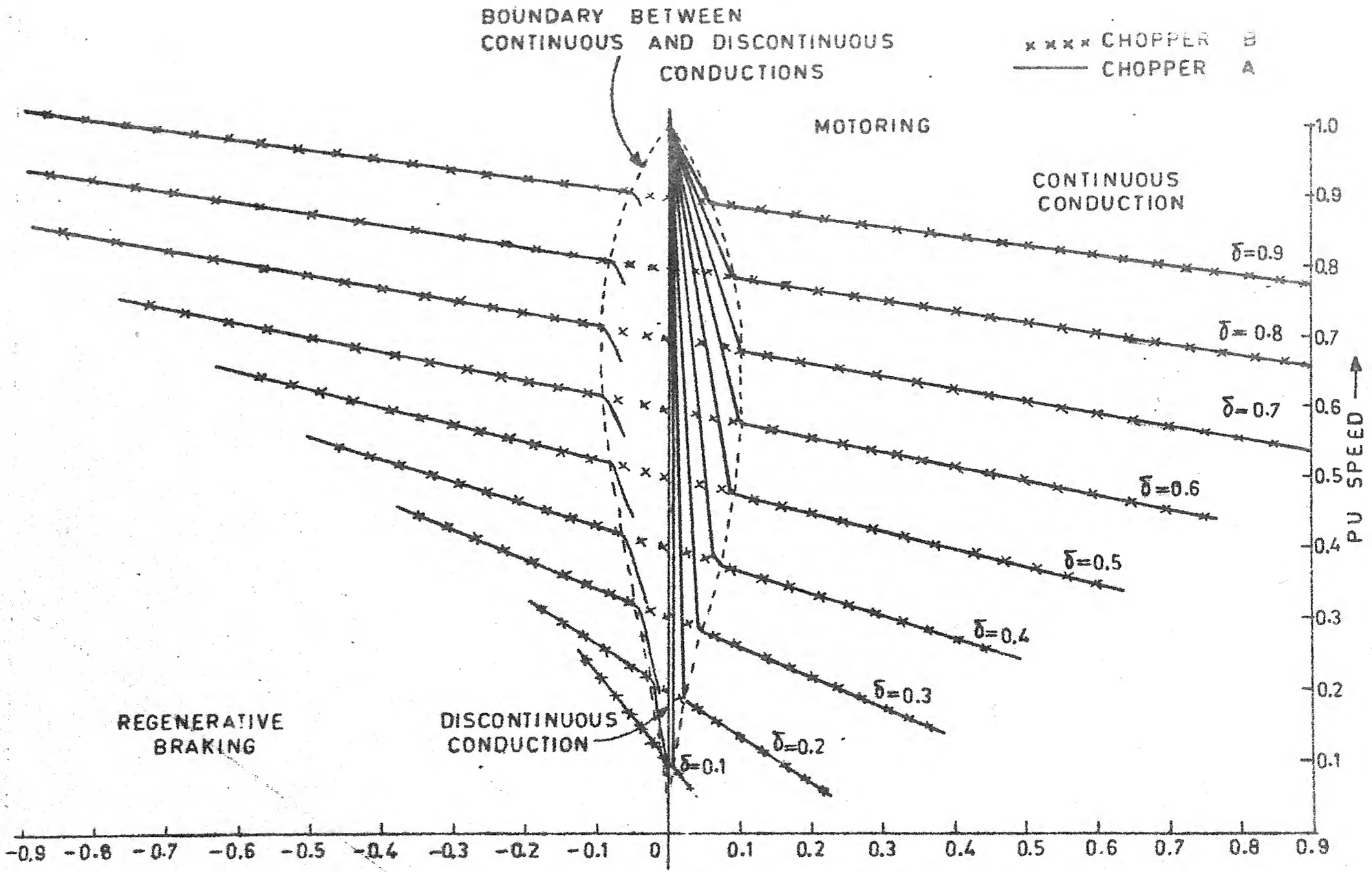

Fig. 2.9 Dc component of Supply Current vs. p.u. Speed for Chopper A and Chopper B.

in Figs. 2.10 and 2.11. These figs. show that contents of harmonics in supply current in case of chopper A operating in discontinuous conduction region is very less compared to contents of harmonics in supply current while operating with chopper B in the same range.

2.4.4 The Regenerated Power and Efficiency of Regeneration:

The normalized regenerated power vs. p.u. speed for choppers A and B has been shown in Fig. 2.12. The efficiency of regenerated power vs. p.u. speed for both choppers is shown in Fig. 2.13. Chopper B gives more efficiency of regeneration for all values of δ in comparison to chopper A. For regeneration down to zero speed in case of chopper B, a continuous decrease in value of δ is required while it can be achieved at any particular value of δ in case of chopper A.

2.4.5 Transfer Characteristics:

The normalised output voltage is shown as a function of the normalized control voltage in Fig. 2.14 for three values of E/V in case of both the choppers A and B operated in both the quadrants i.e. I and II. The incremental gain for both the choppers is also illustrated as a function of normalized control voltage in Fig. 2.15. It can be noticed that there occurs a

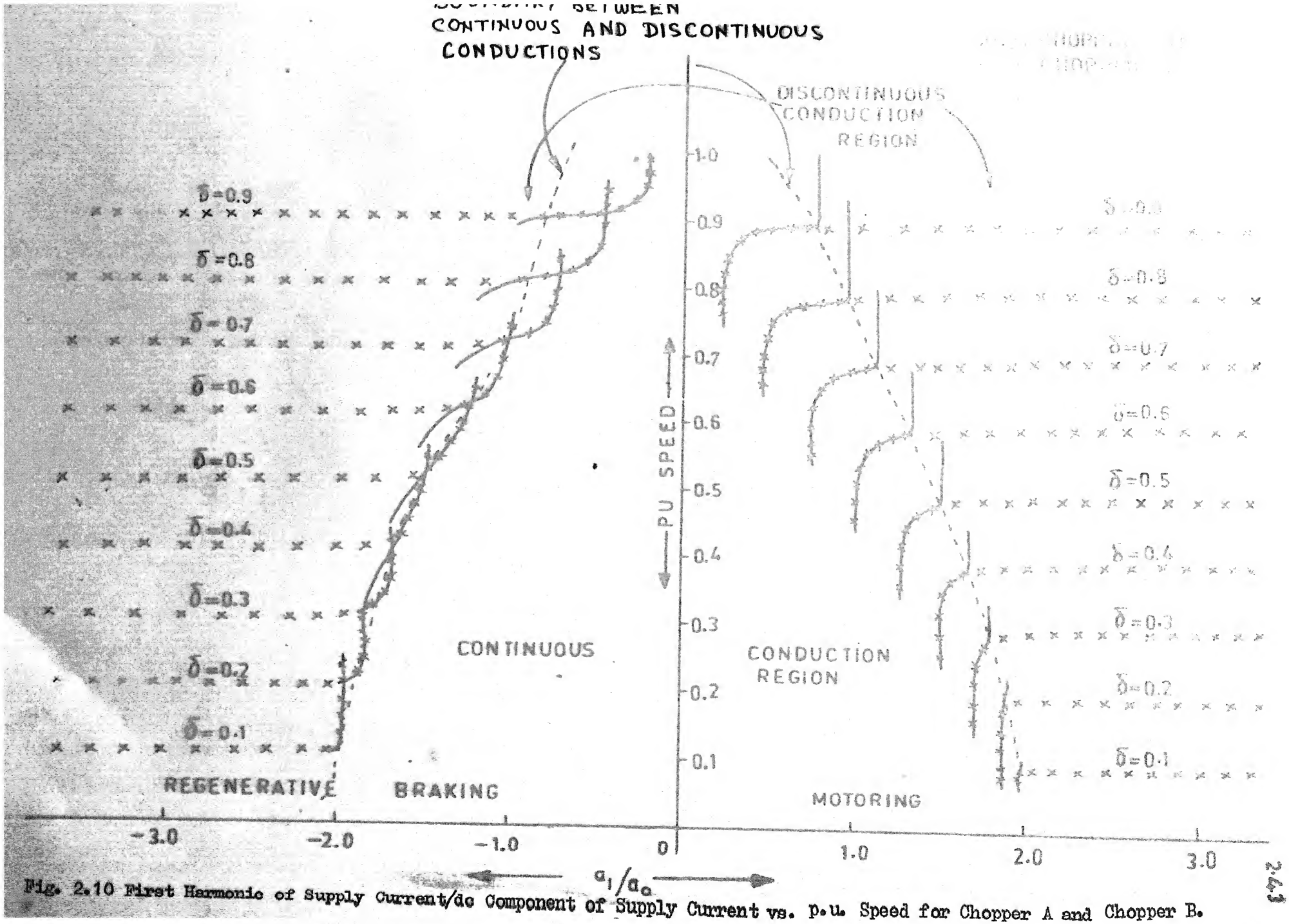

Fig. 2.10 First Harmonic of Supply Current/dc Component of Supply Current vs. p.u. Speed for Chopper A and Chopper B.

2.4.1

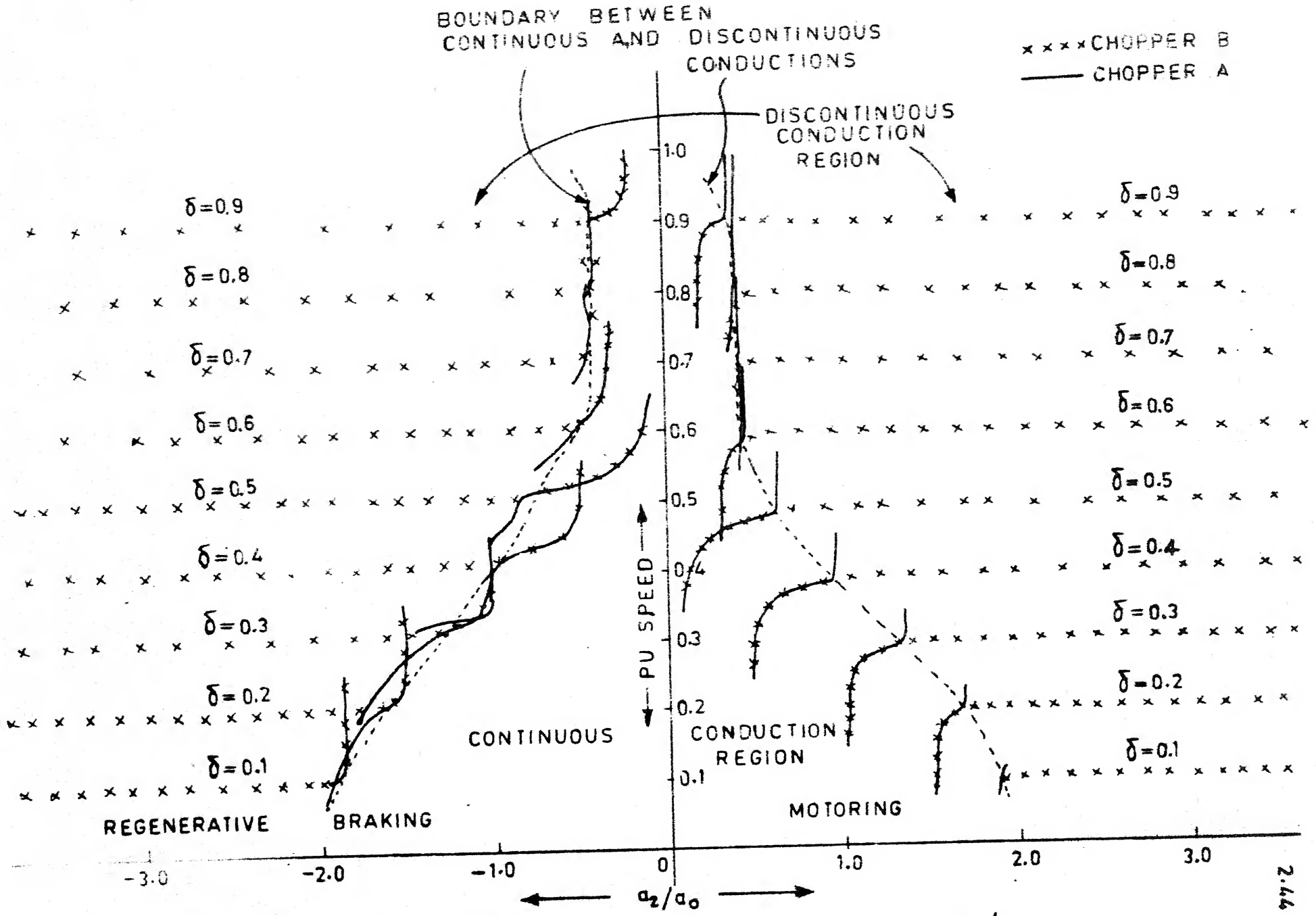

Fig. 2.11 Second Harmonic of Supply Current/dc component of Supply Current vs. p.u. Speed for Chopper A and Chopper B

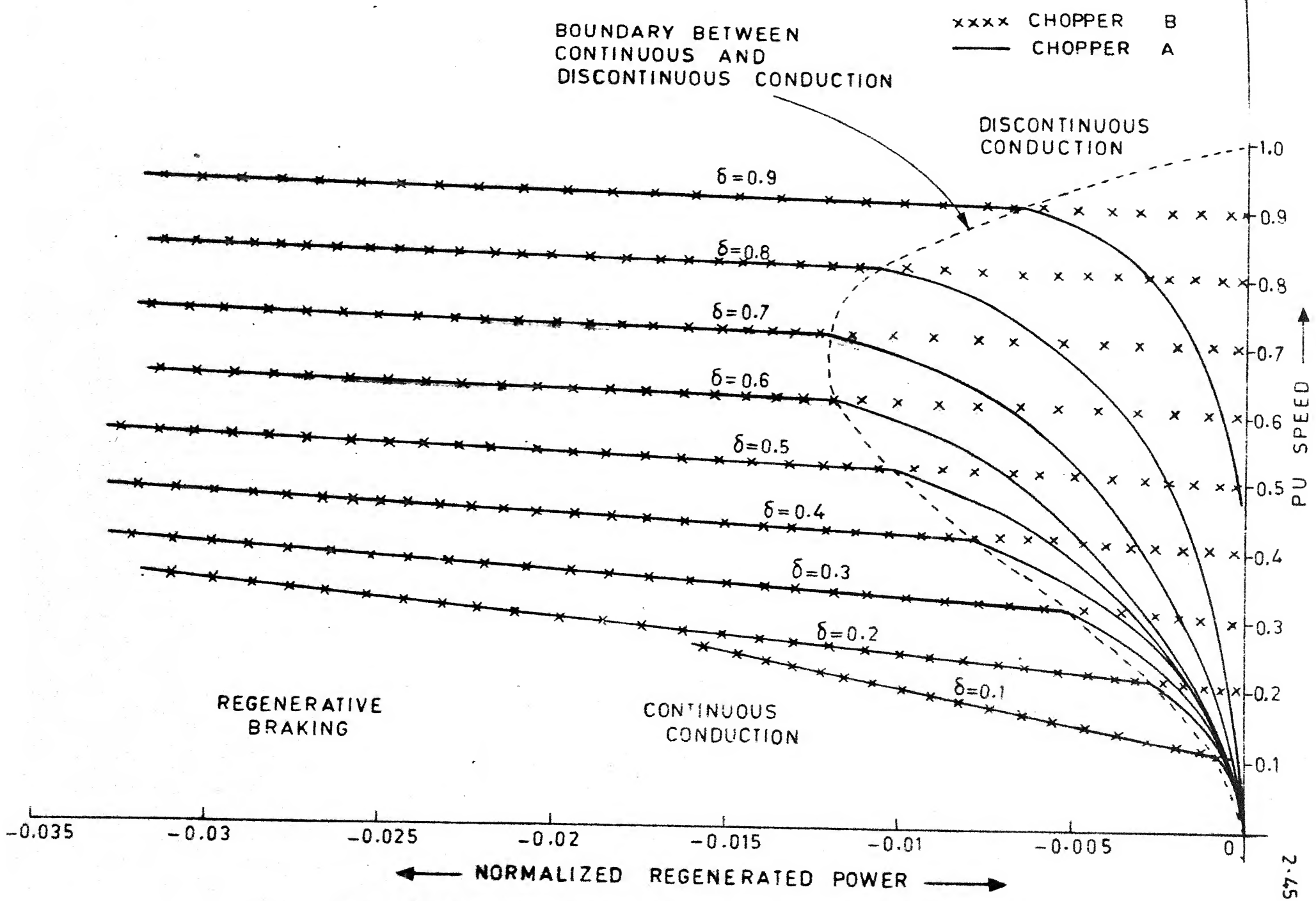

Fig. 2.12 Normalized Regenerated Power vs. p.u. Speed for Chopper A and Chopper B

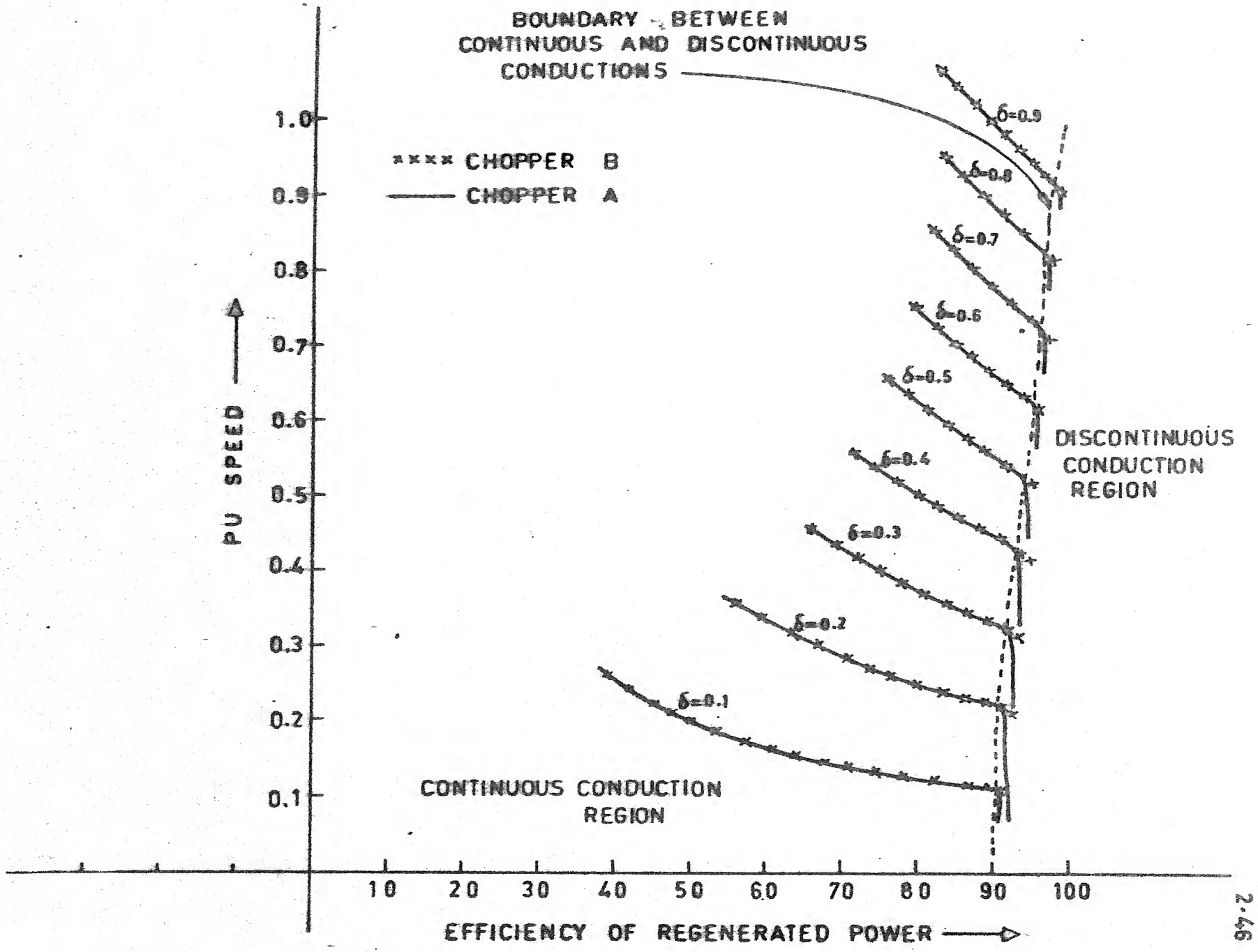

Fig. 2.13 Efficiency of Regenerated Power vs. p.u. Speed for Chopper A and Chopper B

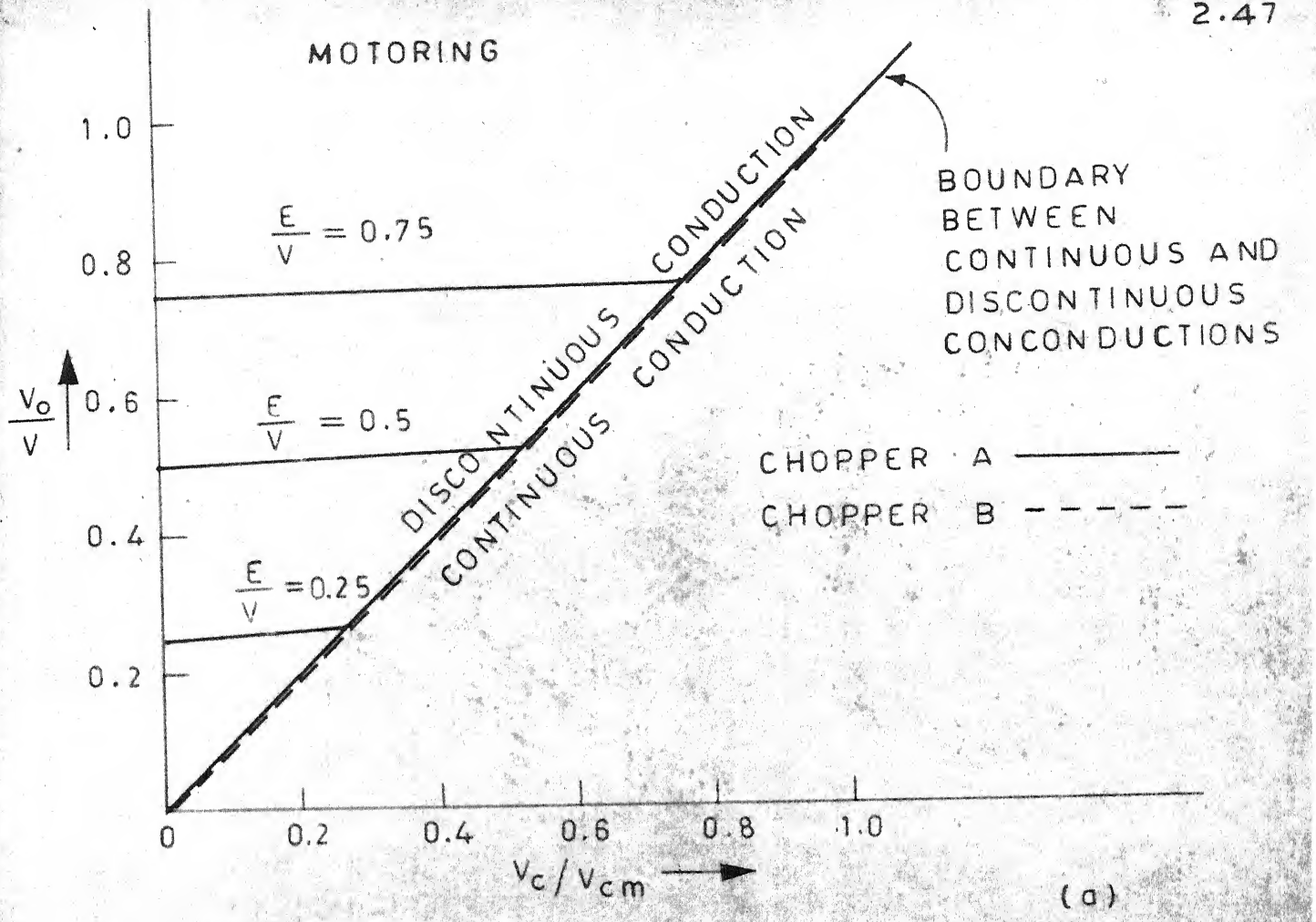
MOTORING
1.0
0.8
0.6
0.4
0.2
$\frac{V_o}{V}$
$\frac{E}{V} = 0.75$
$\frac{E}{V} = 0.5$
$\frac{E}{V} = 0.25$
DISCONTINUOUS CONDUCTION
CONTINUOUS CONDUCTION
BOUNDARY BETWEEN CONTINUOUS AND DISCONTINUOUS CONCONDUCTIONS
CHOPPER A
CHOPPER B
0
0.2
0.4
0.6
0.8
1.0
V_c / V_{cm}

(a)

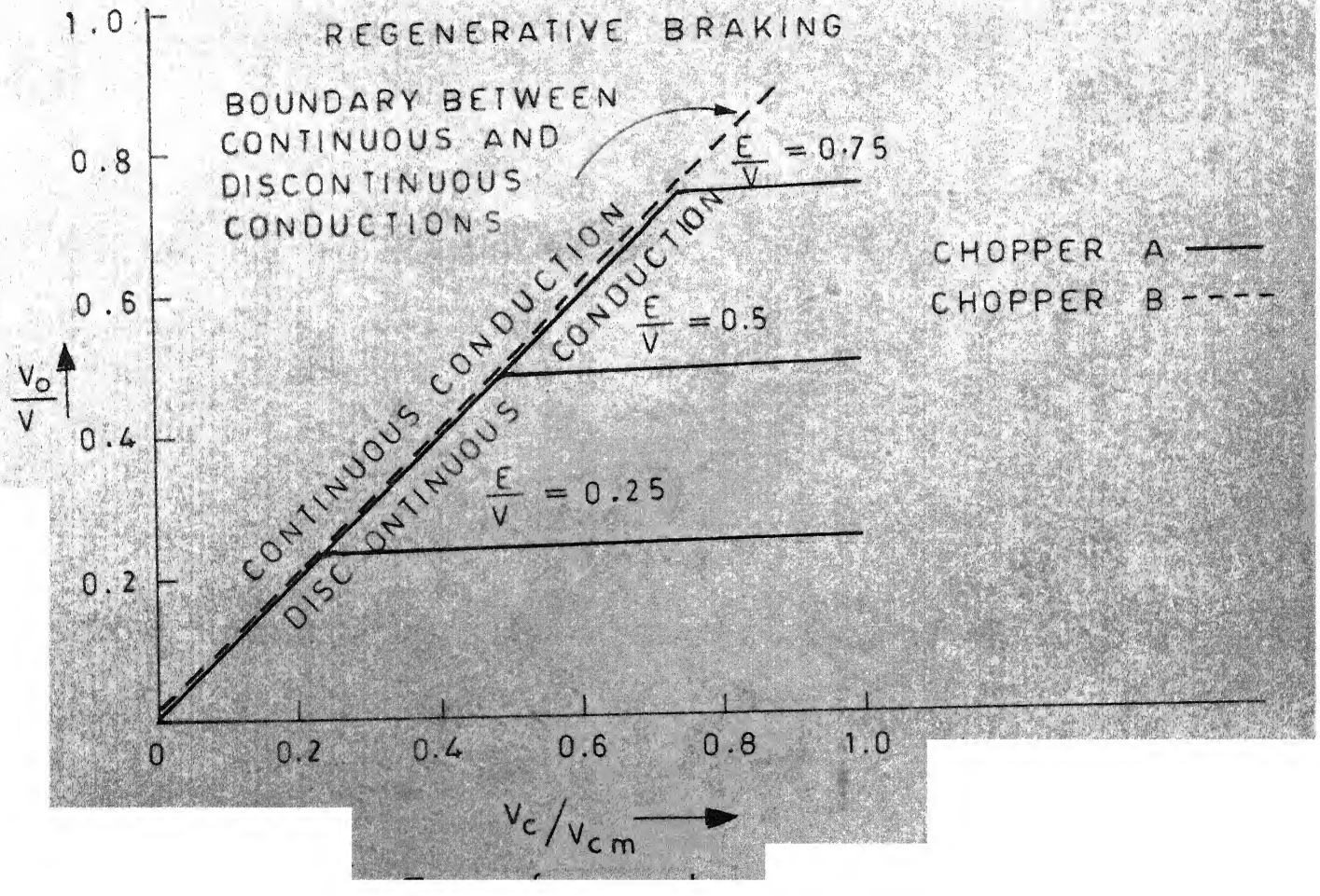
REGENERATIVE BRAKING
BOUNDARY BETWEEN CONTINUOUS AND DISCONTINUOUS CONDUCTIONS
1.0
0.8
0.6
0.4
0.2
$\frac{V_o}{V}$
$\frac{E}{V} = 0.75$
$\frac{E}{V} = 0.5$
$\frac{E}{V} = 0.25$
CONTINUOUS CONDUCTION
DISCONTINUOUS CONDUCTION
CHOPPER A
CHOPPER B
0
0.2
0.4
0.6
0.8
1.0
V_c / V_{cm}

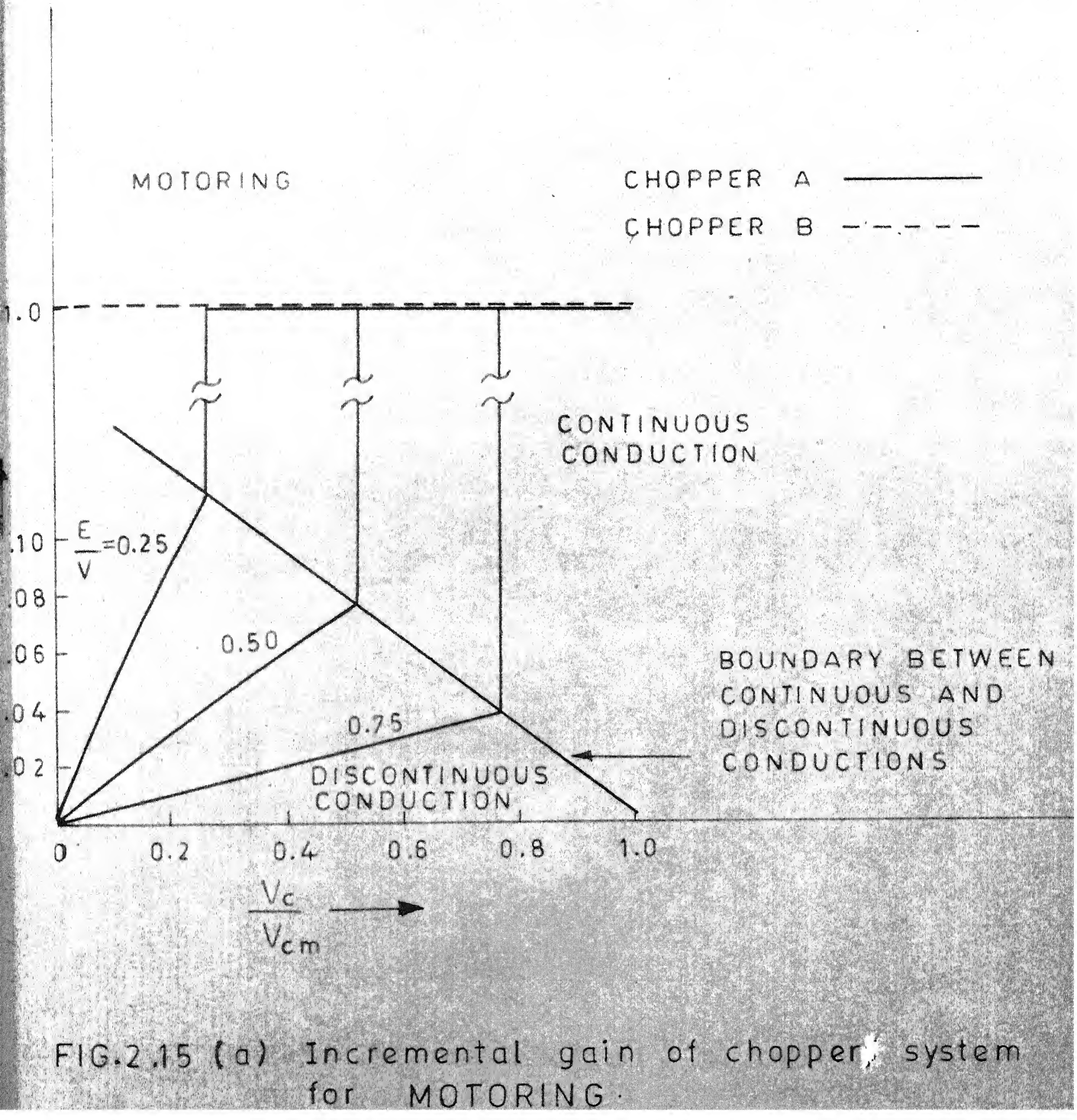

FIG.2.15 (a) Incremental gain of chopper system for MOTORING.

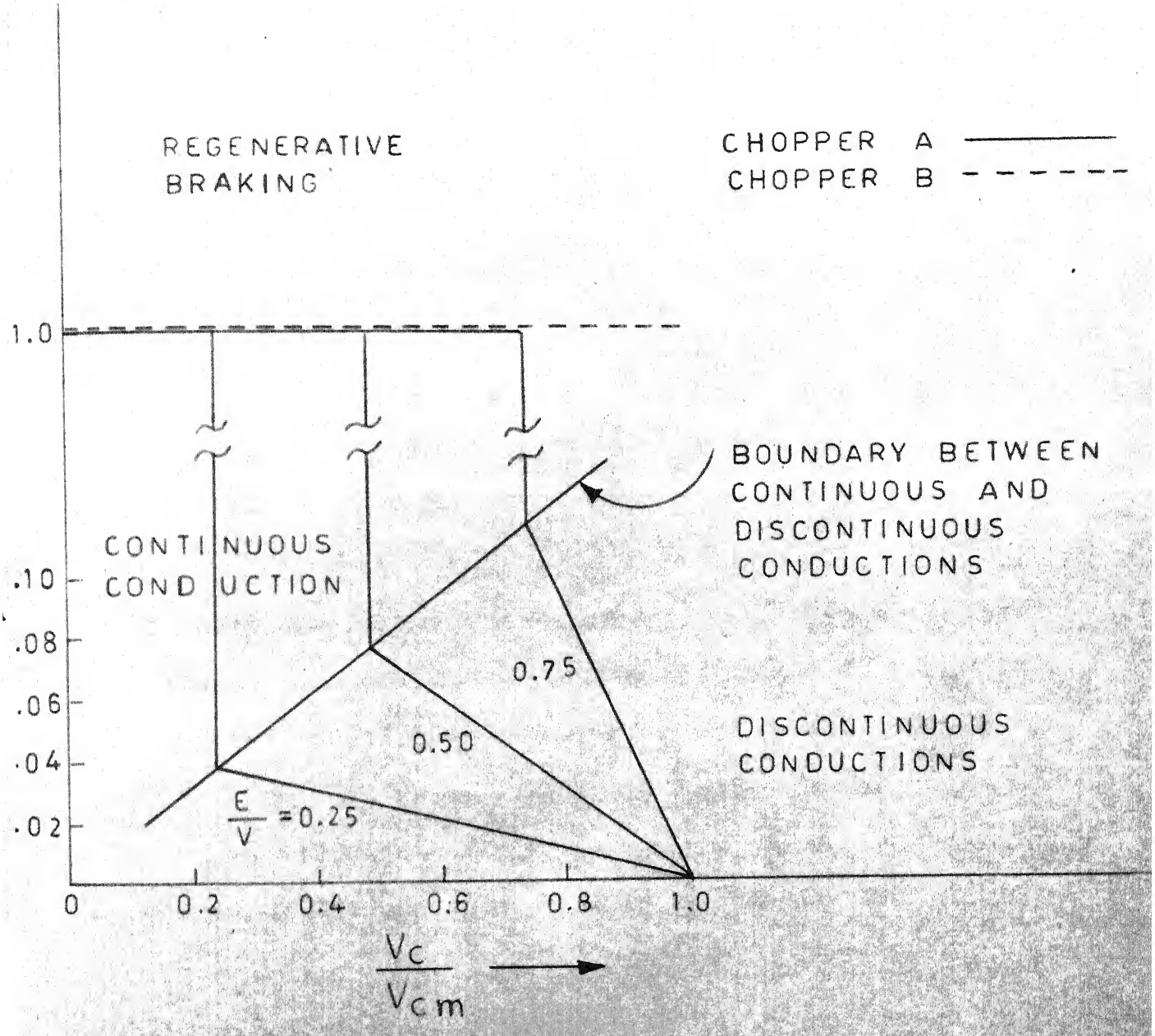

FIG.2.15(b) Incremental gain of chopper system for REGENERATIVE BRAKING.

sudden decrease in incremental gain when chopper A passes into discontinuous conduction region. This adversely affects the transient response of a closed loop chopper fed dc drive.

2.5 CONCLUSION:

From the above discussion, following conclusions can be drawn.

(1) Chopper A suffers fron the disadvantage of discontinuous conduction while this does not occur in case of chopper B.

(2) With chopper A, one can get regeneration down to zero speed at any value of δ ; while operating with chopper B, a continuous decrease in value of δ is required to get the regeneration down to zero speed.

(3) Change-over from one quadrant to another is achieved through control circuit for chopper B, while it requires a change of circuit for chopper A.

(4) Chopper B has got very high values of maximum CRF in comparison to chopper A.

(5) In case of chopper A, a small change in dc component of supply current results in a large change in p.u. speed; while the same cause is responsible for a comparatively

very small change in p.u. speed in case of chopper B.

(6) A change in p.u. speed does not affect the ratios of harmonics of supply current to dc component of supply current in case of chopper A operating in discontinuous conduction region. On the other hand, working with chopper B in the same range, the ratios of harmonics of supply current to dc component of supply current increase enormously with a small change in p.u. speed.

(7) More efficiency of regeneration is obtainable for all values of δ with chopper B compared to chopper A.

(8) When chopper A passes into discontinuous conduction region, its incremental gain goes down suddenly.

CHAPTER III

CHOPPER - DESIGN AND PERFORMANCE

On the basis of the comparison done in Chapter II, it was decided to go for two quadrant chopper or dual chopper. There are two kinds of dual choppers discussed in reference[1]. Both the circuits have been tried. Circuit with type 2 current commutation [1] could not be made to work. Another circuit with type 1 current commutation gave considerable problems after $\delta = 0.5$. In view of this a single quadrant chopper was selected and used for study of closed loop-speed control system. In this chapter steady-state and transient performance of the dc seperately excited motor fed by 1-quadrant chopper has also been presented.

3.1 DUAL CHOPPER WITH TYPE 2 CURRENT COMMUTATION:

The circuit of a dual chopper with type 2 current commutation is shown in Fig. 3.1(a). Following assumptions are made for analyzing the behaviour of this circuit.

(i) i_o remains constant throughout the commutation interval at the value I_{max}, and

(ii) Resistance R_1 is high enough to damp out

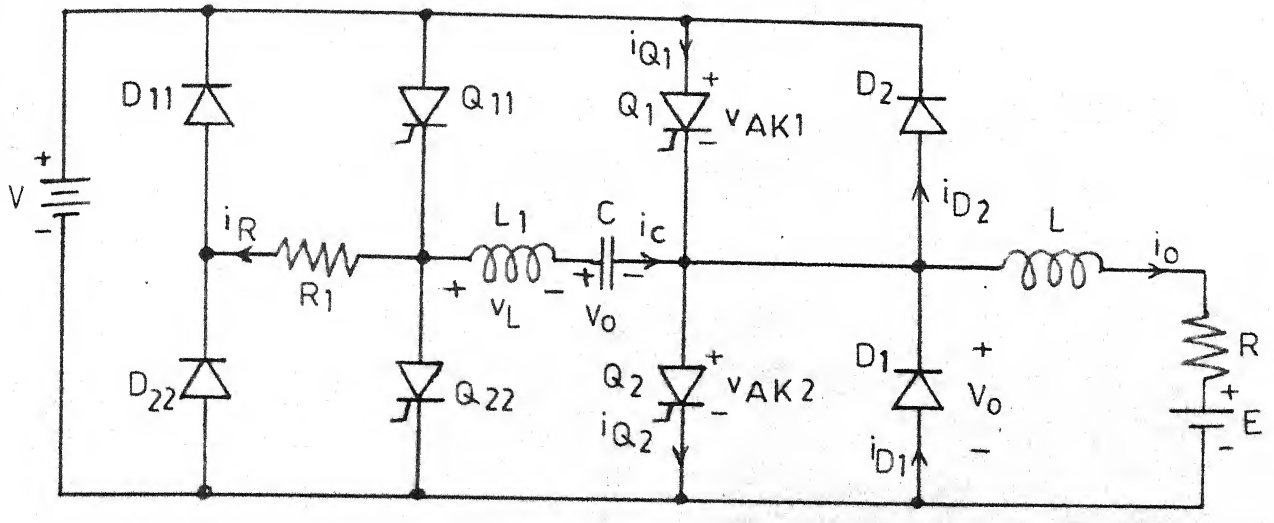

(a)

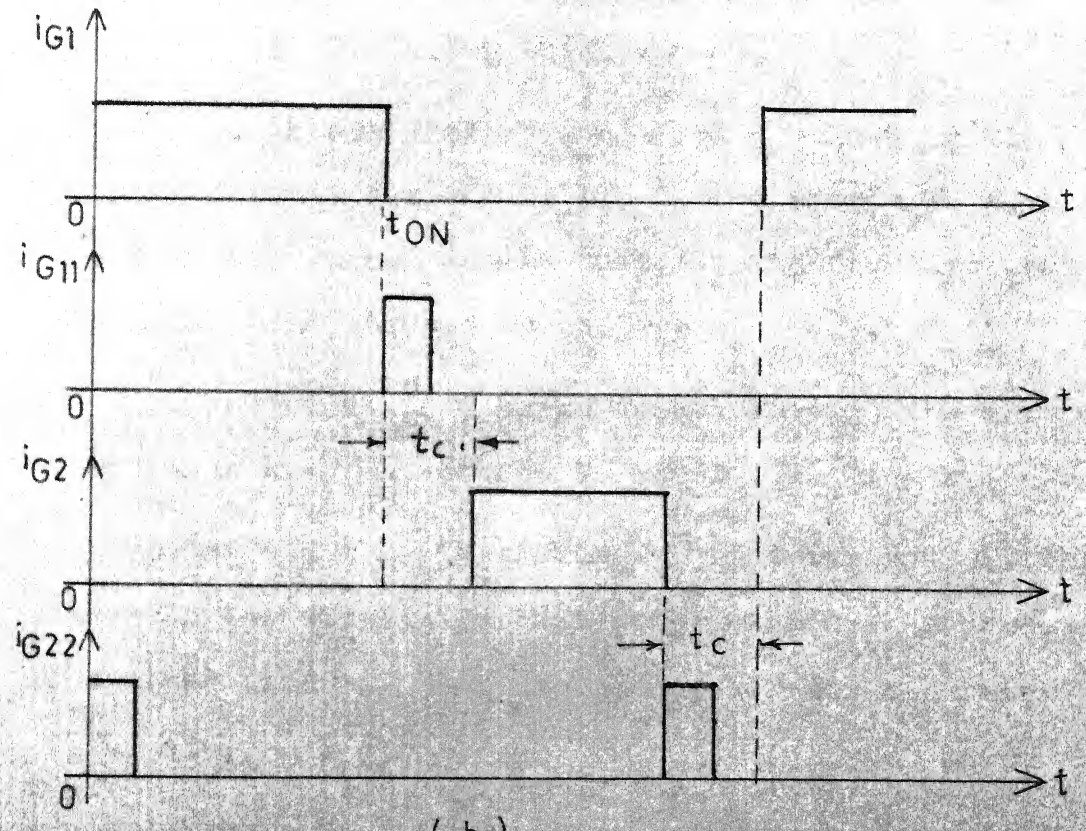

(b)

FIG.3.1 (a) Dual chopper with type 2 current commutation
(b) Firing sequence for (a)

oscillation in $R_1 L_1 C$ series circuit, consequently, i_R is small enough to be ignored during the commutation interval.

Operation of the circuit shown in Fig. 3.1(a) in first quadrant i.e. with i_o always positive is as follows:

1. At $t = 0$, thyristors Q_1 and Q_{22} are turned on, as a consequence of which, simultaneously:

a) i_o increases exponentially to the value I_{max}, during which $v_o = V$.

b) An oscillatory current i_c flows in the ringing circuit comprising L_1, C, and source V, with the result that, when i_c falls to zero, and Q_{22} turns off, capacitor C is charged to voltage $v_c = -2V$.

2. The capacitor charge decays through the circuit comprising R_1, D_{22}, source V, and D_2, leaving $v_c = -V$.

3. At $t = t_{oN}$, thyristor Q_{11} is turned on; i_c then flows in the ringing circuit comprising Q_{11}, source V and the load circuit, thus decreasing current i_{Q1} below the value of $i_o = I_{max}$.

4. When i_{Q1} is reduced to zero by the increasing value of i_c, that is, when $i_c = I_{o1} = I_{max}$, diode D_2 begins to conduct, and the forward voltage across D_2

results in a negative value of v_{AK1}, so that thyristor Q_1 is commutated.

5. When i_c again falls to the value I_{o1}, period I of the commutation interval is completed as illustrated in Fig. 3.2. Diode D_1 now tends to begin to conduct and period II of the commutation interval ensues, during which capacitor C is charged at constant current $i_c = I_{o1}$.

6. When capacitor C has been charged to voltage $v_c = V$, D_1 begins to conduct, and $v_o=0$. This instant marks the beginning of period III of the commutation interval. Simultaneously;

a) i_o decays exponentially through D_1.

b) An oscillatory current i_c flows in the ringing circuit comprising Q_{11}, source V, and the load circuit, for which now $v_o = 0$.

7. i_c falls to zero, and thyristor Q_{11} turns off, leaving $v_c > V$ at the end of period III of the commutation interval.

8. The capacitor charge decays through the circuit comprising R_1, D_{11}, source V, and D_1 to give $v_c = V$.

9. At $t = T$, when i_o has fallen to value I_{min}, Q_1 and Q_{22} are again turned on, and the resulting current

i_c in the ringing circuit produces a capacitor voltage $v_c = -V$, ready for the next commutation cycle.

The time variations of some of the principal circuit variables are shown in Fig. 3.2.

Operation of the dual chopper in the second quadrant of the V_o vs. I_o diagram with I_o always negative is as follows:

1. At t =0, thyristors Q_2 and Q_{11} are turned on, as a consequence of which simultaneously:

   a) i_o increases in a negative direction to the value I_{min}, during which $v_o = 0$.

   b) An oscillatory current i_c flows in the ringing circuit until, when $i_c = 0$, thyristor Q_{11} turns off, and $v_c = 2V$.

2. The capacitor charge decays through D_{11}, R_1, and D_1, leaving $v_c = V$.

3. At $t = t_{oN}$, thyristor Q_{22} is turned on; i_c then flows in a negative direction, thus decreasing the current i_{Q2} below the value of $-i_o = -I_{min}$.

4. When i_{Q2} is reduced to zero, that is when $i_c = I_{o1} = I_{min}$, diode D_1 begins to conduct, and the forward voltage across D_1 results in a negative value of v_{AK2}, so that thyristor Q_2 is commutated.

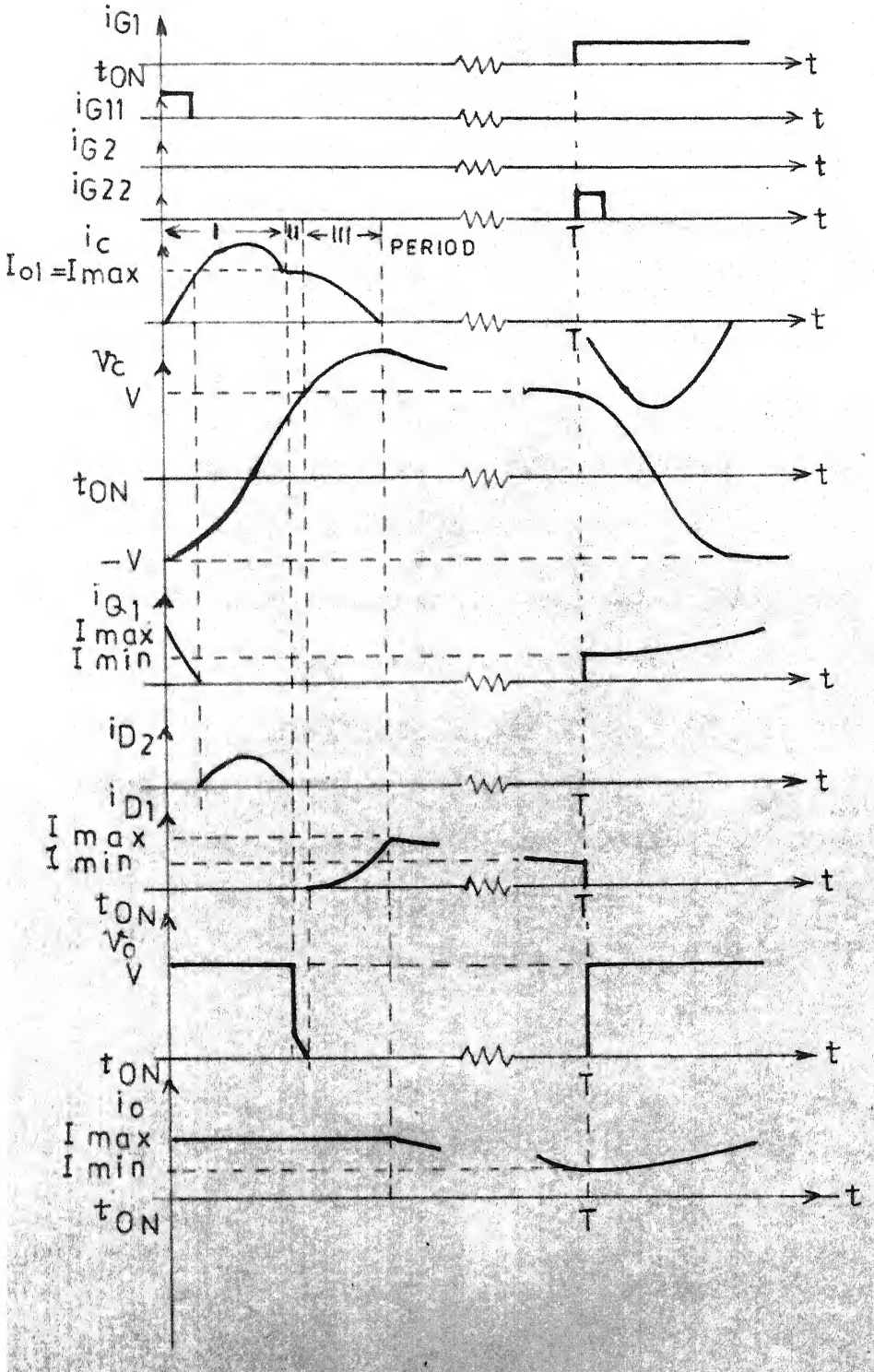

FIG. 3.2 Time variations of different variables during commutation process of dual chopper of Fig. 3.1 (a) — First quadrant operation

5. When i_c again becomes equal to I_{o1}, period I of the commutation interval is completed, as shown in Fig. 3.3. Diode D_2 now tends to begin to conduct, and period II of the commutation interval ensues during which capacitor C is charged at constant current $i_c = I_{o1}$.

6. When capacitor C has been charged to voltage $v_c = -V$, D_2 begins to conduct, and $v_o = V$. This instant marks the beginning of period III of the commutation interval, simultaneously;

a) i_o decays exponentially through D_2 and source V.

b) An oscillatory current i_c flows in the ringing circuit comprising Q_{22} and the load circuit, for which now $v_o = V$.

7. i_c falls to zero, and Q_{22} turns off, leaving $v_c = -V$ at the end of period III of the commutation interval.

8. The capacitor charge decays through D_2, source V, D_{22}, and R_1 to give $v_c = -V$.

9. At $t = T'$, when $i_o = I_{max}$, Q_2 and Q_{11} are again turned on, and the resulting current i_c in the ringing circuit produces a capacitor voltage $v_c = V$, ready for the next commutation cycle.

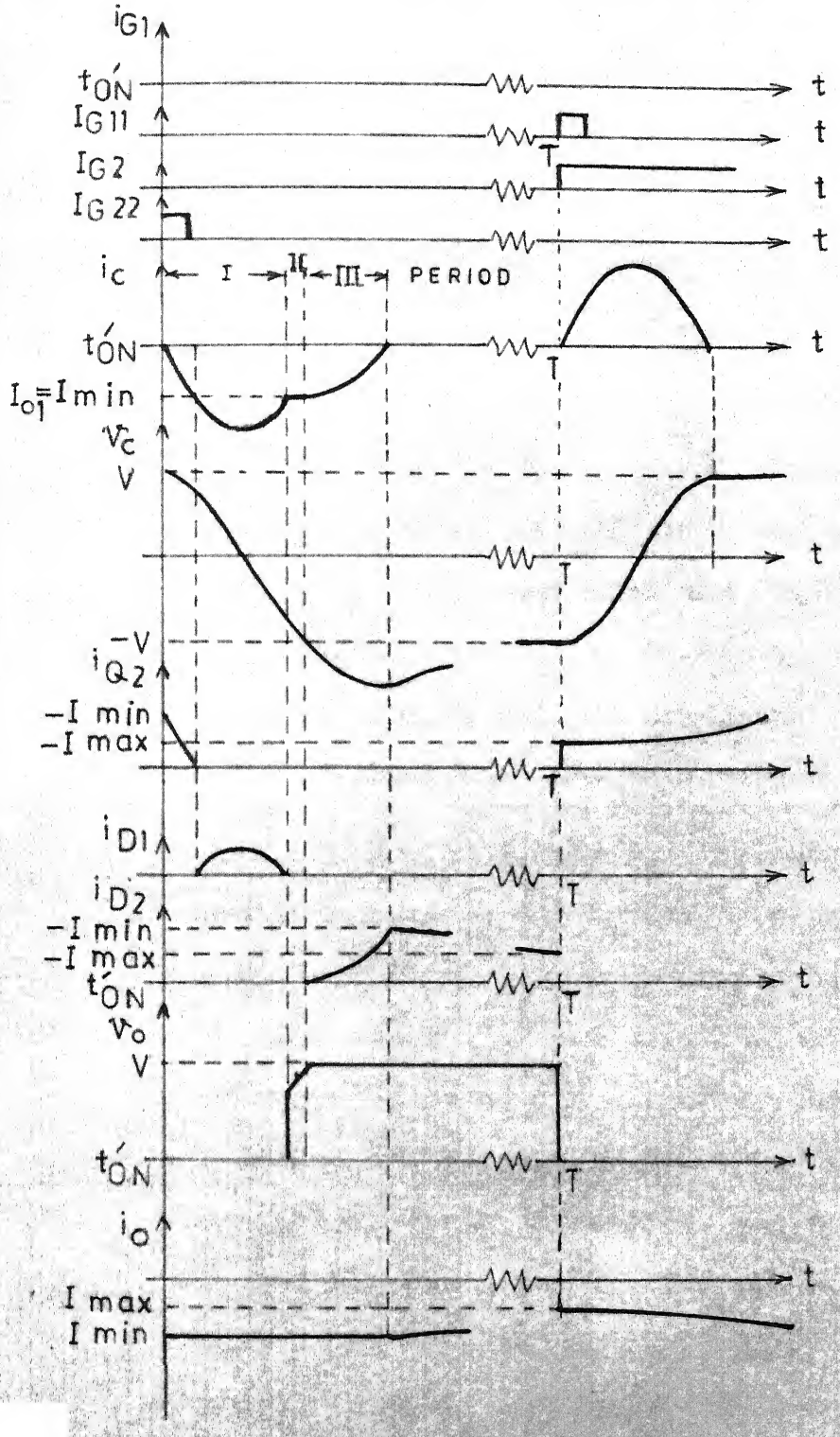

FIG. 3.3 Time variations of different variables during commutation process of dual chopper of Fig. 3.1(a) — Second quadrant operation

The time variations of some of the principal variables are shown in Fig. 3.3.

When current is in both the quadrants such that $I_{max} > 0$ and $I_{min} < 0$, in that case if at $t = 0$ thyristor Q_1 is turned on, then Q_{22} will already have been conducting at $t < 0$ in order to commutate Q_2. As a result $v_c = -V$, ready for the commutation cycle of Q_1. Conversely , when Q_2 is turned on, then Q_{11} will already have been conducting to commutate Q_1. As a consequence $v_c = +V$, ready for the commutation cycle of Q_2.

A gap of length t_c i.e. commutation interval is required between the end of the gating signal for one main thyristor and the beginning of the gating signal for the other to avoid possibility of short circuiting of source V by Q_1 and Q_2. Also when system is switched on, before any steady-state cycle of the circuit variables has been reached, it is necessary to have Q_1 and Q_{22} or Q_2 and Q_{11} turned on simultaneously in order that C may be charged, This can be achieved by allowing a small overlap of the gating signals, as shown in Fig. 3.1(b).

3.2 ANALYSIS OF THE COMMUTATION CIRCUIT FOR DUAL CHOPPER WITH TYPE 2 CURRENT COMMUTATION:

The analysis of the commutation circuit of Fig. 3.1(a)

has been carried out using the assumptions made in the previous section.

At t=0, Q_1 and Q_{22} are turned on. Hence for the circuit V, Q_1, C, L_1 and Q_{22}

$$V = \frac{1}{C}\int i_c\,dt + L_1\,\frac{di_c}{dt} \qquad (3.1)$$

The initial conditions for the above eqn. are

$$i_c = 0\,, \qquad \text{and} \qquad (3.2)$$

$$\frac{di_c}{dt} = \frac{V}{L_1} \quad \text{at} \quad t = 0 \qquad (3.3)$$

From above eqns.

$$i_c = -\frac{V}{\sqrt{L_1/C}}\,\sin\frac{1}{\sqrt{L_1C}}\,t \qquad (3.4)$$

$$v_L = -V\cos\frac{1}{\sqrt{L_1C}}\,t \qquad (3.5)$$

$$v_c = -V\left(1-\cos\frac{1}{\sqrt{L_1C}}\,t\right) \qquad (3.6)$$

Q_{22} will be turned off at $t = \pi\sqrt{L_1C}$. When capacitor is charged with 2V, i_c starts flowing in the path comprising of D_2, V, R_1, L_1 and C. It continues to flow until capacitor voltage comes back to V. Following are the eqns. for i_c, V_L and V_C.

$$i_c = e^{-\varepsilon t} \times \frac{V}{2L_1\sqrt{\varepsilon^2 - w_o^2}}\left[e^{\sqrt{\varepsilon^2-w_o^2}\,t} - e^{-\sqrt{\varepsilon^2-w_o^2}\,t}\right] \qquad (3.7)$$

$$v_L = V e^{-\varepsilon t} \left[e^{\sqrt{\varepsilon^2 - w_o^2}\, t} - e^{-\sqrt{\varepsilon^2 - w_o^2}\, t} \right] \left[1 - \frac{\varepsilon}{\sqrt{\varepsilon^2 - w_o^2}} \right] \quad (3.8)$$

$$v_c = -V - v_L - R_1 i_c \quad (3.9)$$

where

$$\varepsilon = \frac{R_1}{2L_1} \text{ and } w_o = \frac{1}{\sqrt{L_1 C}}$$

Assuming a new time scale i.e. t = 0 when the commutating cycle is initiated by the application of the gating signal to thyristor Q_{11}. Thus for the circuit mesh comprising C, Q_1, Q_{11} and L_1

$$-V + \frac{1}{C} \int i_c \, dt + L_1 \frac{di_c}{dt} = 0 \quad (3.10)$$

The initial conditions required for the solution of (3.10) are

$i_c = 0$ and $v_c = -V$ at $t = 0$.

So, from eqn. (3.10)

$$i_c = \frac{V}{\sqrt{L_1/C}} \sin \frac{1}{\sqrt{L_1 C}} t \quad (3.11)$$

$$v_L = V \cos \frac{1}{\sqrt{L_1 C}} t \quad (3.12)$$

$$v_c = -V \cos \frac{1}{\sqrt{L_1 C}} \quad (3.13)$$

When i_c becomes equal to the current flowing through

Q_1 i.e., I_{o1}, $i_{Q1} = 0$, and diode D_2 starts conducting, so that

$$i_{D2} = i_c - I_{o1} \quad A \qquad (3.14)$$

Also $$v_{AK1} = -v_{D2} \quad V \qquad (3.15)$$

and Q_1 is commutated.

The time at which Q_1 goes off is given by

$$t_1 = \frac{1}{w_r} \sin^{-1} \frac{w_r L_1 I_{o1}}{V} \quad S \qquad (3.16)$$

where $w_r = \frac{1}{\sqrt{L_1 C}}$

Assuming that at $t = t_2$, i_c has passed its positive maximum and fallen to the value I_{o1}. Thus

$$t_2 = \frac{\pi}{w_r} - t_1 \quad S \qquad (3.17)$$

At t_2, diode D_1 tends to begin to conduct. Since $v_c < V$, capacitor C is charged at constant current $i_c = I_{o1}$ until $v_c = V$. During this charging interval

$$v_o = V - v_c \quad V \qquad (3.18)$$

Constant current charging of capacitor continues for the period t_1' given by

$$t_1' = \frac{CV}{I_{o1}} (1 - \cos w_r t_2) \quad S \qquad (3.19)$$

At this instant v_o becomes zero, and diode D_1 begins

to conduct; $i_c = I_{o1}$ now becomes the initial current in an oscillatory circuit comprising C, L_1, D_1, Q_{11} and source V. The current in this circuit may be considered to flow in the reverse direction through D_1, that is

$$i_{D1} = i_o - i_c > 0 \qquad A \qquad (3.20)$$

i_c is given by the following eqn. for this interval

$$i_c = I_{o1} \cos w_r t'' \qquad A \qquad (3.21)$$

i_c becomes zero at $t_1'' = \frac{\pi}{2w_r}$ S

The maximum capacitor voltage is given by

$$v_{cmax} = V + \frac{I_{o1}}{w_r C} \qquad (3.22)$$

This capacitor voltage then decays through R_1 to $v_c = V$.

The length of the entire commutation interval is

$$t_c = t_2 + t_1' + t_1'' \qquad S \qquad (3.23)$$

The turn-off time available for thyristor Q_1 is

$$t_q = \frac{\pi}{w_r} - \frac{2}{w_r} \sin^{-1} \frac{w_r L_1 I_{o1}}{V} \quad S \quad (3.24)$$

3.3 DESIGN OF THE CURRENT COMMUTATION CIRCUIT:

The commutation circuit design is carried out in terms of a dimensionless quantity [1]

$$x = \frac{V}{w_r L_1 I_{o1}} = \frac{V}{(L_1/C)^2 I_{o1}} \qquad (3.25)$$

Typically for a current commutated converter $1.4 < x < 3.0$. That value of x must be chosen which yields circuit parameters giving acceptable values of

1. Maximum capacitor voltage v_{cmax}
2. Peak commutating thyristor current I_{peak}
3. Charging circuit losses in resistance R_1.

A function has been defined from (3.24) and (3.25)

$$G(x) = w_r t_q = (\pi - 2 \sin^{-1} \frac{1}{x}) \text{ rad} \qquad (3.26)$$

The above function has been employed for finding L_1 and C. Following expressions give values of L_1 and C.

$$L_1 = \frac{V(t_{off} + \Delta t)}{x\, G(x) I_{o1}} \quad \text{H} \qquad (3.28)$$

$$C = \frac{x\, I_{o1}\, (t_{off} + \Delta t)}{G(x) V} \quad \text{F} \qquad (3.29)$$

The value of R_1 must be chosen such that

$$T \geq 3 R_1 C \quad \text{S} \qquad (3.30)$$

since, if this were not the ease, there would be insufficient time for the capacitor voltage to fall from v_{cmax} to V before another commutation cycle was initiated.

The average power dissipated in resistor R_1 is given by

$$P_R = \frac{1}{2} \frac{CV^2}{x^2 T} \quad W \qquad (3.31)$$

Taking $(t_{off} + \Delta t) = 50$ μs, design for commutation circuit is carried out for three different values of x. Different parameters are listed in the following table.

Table 3.1

x	L_1 mH	C μf	R_1 ohms	V_{cmax} V	Losses in R_1 W	I_{peak} A
1.5	1.7	0.527	125	367.7	2.834	3.87
2.0	1.01	0.564	100	330	1.706	5.2
2.5	0.73	0.637	75	308	1.233	6.499

From the voltage and current considerations, values for x = 2.0 has been chosen. Different waveforms for commutation interval are shown in Fig. 3.4 for L_1 = 1 mH and C = 0.6 μf. Details of thyristors are given in appendix B.

3.4 CONTROL CIRCUIT FOR DUAL CHOPPER WITH TYPE 2 CURRENT COMMUTATION:

Block diagram of the firing circuit for dual chopper of Fig. 3.1(a) is shown in Fig. 3.5. The basic waveforms are shown in Fig. 3.6. The waveform A is generated using astable circuit which has off time equal

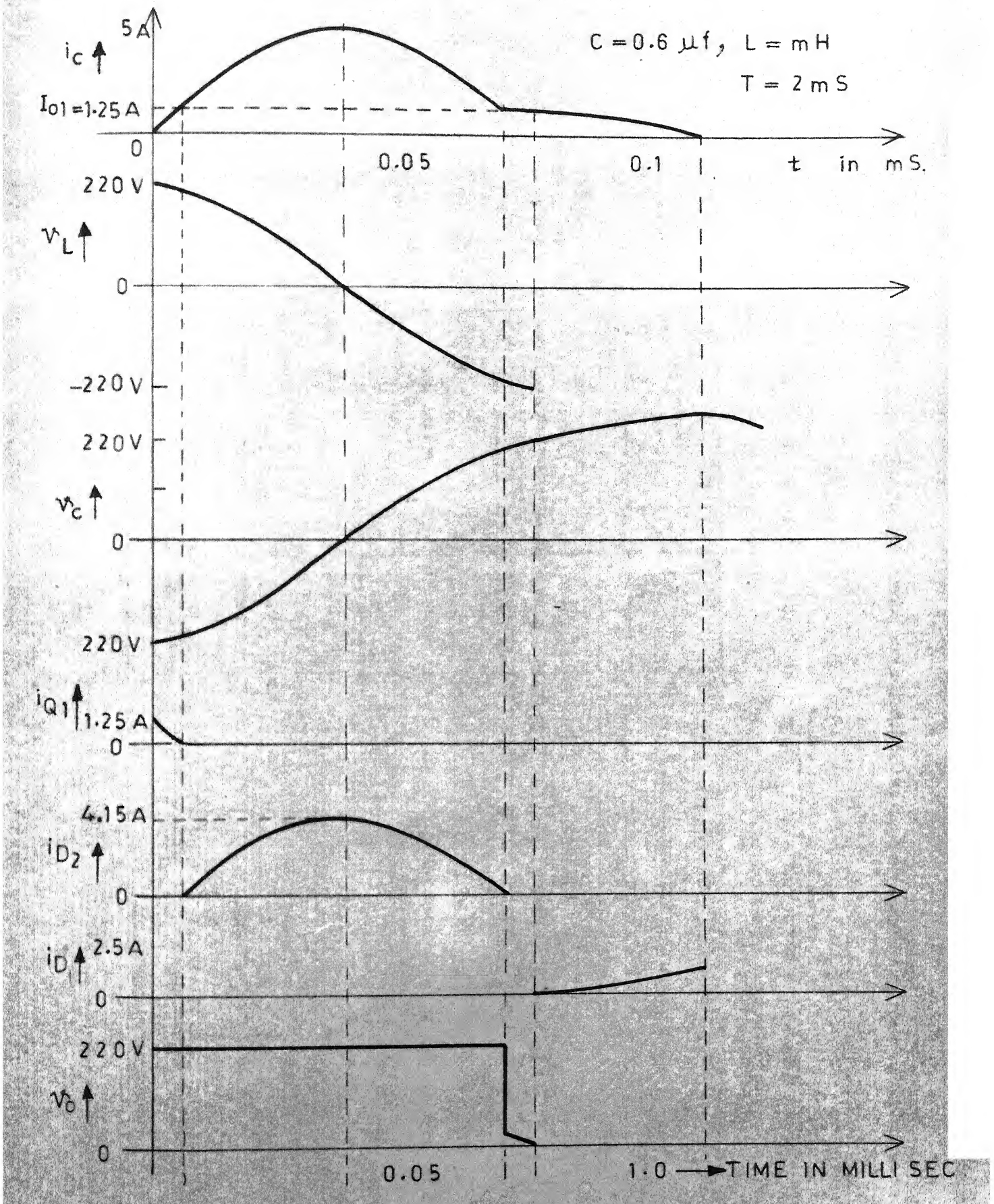

FIG.3.4 Waveforms for commutation interval of dual chopper of Fig. 3.1(a)

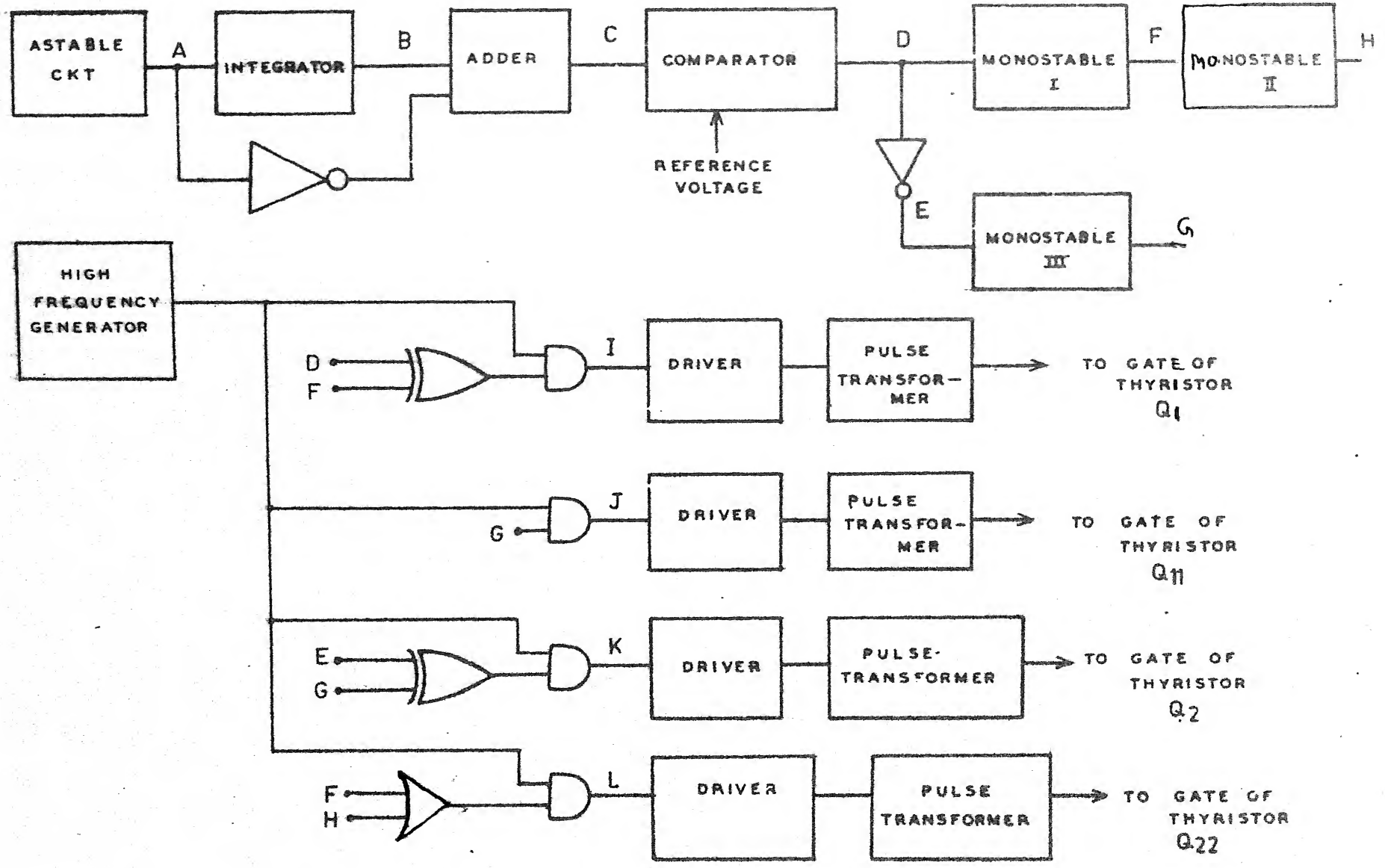

FIG.3.5 BLOCK DIAGRAM OF FIRING SCHEME FOR DUAL CHOPPER OF FIG. 3.1(a)

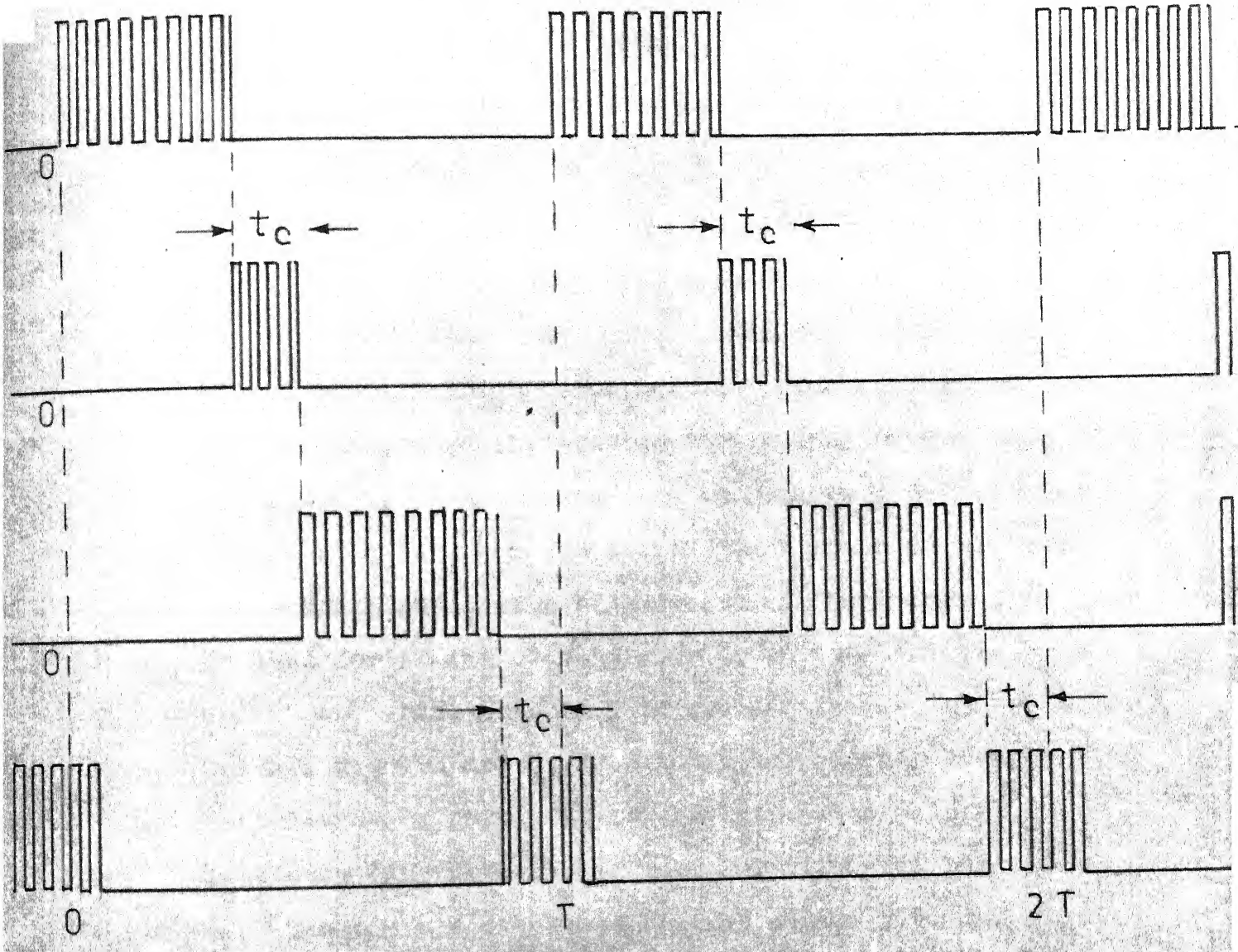

FIG. 3.6 Waveforms at different stages of FIG. 3.5

to t_c. This is integrated to get a waveform B.

A and B are added together for obtaining waveform C which is compared with a reference voltage to generate D. E is $\bar{D}$. F is generated by monostable I which is set for the rising edge of D. G is the output of the monostable III which is triggered by the rising edge of E. Monostable II, set for the falling edge of F, generates H. A high frequency is generated for carrier frequency gating. D and F are ored exclusively and the output, gated with high frequency (waveform I), is used for firing of thyristor Q_1 of Fig. 3.1(a). G is anded with high frequency to get J which is the triggering pulse for thyristor Q_{11}. E and G are passed through an exclusive - or gate and its output, gated with high frequency (waveform K), is used for firing of thyristor Q_2. F and H are processed through an AND gate and the result is gated with high frequency (waveform L). L is used for the triggering of thyristor Q_{22}.

3.4.1 Realization:

The circuit diagram for above firing scheme is shown in Fig. 3.7. Op-amps and C-MOS gates are used to have the system compatibility. NE 555 is used for

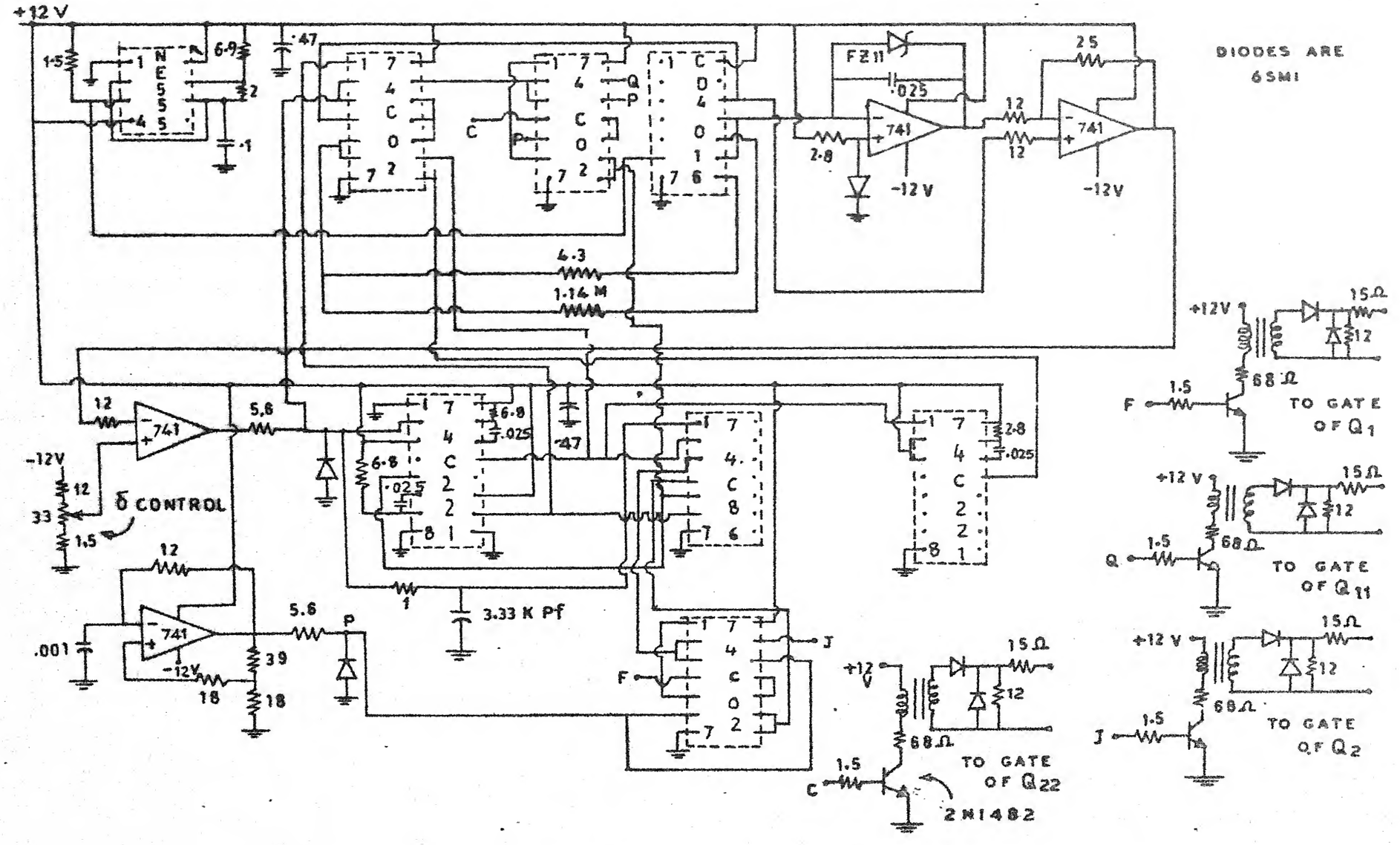

FIG.3.7 Firing circuit for Fig. 3.1(a) (Resistances are in kΩ, Capacitances are in μf, unless specified)

the astable circuit to generate a signal of period 2 ms with off time equal to 0.2 ms.

An analogue switch (IC CD 4016) is used with op-amp constant current integrator to provide different values of resistors in charging and discharging paths of capacitor in integrator. NOR gates (IC 74C02) are used as inverters and adder because of non-availability of HEX inter (IC74C06). Op-amps (IC741) are used for comparing and adding two analogue signals. Monostables (IC74C221) are employed for the generation of pluses of desired magnitudes. An op-amp astable circuit is used for the generation of high frequency of magnitude 10 KHz for the purpose of carrier frequency gating. Exclusive OR-gates (IC74C86) are used for the extraction of required signals.

3.5 EXPERIMENTAL VERIFICATION OF DUAL CHOPPER WITH TYPE 2 CURRENT COMMUTATION:

Dual chopper of Fig. 3.1(a) was built but it could not be made to work because of the following reasons.

1. Commutation problems.
2. lossy capacitors
3. inherent complexity in the functioning of the circuit i.e. the use of the same commutation circuit for both the main thyristors Q_1 and Q_2.

4. operation at high frequency i.e. 500 Hz.

It was decided to go for a circuit with type 1 current commutation [1] because it uses separate commutation circuitry for both the main thyristors. Circuit for motoring and circuit for regeneration can be tested separately before combining them together for dual chopper.

3.6 DUAL CHOPPER WITH TYPE 1 CURRENT COMMUTATION:

The circuit of dual chopper with type 1 current commutation is shown in Fig. 3.8(a). Its firing sequence is shown in Fig. 3.8(b). The sequence of operation of first quadrant is as follows:

1. By closing switch SW, the system is connected to the source V and capacitor C_1 is charged upto $v_{c1}=V$ volts via resistor R_1.

2. After full charging of capacitor C_1, at t = 0, thyristor Q_1 is turned on and load current i_o increases exponentially from zero to I_{max}.

3. At $t = t_{oN}$, thyristor Q_{11} is turned on, initiating the commutation cycle and an oscillatory current flows in the ringing circuit comprising C_1, L_1 and Q_{11}; i_c is initially negative.

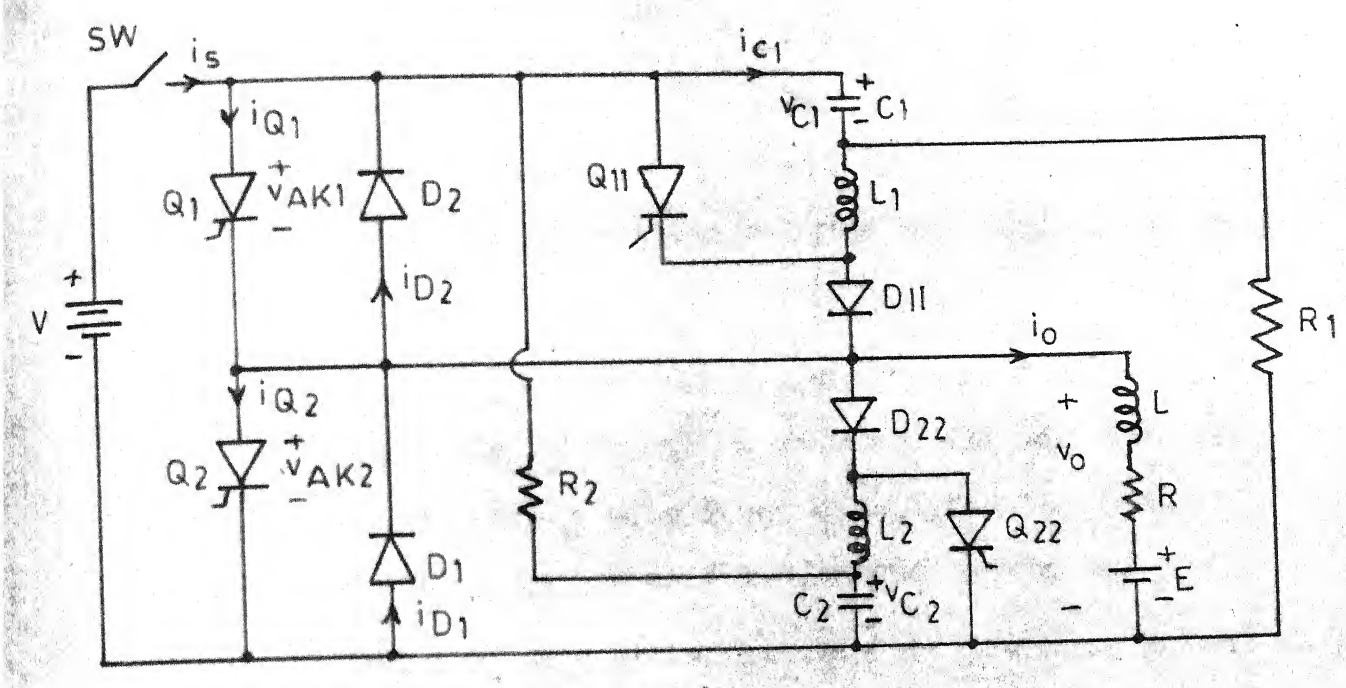

(a)

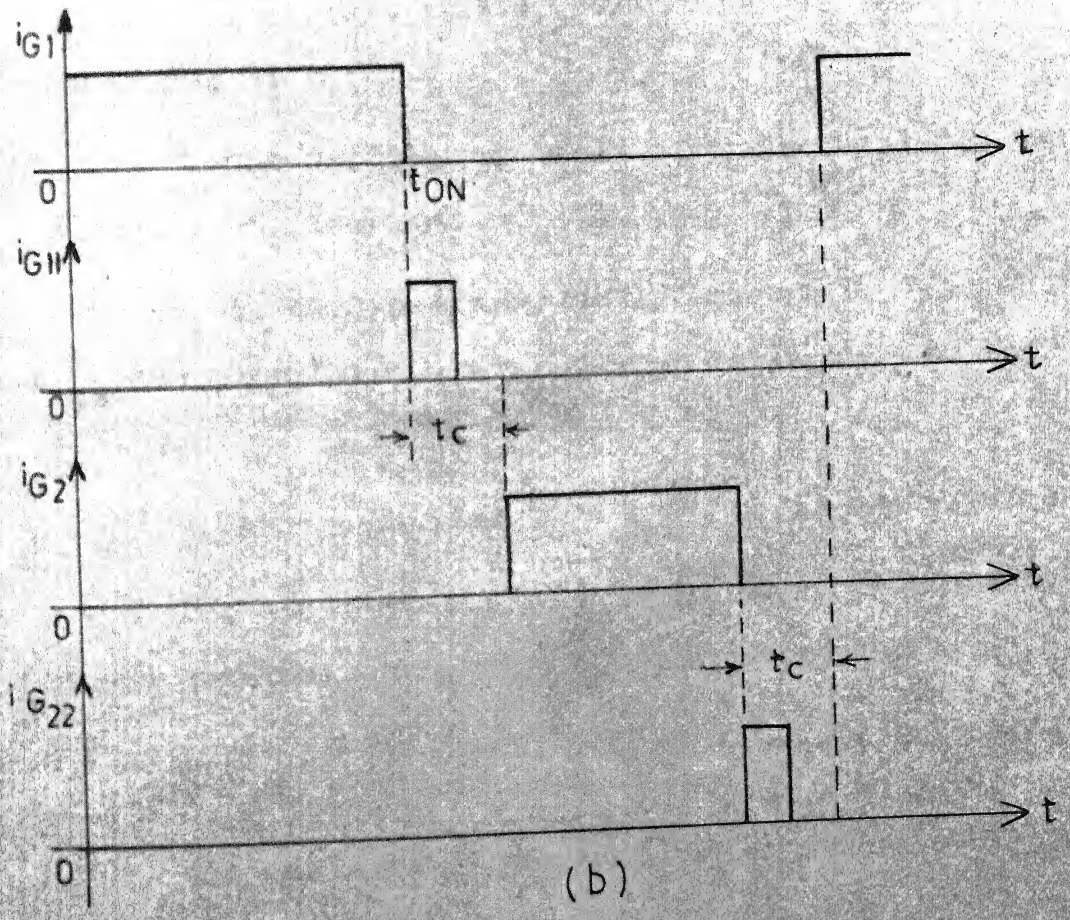

(b)

FIG.3.8 (a) Dual chopper for type 1 current commutation.
(b) Firing sequence for (a).

4. When i_c becomes positive, diode D_{11} conducts, Q_{11} turns off, and since i_o is assumed constant, i_c reduces i_{Q1}.

5. When i_{Q1} is reduced to zero by the increasing value of i_c, diode D_2 begins to conduct, and the forward voltage drop across this diode commutates thyristor Q_1. Current $i_c - I_{max}$ then flows through diode D_2.

6. After i_c has passed its maximum positive value and again become less than I_{max}, diode D_1 conducts. A new oscillatory circuit exists, comprising C_1, L_1, D_{11}, D_1 and source V.

7. The oscillatory cycle of i_c is completed and i_c becomes zero, leaving $v_{c1} > V$.

8. i_o decays exponentially through D_1 from the value I_{max} and simultaneously v_{c1} decays through R_1 to the value $v_{c1} = V$.

9. At $t = T$, when $i_o = I_{min}$, Q_1 is again turned on.

The above explanation can be applied for the second quadrant operation of dual chopper of Fig. 3.8(a).

3.7 ANALYSIS OF THE COMMUTATION CIRCUIT FOR DUAL CHOPPER WITH TYPE 1 CURRENT COMMUTATION:

The analysis of the commutation circuit for the dual chopper shown in Fig. 3.8(a) is done employing the

assumptions made in section 3.1. A time scale is chosen, such that t = 0 when Q_{11} is triggered. i_c and v_c are given by

$$i_c = - \frac{V}{w_r L_1} \sin w_r t \qquad (3.32)$$

$$v_c = V \cos w_r t \qquad (3.33)$$

At $t = \frac{\pi}{w_r}$, i_c reverses and Q_{11} goes off. i_c now, flows through Q_1 so that

$$i_{Q1} = I_{max} - i_c \; ; \; t > \frac{\pi}{w_r} \qquad (3.34)$$

At $t = t_1$, $i_c = I_{max}$, $i_{Q1} = 0$ and diode D_2 begins to conduct, so that

$$i_{D2} = i_c - I_{max} = i_c - I_{o1} \qquad (3.35)$$

Also

$$V_{AK1} = -v_{D2} \quad V \qquad (3.36)$$

and Q_1 is commutated, t_1 is given by

$$t_1 = \frac{\pi}{w_r} + \frac{1}{w_r} \sin^{-1} \frac{w_r L_1 I_{o1}}{V} \quad S \qquad (3.37)$$

At $t = t_2$, i_c has passed its positive maximum and fallen to the value I_{o1}. Thus

$$t_2 = \frac{3\pi}{w_r} - t_1 \quad S \qquad (3.38)$$

At this instant, diode D_1 tends to begin to conduct. Since $v_{c1} < V$, for a short interval capacitor C_1 is charged at constant current $i_c = I_{o1}$, until $V_{c1} = V$. During this interval

$$v_o = V - v_c \qquad V \tag{3.39}$$

The time for which constant current charging of capacitor lasts is given by

$$t_1' = \frac{CV}{I_{o1}} (1 - \cos w_r t_2) \qquad S \tag{3.40}$$

At this instant v_o becomes zero, and diode D_1 begins to conduct. After this i_c falls as per the following eqn.

$$i_c = I_{o1} \cos w_r t'' \tag{3.41}$$

At $t'' = t_1'' = \frac{\pi}{2w_r}$, i_c becomes zero.

The length of the entire commutation interval is

$$t_c = t_2 + t_1' + t_1'' \qquad S \tag{3.42}$$

The turn off time available for the thyristor is

$$t_q = \frac{\pi}{w_r} - \frac{2}{w_r} \sin^{-1} \frac{w_r L_1 I_{o1}}{V} \qquad S \tag{3.43}$$

The time variations of different current and voltages during commutation process are shown in Fig. 3.9. Design of commutation circuit is same as discussed in section 3.3.

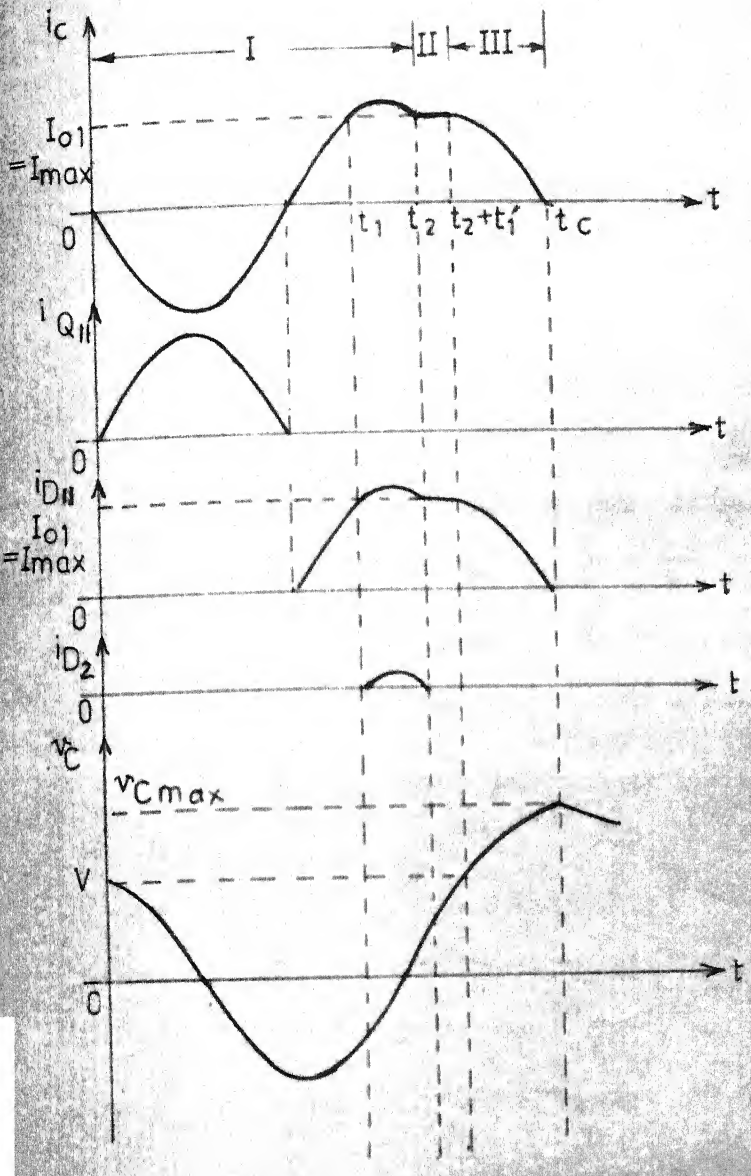

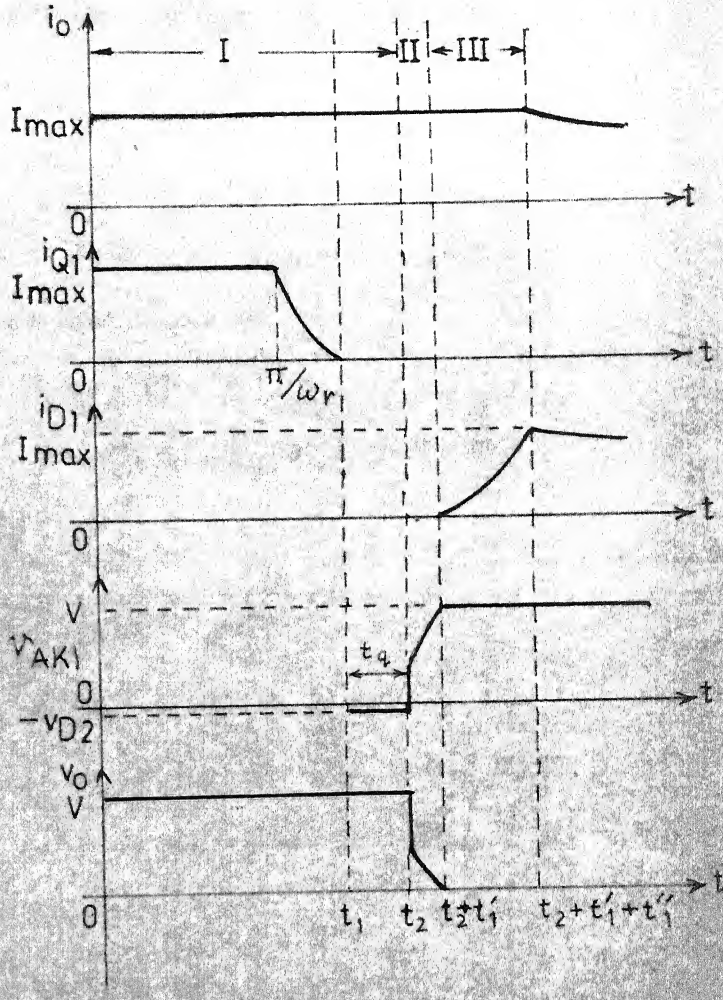

FIG.3.9 Waveforms during commutation process of dual chopper of Fig.3.8(a)

3.7 FIRING CIRCUIT FOR DUAL CHOPPER WITH TYPE 1 CURRENT COMMUTATION:

The firing circuit for dual chopper of Fig. 3.8(a) is obtained by eliminating waveform H from Fig. 3.6. The circuit diagram of firing circuit is shown in Fig. 3.10(a). Waveforms at different stages of firing circuit are shown in Fig. 3.10(b). A RC circuit is used for the compensation of delay caused by monostable before feeding signals to exclusive OR gate.

3.8 EXPERIMENTAL VERIFICATION AND SYSTEM PERFORMANCE OF DUAL CHOPPER WITH TYPE 1 CURRENT COMMUTATION:

The circuit of dual chopper of Fig. 3.8(a) was built and tested at 100 Hz. The values of different components are given in appendix C. Oil filled capacitors are used for commutation purposes.

Photographs of firing pulses for thyristors Q_1, Q_{11} and Q_2 are shown in Fig. 3.11. Two photographs of output voltage of dual chopper and armature current for small δ are shown in Fig. 3.12. Fig. 3.12.1 shows the behaviour of system at no-load. Fig. 3.12.2 depicts operation of the system in regeneration.

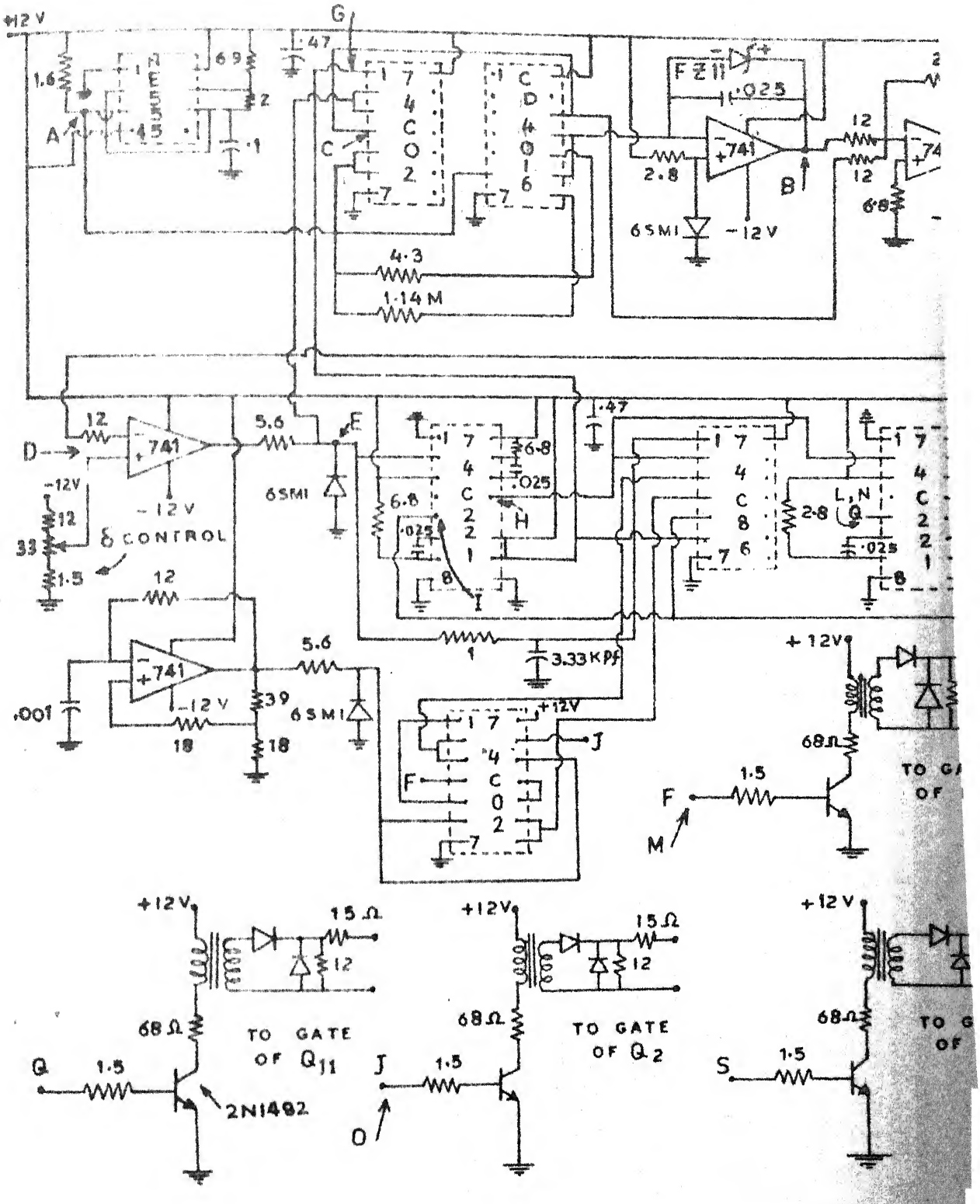

FIG. 3.10 (a) Firing circuit of Fig. 3.8(a) (Resistances are Capacitances are in μf, unless specified)

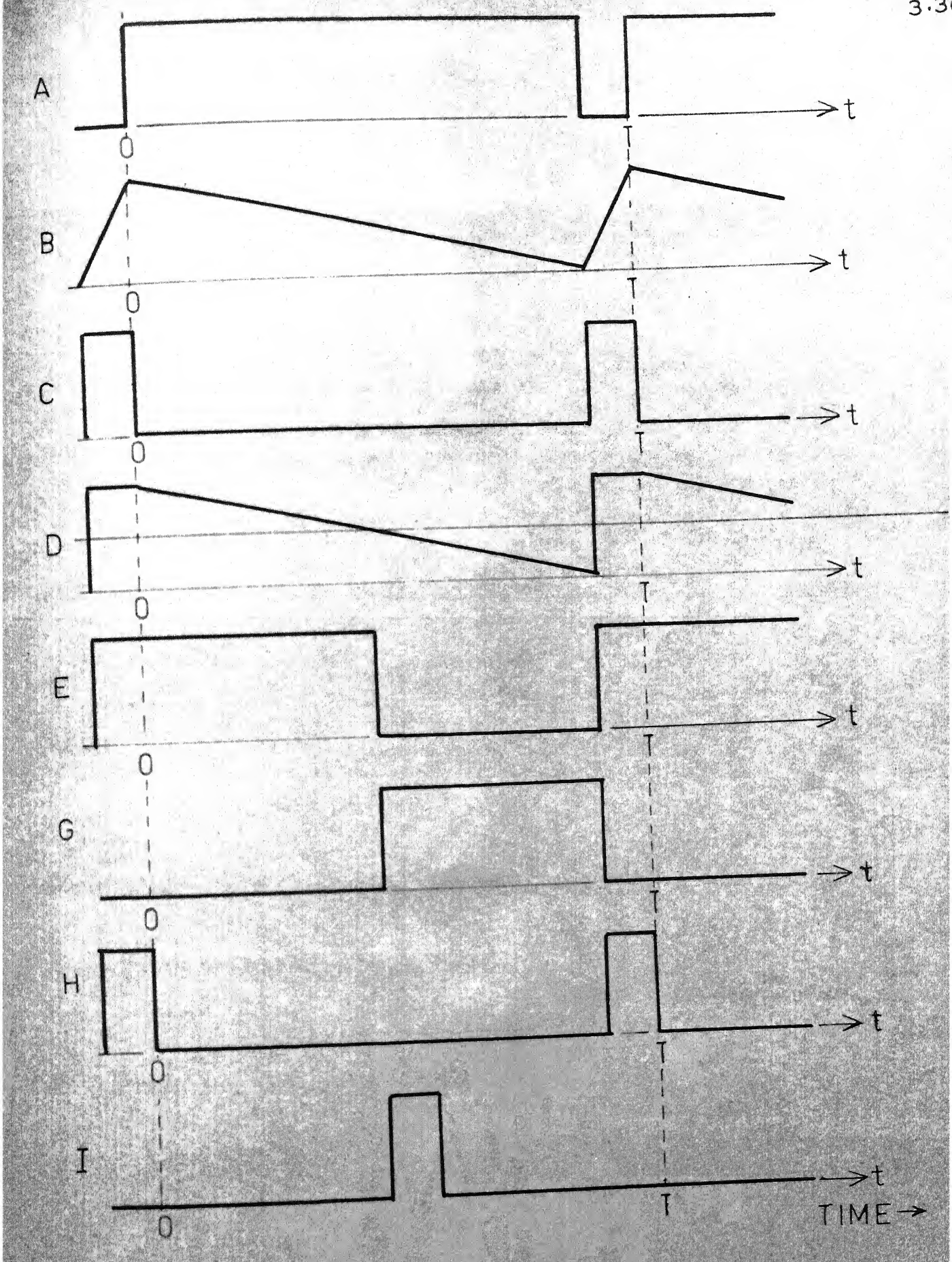

FIG. 3.10 (Contd.)

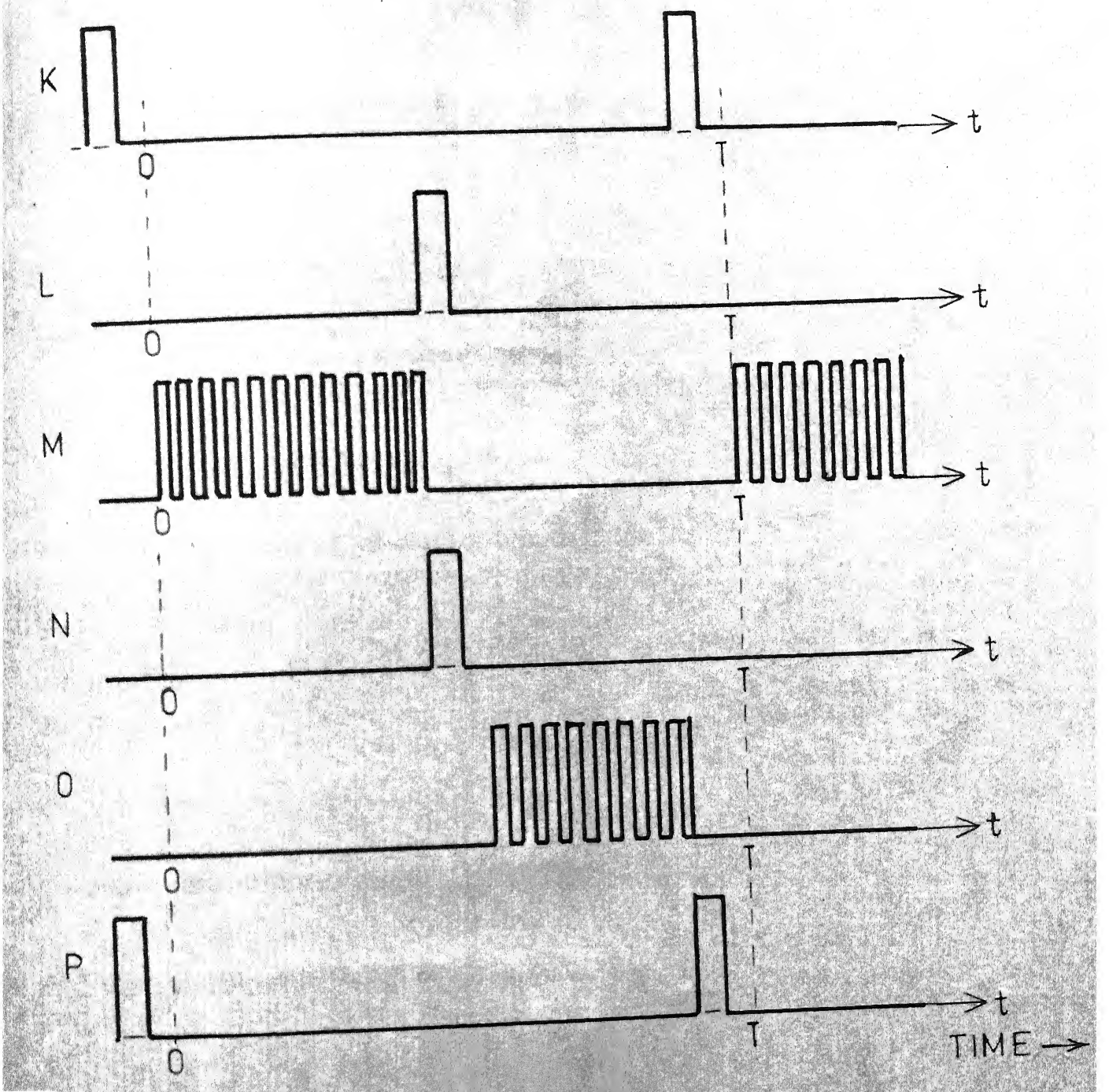

FIG. 3.10(b) Waveforms at different stages of Fig. 3.10(a)

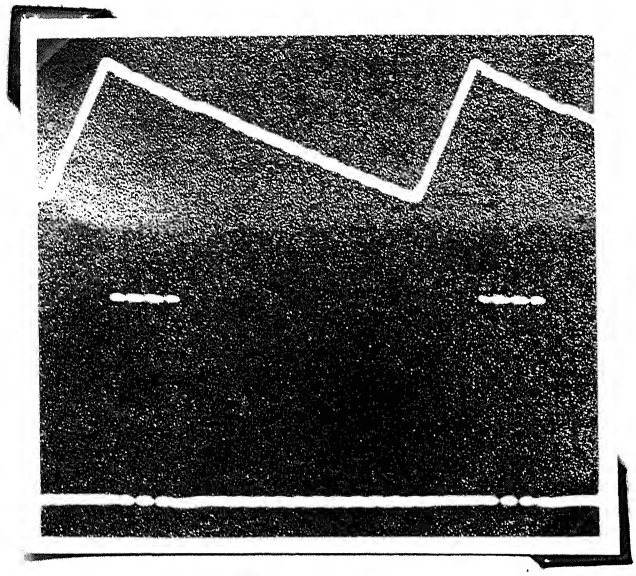

Fig. 3.11.1

Triangle wave
Scale: X-axis 0.5 ms/cm
Y-axis 2V/cm

Firing pulse for Q_1
Scale : X-axis 0.5 ms/cm
Y-axis 5V/cm

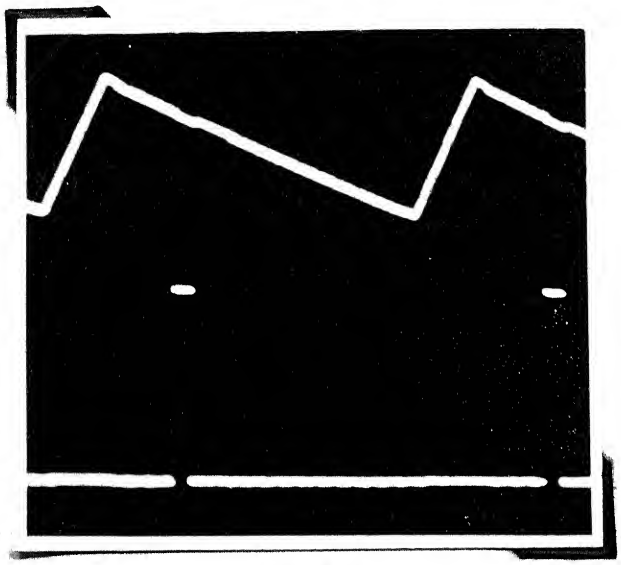

Fig. 3.11.2

Triangle wave
Scale: X-axis 0.5ms/cm
Y-axis 2V/cm

Firing pulse for Q_{11}
Scale : X-axis 0.5 ms/cm
Y-axis 5V/cm

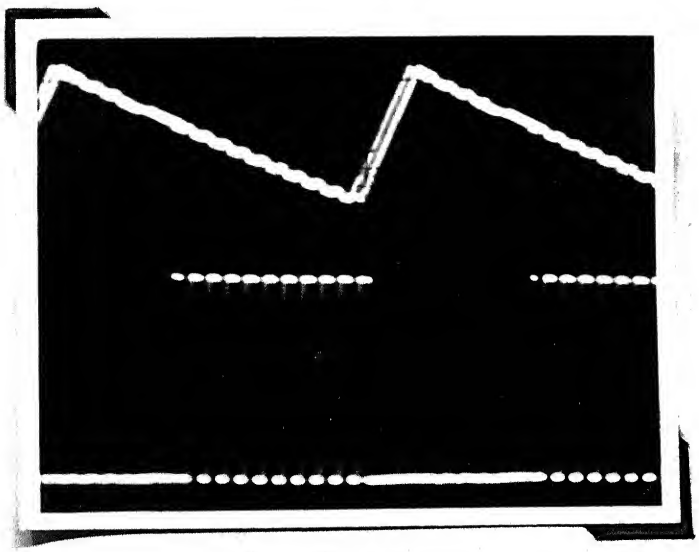

Fig. 3.11.3

Triangle Wave
Scale : X-axis 0.5 ms/cm
Y-axis 2V/cm

Firing pulse for Q_2
Scale : X-axis 0.5 ms/cm
Y-axis 5V/cm

DUAL CHOPPER AT 100 Hz

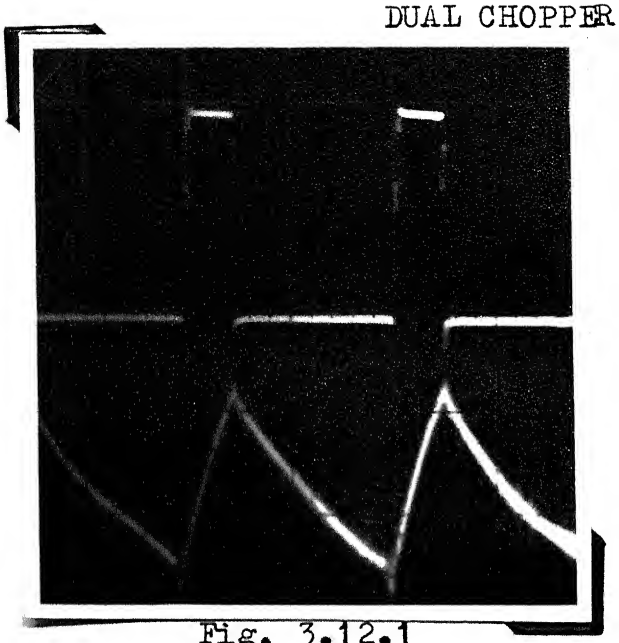

Fig. 3.12.1

Load voltage for small δ at no load

Scale : X-axis 5 ms/cm
Y-axis 100 V/cm

Load current across shunt (10A, 75 mV)

Scale : X-axis 5 ms/cm
Y-axis .1 mV/cm

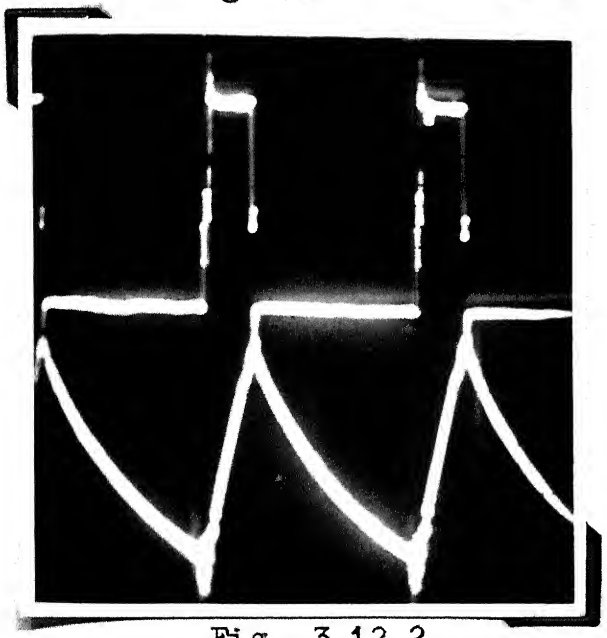

Fig. 3.12.2

Load voltage during regeneration

Scale : X-axis 5 ms/cm
Y-axis 100 V/cm

Load Current

Scale : X-axis 5 ms/cm
Y-axis .1 mV/cm

Speed-torque characteristics for dual chopper or chopper B (from Chapter II) are shown in Fig. 3.13 for two values of δ i.e. $\delta = 0.26$ and 0.4. It can be seen that experimental results are closely matching with theoretical results for low torque ranges. Deviations at large values of torque can be attributed to armature reaction [7]. System did not work beyond $\delta = 0.5$ because of commutation problems.

3.9 PERFORMANCE OF SEPARATELY EXCITED MOTOR WITH SINGLE QUADRANT CHOPPER:

Since dual chopper offered considerable commutation problems, a single quadrant chopper was chosen for the closed loop control of chopper fed dc separately excited motor. This single quadrant chopper (same as chopper A in Chapter II) resembles with the chopper Q_1 of Fig. 3.8(a). Speed torque characteristics of dc motor fed by chopper A at 500 Hz are shown in Fig. 3.14 for three values of δ. Continuous conduction was observed from no load to full load. A closeness between theoretical and experimental results can be seen from Fig. 3.14. Some photographs for chopper A are shown in Fig. 3.15. Fig. 3.15.1 illustrates

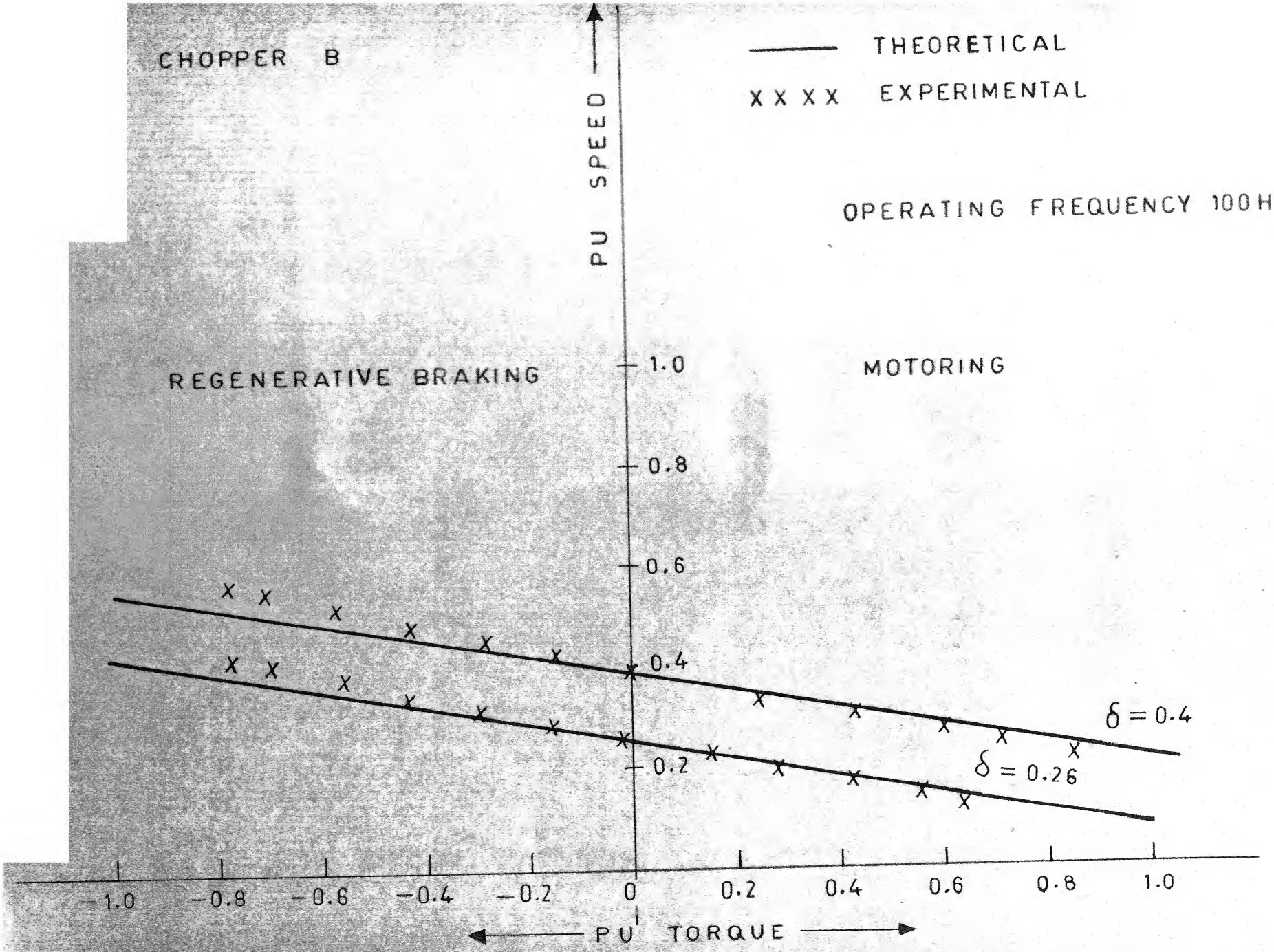

FIG. 3.13 Speed – Torque Characteristics for chopper B

Single Quadrant Chopper at 500 Hz

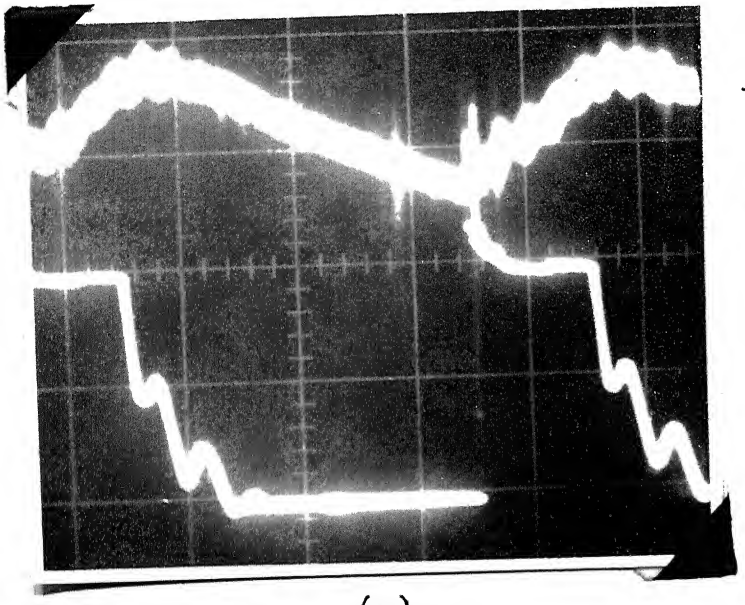

Armature current, shunt (10A, 75 mV), small δ

Scale : X-axis .5 ms/cm
Y-axis 50 mV/cm

Load voltage

Scale : X-axis 0.5 ms/cm
Y-axis 100 V/cm

(a)

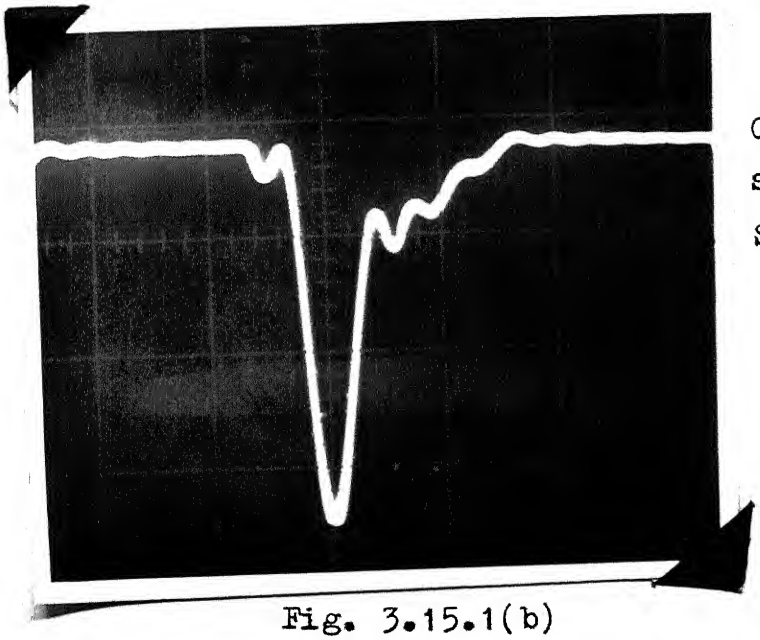

Capacitor Voltage, small δ

Scale : X-axis .5 ms/cm
Y-axis 100 V/cm

Fig. 3.15.1(b)

Single Quadrant Chopper at 500 Hz

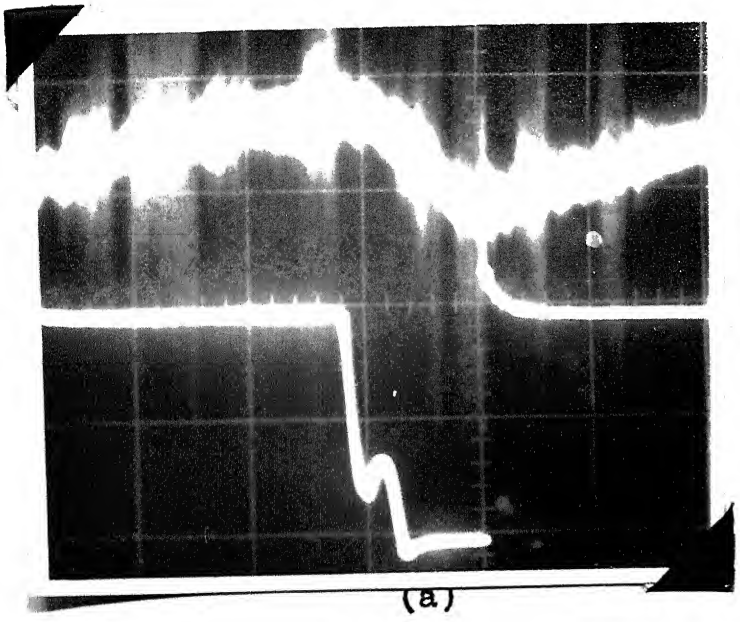

(a)

Armature current, shunt (10A, 75 mV), large δ

Scale : X-axis 0.5 ms/cm
Y-axis 50 mV/cm

Load voltage

Scale : X-axis 0.5 ms/cm
Y-axis 100V/cm

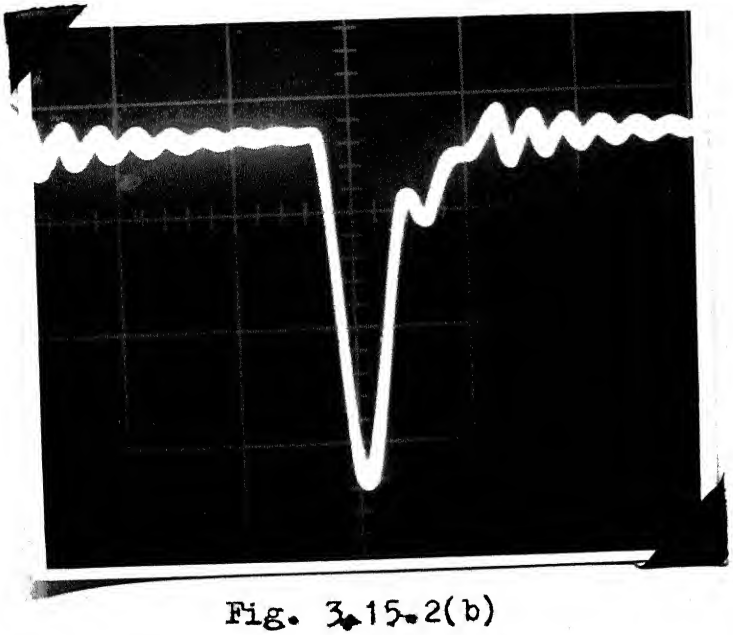

Capacitor voltage, large δ

Scale : X-axis 15 ms/cm
Y-axis 100 V/cm

Fig. 3.15.2(b)

the output voltage of chopper and armature current for small value of δ . Commutation capacitor voltage for the same δ is shown in Fig. 3.15.2. Load voltage, load current and commutation capacitor voltage for large δ have been shown in Fig. 3.15.3 and 3.15.4 respectively.

Open loop speed transient responses have been calculated theoretically and recorded experimentally during starting and during perturbation in δ and load. They are shown in Figs. 3.16 to 3.18.

Fig. 3.16(a) shows open loop speed transient response of the motor at no load for $\delta = 0.4$. Fig. 3.16(b) depicts speed transient response at 0.6 p.u. load for $\delta = 0.3$.

Transient response of speed in open loop for 10% perturbation in δ (=0.6) at no load is shown in Fig. 3.17(a). Speed transient response for 5% perturbation in δ (=0.6) at full load is shown in Fig. 3.17(b).

Speed transients for 20% and 80% perturbation in load at $\delta = 0.5$ are shown in Fig. 3.18.

3.10 CONCLUSION :

Two different circuits for dual chopper were designed and fabricated. Dual chopper with type 2 current commutation did not work due to commutation problems. Dual chopper with type 1 current commutation gave results upto $\delta = 0.5$, afterwards it also offered commutation problems. A digital circuitry for the control of dual chopper has been developed. An investigation of single quadrant chopper fed dc separately excited motor for steady state and transient operation was carried out for the purpose of using it later in closed loop system. Closed loop operation has been reported in the next chapter.

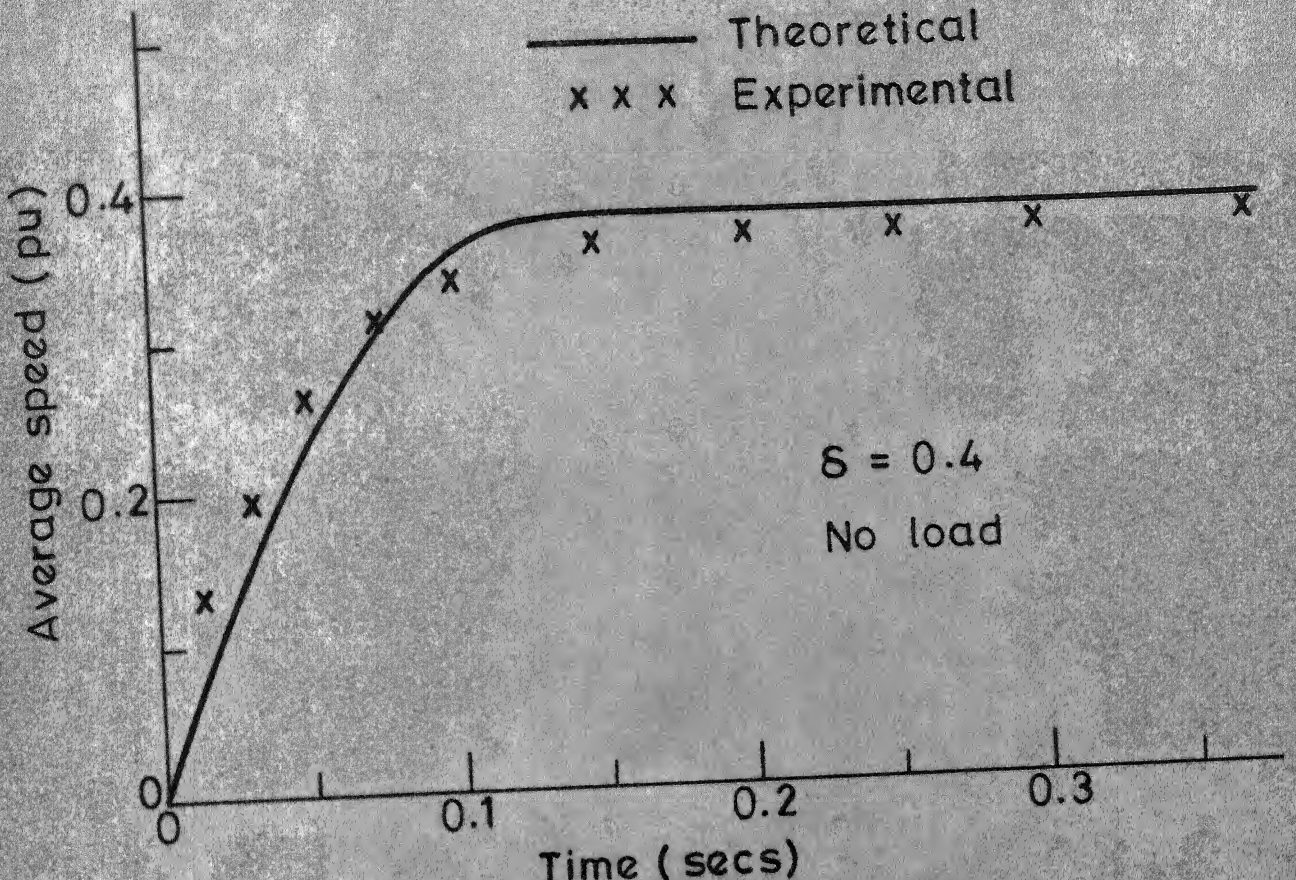

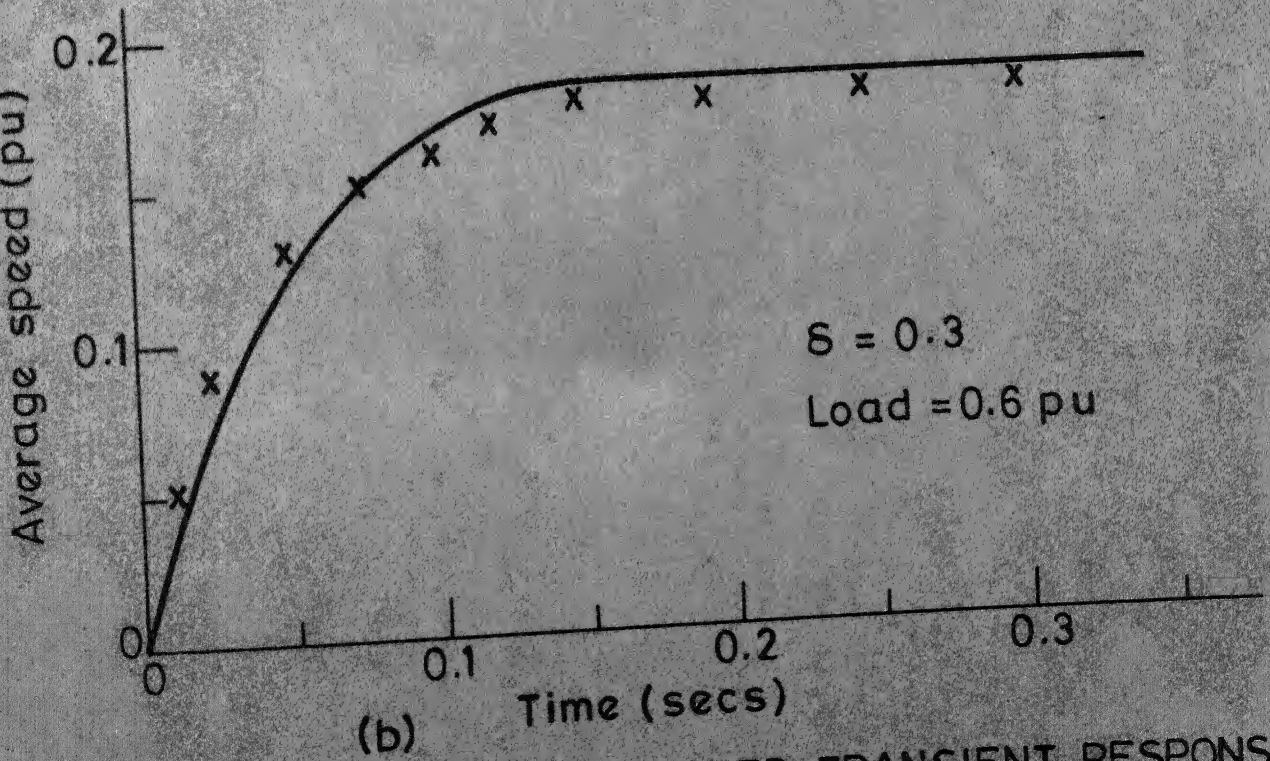

FIG. 3.16 OPEN LOOP SPEED TRANSIENT RESPONSE DURING STARTING.

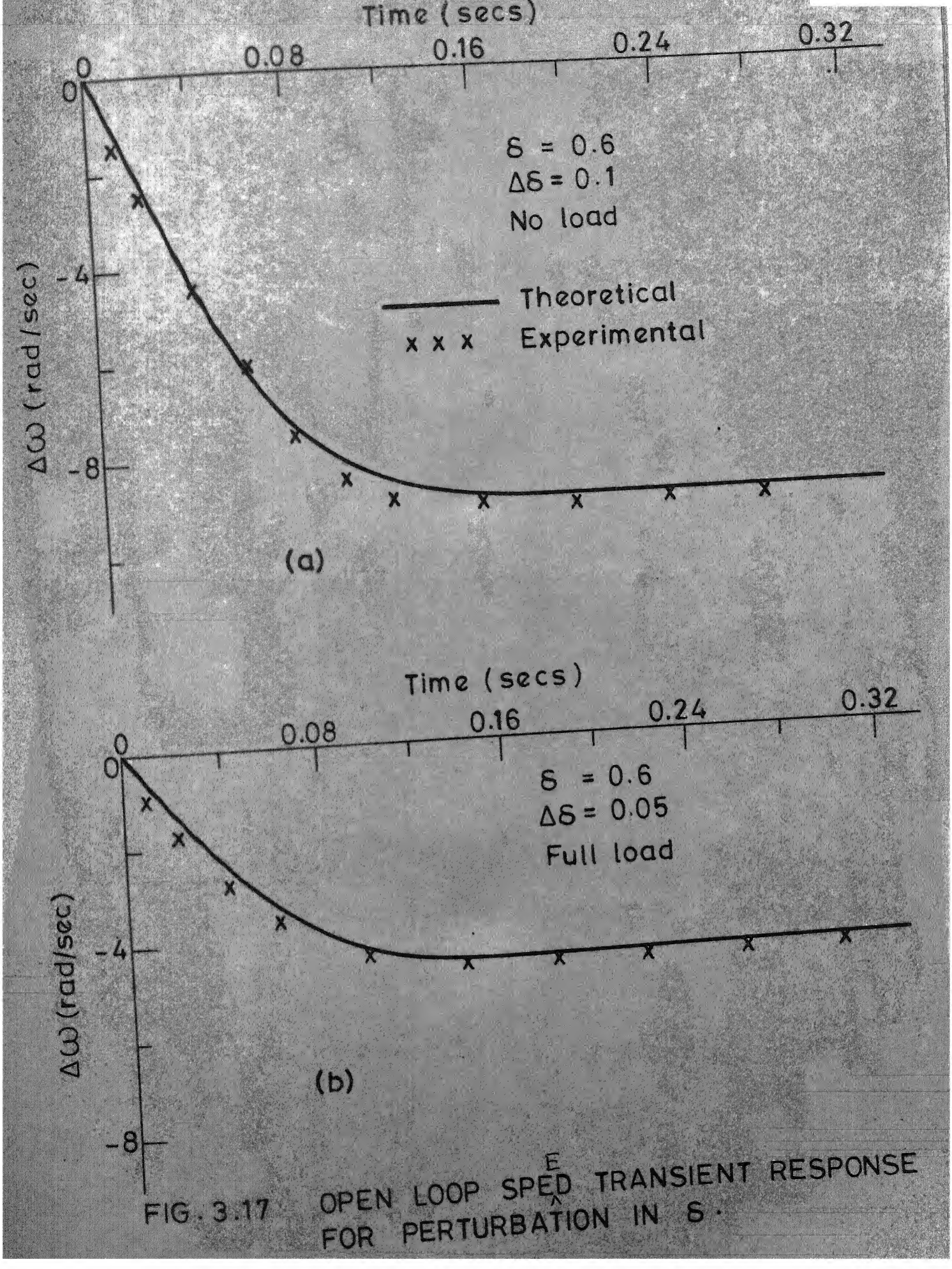

FIG. 3.17 OPEN LOOP SPED TRANSIENT RESPONSE FOR PERTURBATION IN $\hat{E}$ δ.

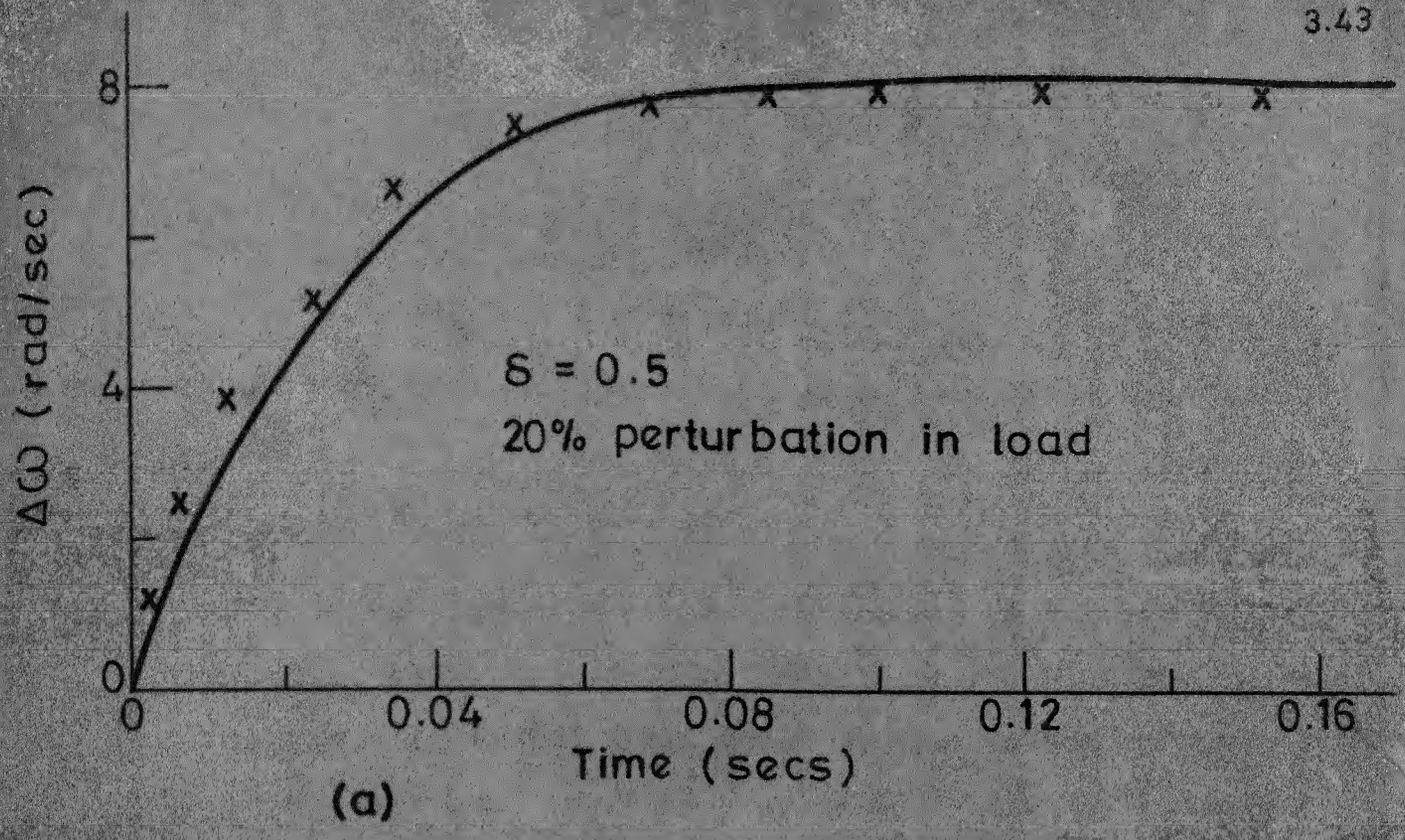

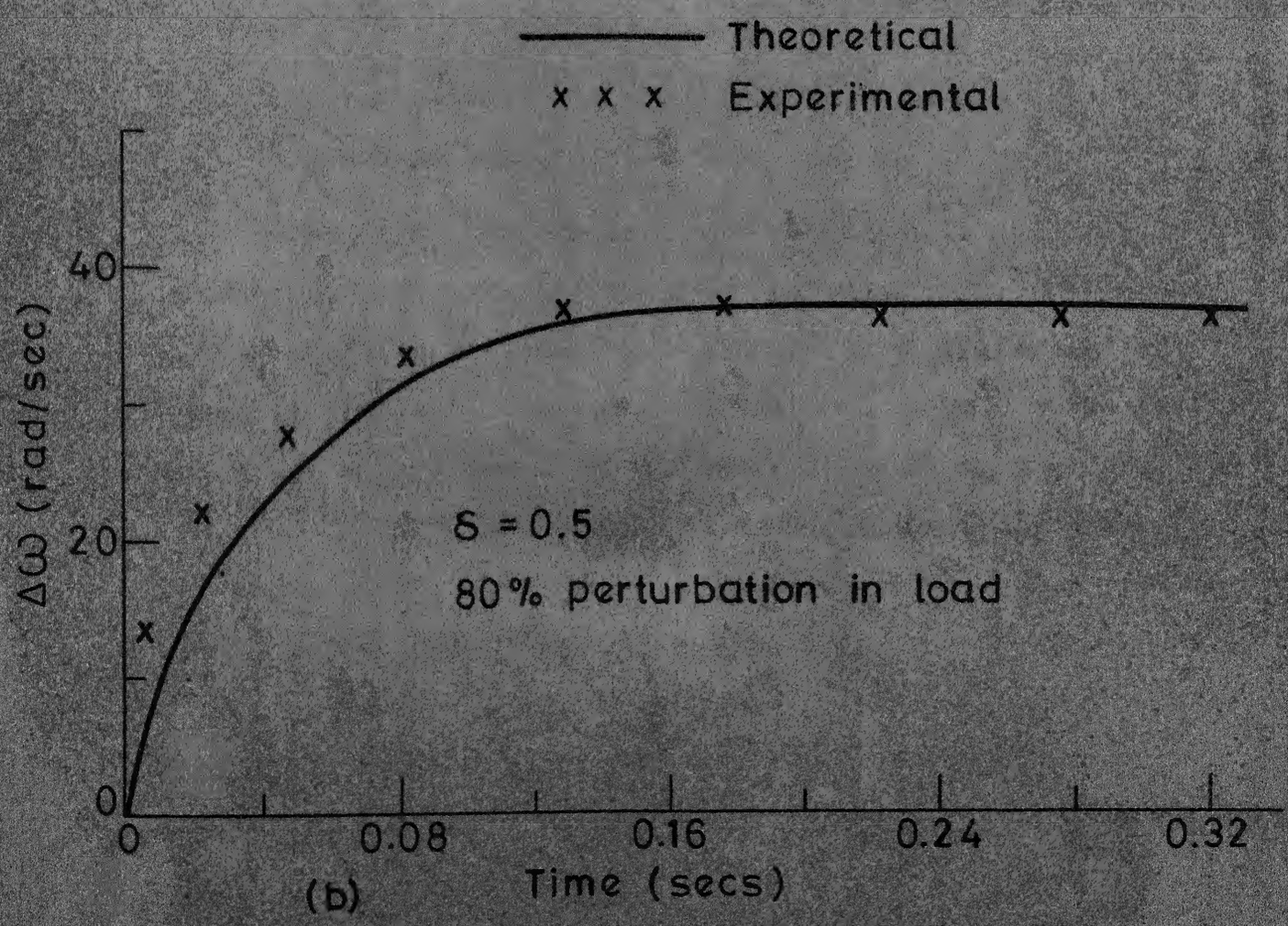

FIG. 3.18 OPEN LOOP SPEED TRANSIENT RESPONSE FOR LOAD PERTURBATION.

CHAPTER IV

CLOSED LOOP CONTROL OF CHOPPER FED DC SEPARATELY EXCITED MOTOR

4.1 INTRODUCTION:

DC separately excited motors are widely used for precision control of speed in industries. One of the common mode is to use fixed field excitation and variable armature voltage. There are two basic schemes of getting variable armature voltage.

1. scheme with current limit control, and
2. scheme with inner current control loop.

The first scheme is shown in Fig. 4.1. In this scheme, V_{ref} is used to set the reference speed. The sensed speed is filtered through a low pass filter and is compared with speed reference. The error signal is fed to the speed controller which is generally a PI controller. It tries to make the system steady-state speed error zero. The armature current is sensed by a current transducer. If the motor current is less than I_{limit}, current controller remains inactive. But, as soon as I_a exceeds I_{limit} even by a small amount, large output voltage is developed by current controller. The speed control goes out of action

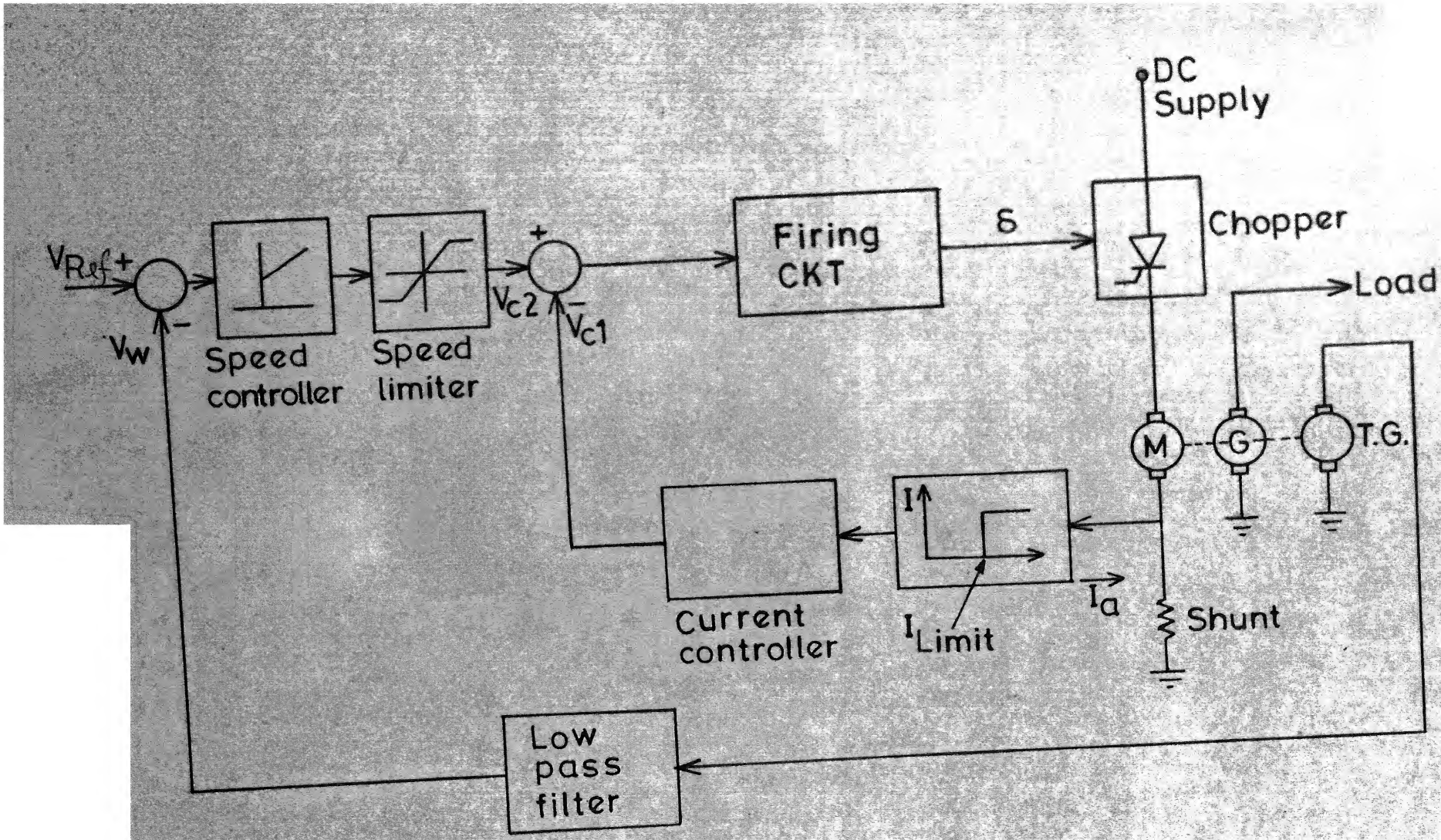

Eig. 4.1 Scheme of speed control system with current limit control.

motor, the armature current rather than the speed drops almost instantaneously whenever the supply voltage falls. In the absence of the inner current control loop, the motor decelerates to cope with the load torque. The speed comes back to the original value after the drop in speed is processed by the speed controller to give a new firing angle. Hence, for corrective action to take place, a change in speed has to accompany a change in supply and the response is poor owing to the large mechanical time constant involved. With the inner current control loop present, a drop in armature current itself results in a new firing angle and the fall in supply voltage is counteracted by correcting the armature current at a fast rate.

4.2 REALISATION OF THE SYSTEM:-

On the basis of above mentioned advantages, the inner current control scheme has been chosen. The different blocks and their details are given below.

1. Speed Sensor:

There are two methods used for sensing the speed of dc separately excited motor. Since the speed of dc motor is proportional to its back emf, hence in order to sense the speed the induced voltage is sensed by sensing the motor terminal voltage and armature resistance drop

obtained from the shunt resistor is first amplified and then it is filtered through a low pass filter. This filtered output is inverted with some amplification to get a negative feedback of armature current.

3. Speed Controller and Limiter:

Following are the two common types of speed controllers.

i) Proportional controller (known as P controller).

ii) Proportional plus integral controller (called as PI controller).

Proportional controller gives appreciable steady - state error whereas PI gives zero steady state error. Hence, a PI controller has been chosen for the speed loop. The output of PI controller is passed through a limiter as shown in Fig. 4.2 whose design procedure is given in reference [6]

4. Current Controller and Limiter:

In the beginning, a P-controller was chosen for current controller. But after analysis, it was found that to get a steady state error equal to 5%, the gain of the P controller should be around 200 which can not be achieved in practice because of the saturation problems in op-amp. A limiter as shown in Fig. 4.2 was used after current controller.

5. Firing Circuit:

Firing circuit has been discussed in Chapter III. The relationship between the control voltage and the firing angle is linear.

4.3 TRANSFER FUNCTIONS OF VARIOUS BLOCKS:

The transfer functions of various blocks are derived below.

A. DC Motor:

The differential equations governing the operation of a dc motor with constant field excitation and no mechanical friction are

$$L \frac{di_a}{dt} + R i_a + K_v w = v_a(t) \qquad (4.1)$$

$$J \frac{dw}{dt} = T_m - T_l \qquad (4.2)$$

The coulomb and static frictions are neglected for getting a linear model. Viscous friction is included in the load-torque T_l. In the experimental set up used, the dc motor is loaded by means of a dc generator supplying a resistive load. Neglecting the electrical time constant of the dc generator armature circuit it can be easily shown that the load torque on the dc motor is proportional to speed. The viscous friction only increases this proportionality constant.

Dividing eqn. (4.1) by V_R(V_R=RI_{st} = $K_v w_o$).

$$\frac{L}{R}\ \frac{d(i_a/I_{st})}{dt} + \frac{i_a}{I_{st}} + \frac{w}{w_o} = \frac{v_a(t)}{V_R} \qquad (4.3)$$

Taking the Laplace transform of (4.3) and rearranging the terms

$$(1+ s\ \tau_e)I_a(s) = V_a(s) - w(s) \qquad (4.4)$$

Dividing (4.2) by T_{st} ($T_{st} = K_v I_{st}$)

$$\frac{Jw_o}{T_{st}}\ \frac{d(w/w_o)}{dt} = \frac{i_a}{I_{st}} - \frac{T_l}{T_{st}} \qquad (4.5)$$

Taking the Laplace transform of (4.5)

$$\tau_m\ s\ w(s) = I_a(s) - T_l(s) \qquad (4.6)$$

The load torque of dc motor is proportional to the speed w, and the proportionality constant B is defined by (4.7).

$$\frac{T_l}{T_{st}} = B\ \frac{w}{w_o}$$

or

$$T_l(s) = B\ w(s) \qquad (4.7)$$

The block diagram of dc motor with normalised quantities shown in Fig. 4.3(a) is obtained from (4.4), (4.6) and (4.7).

From (4.6) and (4.7), the transfer function between w and I_a can be written as

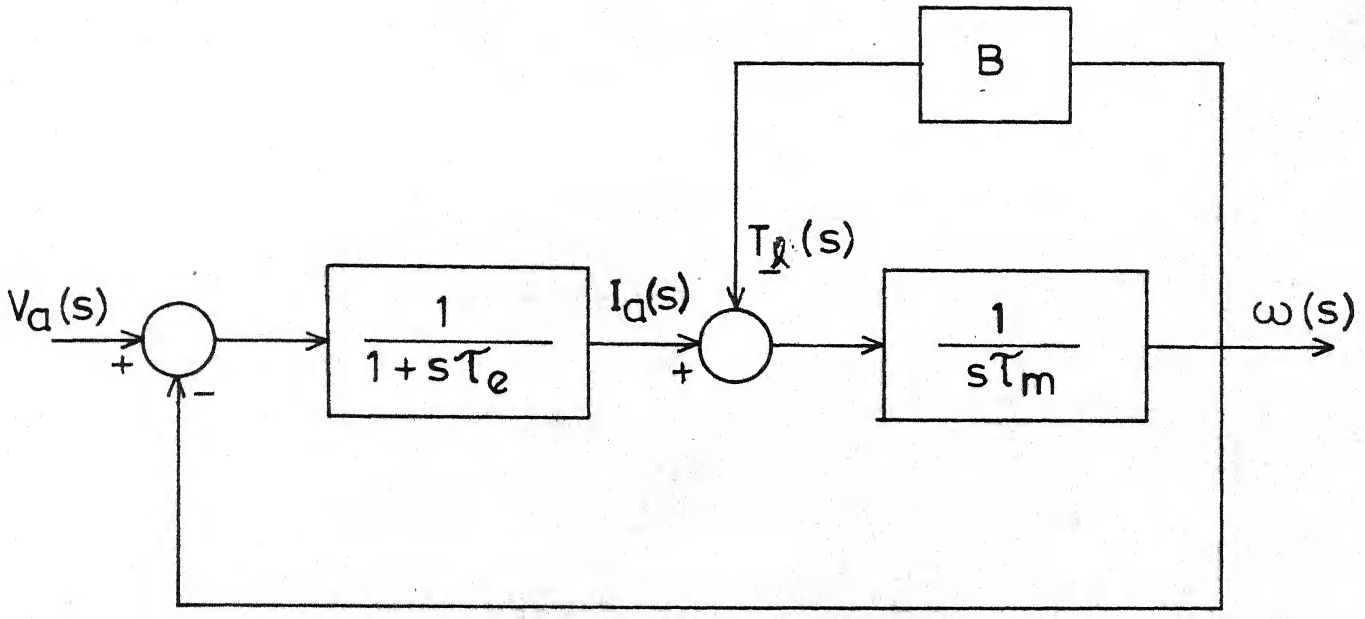

(a)

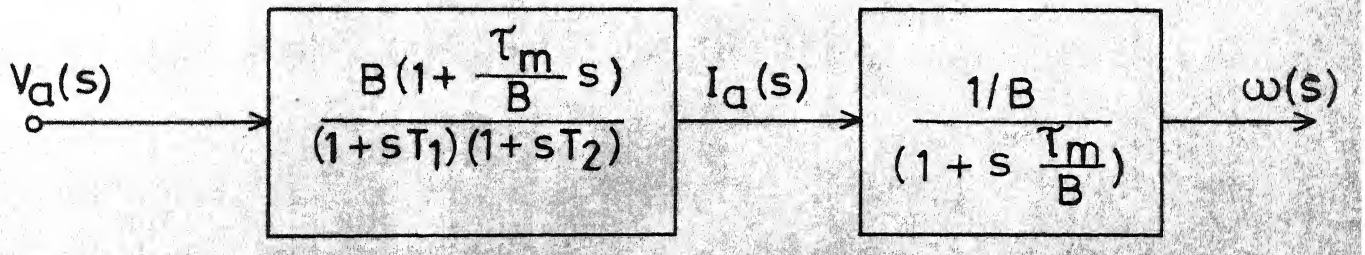

(b)

Fig. 4.3 (a) Block diagram of dc motor.

(b) Reduced block diagram of dc motor.

$$\frac{w(s)}{I_a(s)} = \frac{1}{B} \cdot \frac{1}{(1+\frac{\tau_m}{B}s)} \qquad (4.8)$$

The block diagram of the motor given in Fig. 4.3(a) is reduced to the one shown in Fig. 4.3(b), where

$$-\frac{1}{T_1}, -\frac{1}{T_2} = \frac{1}{2}\left\{-\left(\frac{B}{\tau_m}+\frac{1}{\tau_e}\right) \pm \sqrt{\left(\frac{B}{\tau_m}+\frac{1}{\tau_e}\right)^2 - \frac{4(B+1)}{\tau_e \tau_m}}\right\} \qquad (4.9)$$

B. Thyristor Chopper and Firing Unit:

The relation between input voltage and output voltage of a chopper is

$$V_a = \delta V_R \qquad (4.10)$$

since from our assumption in chapter II

$$\delta = \frac{V_c}{V_{cm}} \qquad (2.79)$$

Hence, from (4.10) and (2.79)

$$\frac{V_a}{V_R} = \delta = \frac{V_c}{V_{cm}} \qquad (4.11)$$

Taking the Laplace transform of (4.11)

$$V_a(s) = V_c(s) \qquad (4.12)$$

C. Current Controller:

In the beginning, a proportional controller was chosen. Its transfer function can be represented

by a pure gain K_1. But after analysis which is shown in section 4.4A, it was found that for getting a steady state error within 5%, the gain of the P-controller i.e. K_1 should be around 200. Since it poses problems of saturation in op-amps a PI controller was chosen for current control since this provides quick response with zero steady state error. The transfer function of this can be written as $\frac{K_1(1+\tau_{c1}s)}{\tau_{c1}s}$, and the design of this (i.e. choosing the parameters K_1 and τ_{c1}) is considered in section 4.4A.

D. Current Transducer:

It is designed such that the output voltage v_i is proportional to armature current i_a. The current pick-up gain, v_i/i_a is found to be 1.0V/A from the experiment. The normalized gain H_i is

$$H_i = \frac{v_i/V_{cm}}{i_a/I_{st}} = \frac{1.0 \times 7.5}{12} = 0.7 \qquad (4.13)$$

E. Speed Controller and Speed Transducer:

The speed control loop is required to provide a zero steady-state error and a fast response. Hence a PI controller has been chosen for speed control. The transfer function of the controller is $\frac{K_2(1+\tau_{c2}s)}{\tau_{c2}s}$ and the design of this controller is discussed in section 4.4B.

A tachogenerator mounted on the motor shaft provides the speed feedback signal. The tachogenerator gain v_w/w is found to be .0762 V/rad/S from experiment. The normalized gain of the speed transducer H_w is given by

$$H_w = \frac{v_w/V_{cm}}{w/w_o} = \frac{.0762 \times 157.07}{12} = 1.0 \qquad (4.14)$$

4.4 DESIGN OF CONTROLLERS:

A. Current Controller:

The current control loop with P-controller is obtained as shown in Fig. 4.4. This is third order system. The loop gain function is

$$GH_i(s) = \frac{K_1 B H_i (1 + \frac{\tau_m}{B} s)}{(1+sT_1)(1+sT_2)} \qquad (4.15)$$

Substituting the values of B, τ_m and τ_e (given in appendix A) into (4.9)

$$T_1 = 1.21 \text{ S}, \quad T_2 = 0.01 \text{ S}$$

Hence

$$GH_i(s) = \frac{86.8K_1(s+0.1)}{(s+0.83)(s+100)} \qquad (4.16)$$

The root locus of current control loop with P - controller is shown in Fig. 4.6.

The expression for steady-state error of current loop is

$$e_{ss} = \frac{83}{83+8.68\,K_1} \qquad (4.17)$$

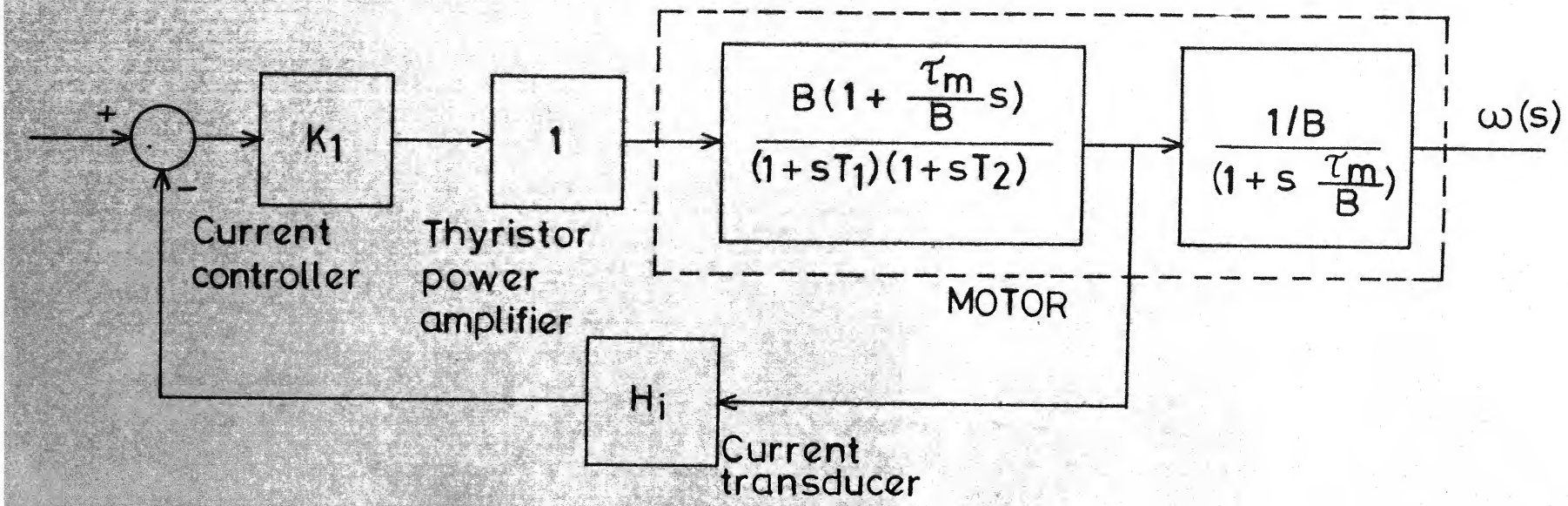

Fig. 4.4 Current control loop with P controller

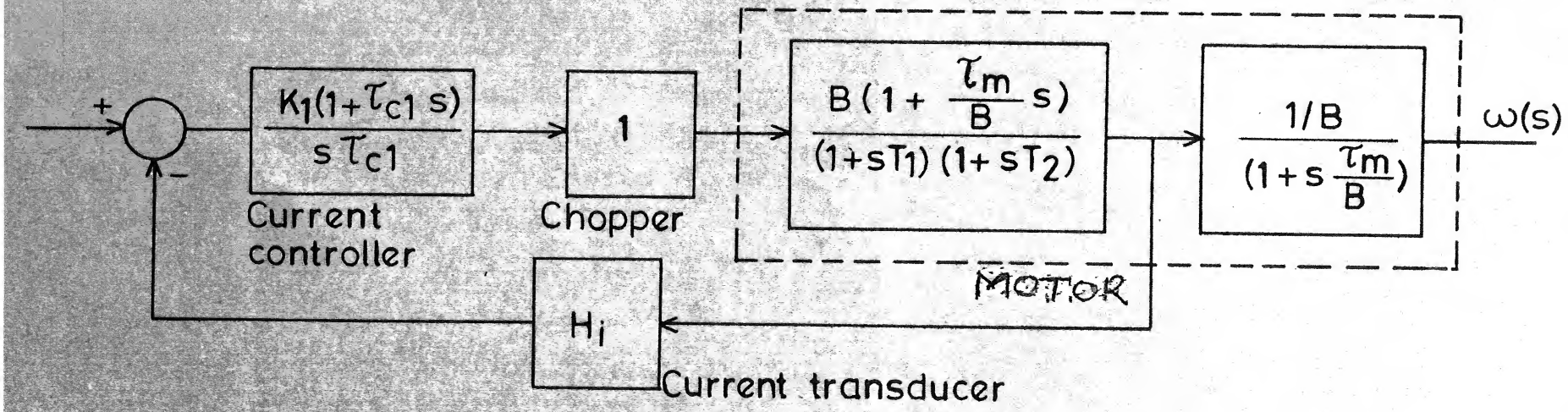

Fig. 4.5 Current control loop with PI controller.

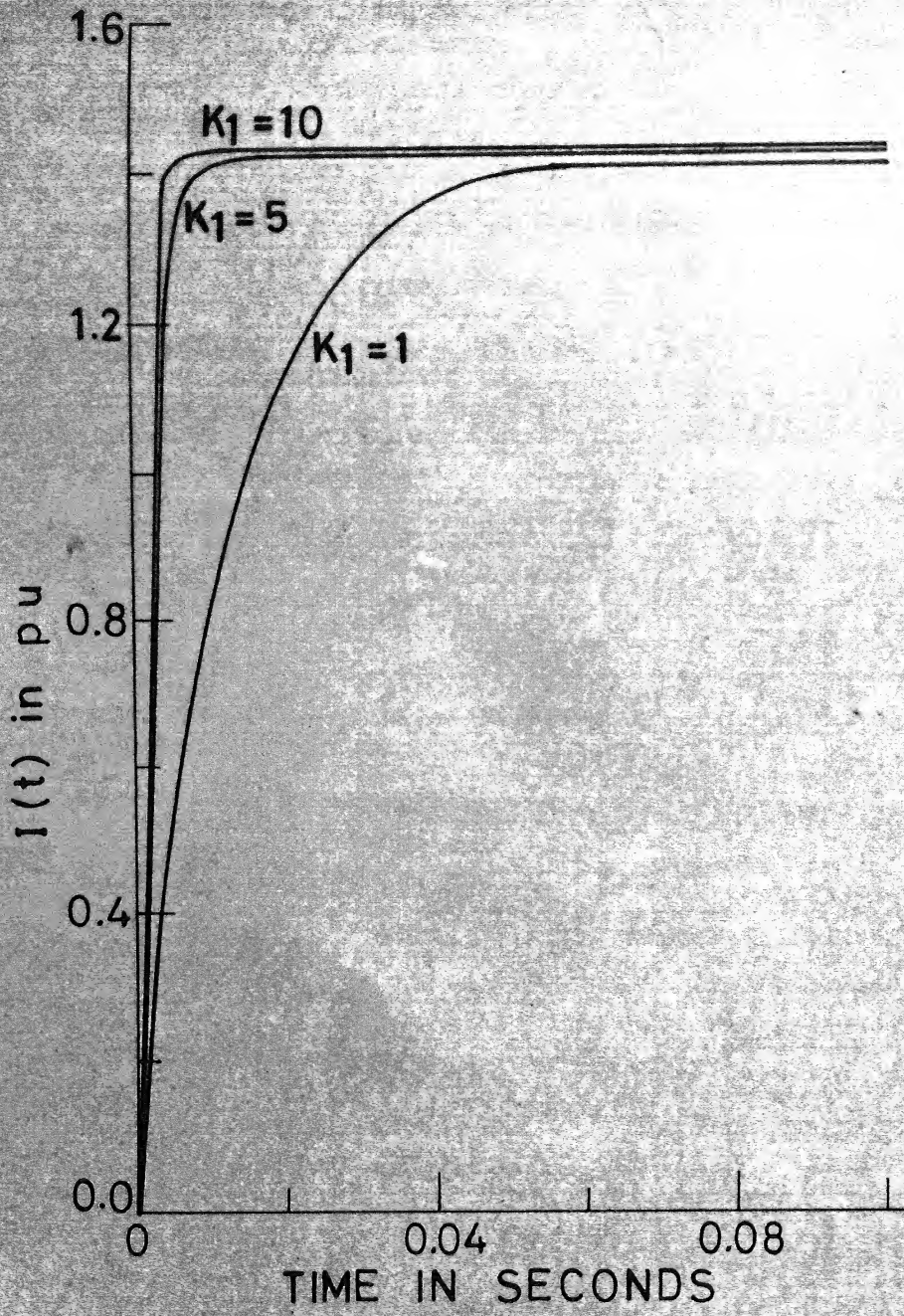

Fig.4.8 Current loop response.

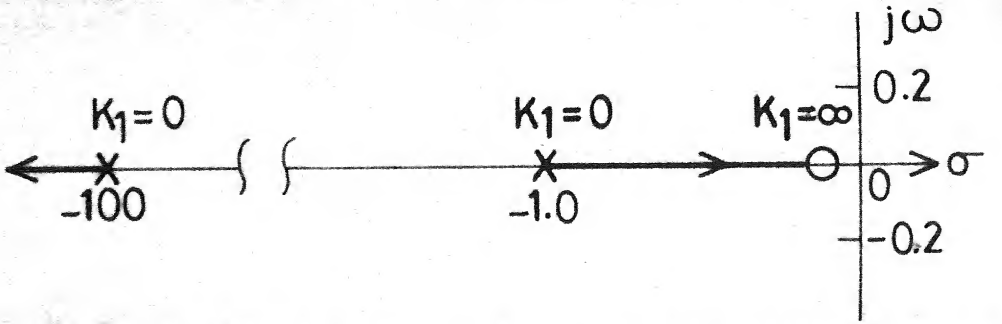

Fig.4.6 Root locus of current control loop with P controller.

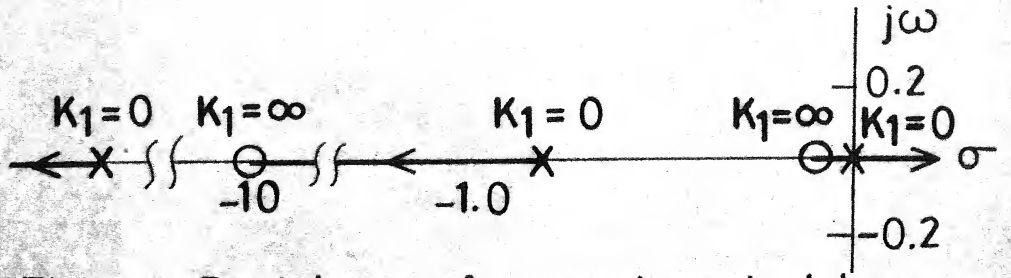

Fig.4.7 Root locus of current control loop with PI controller.

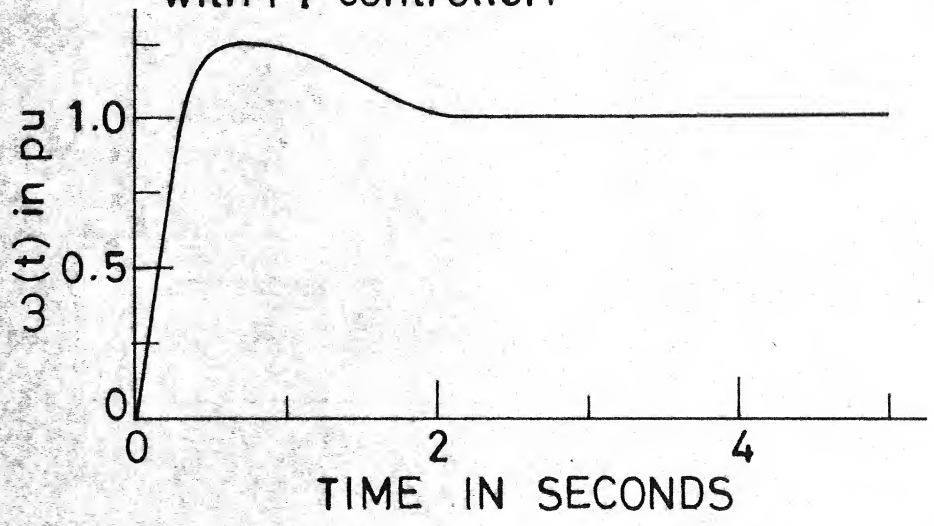

Fig.4.9 Step response of speed (theoretical).

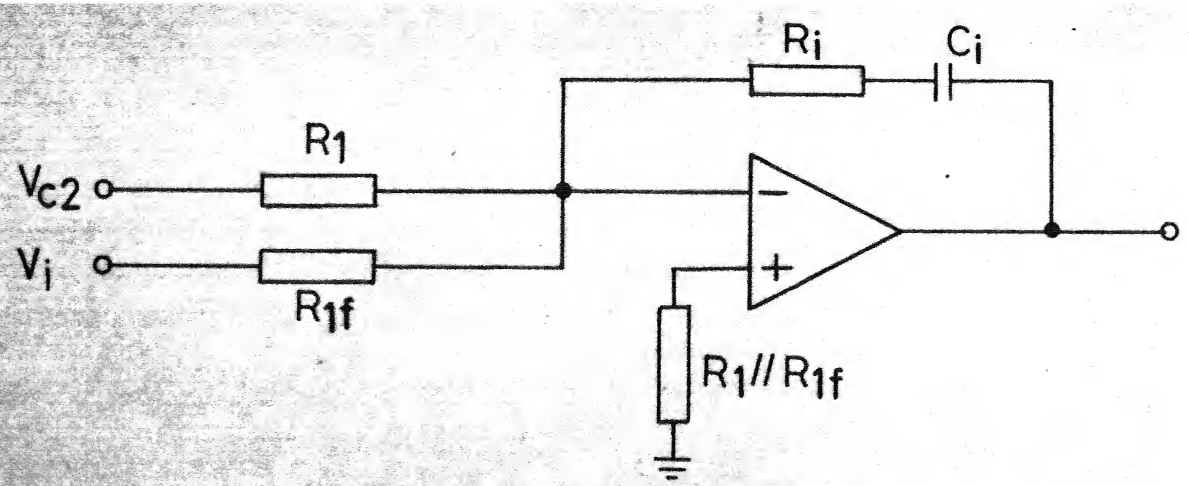

Fig. 4.10 Current controller

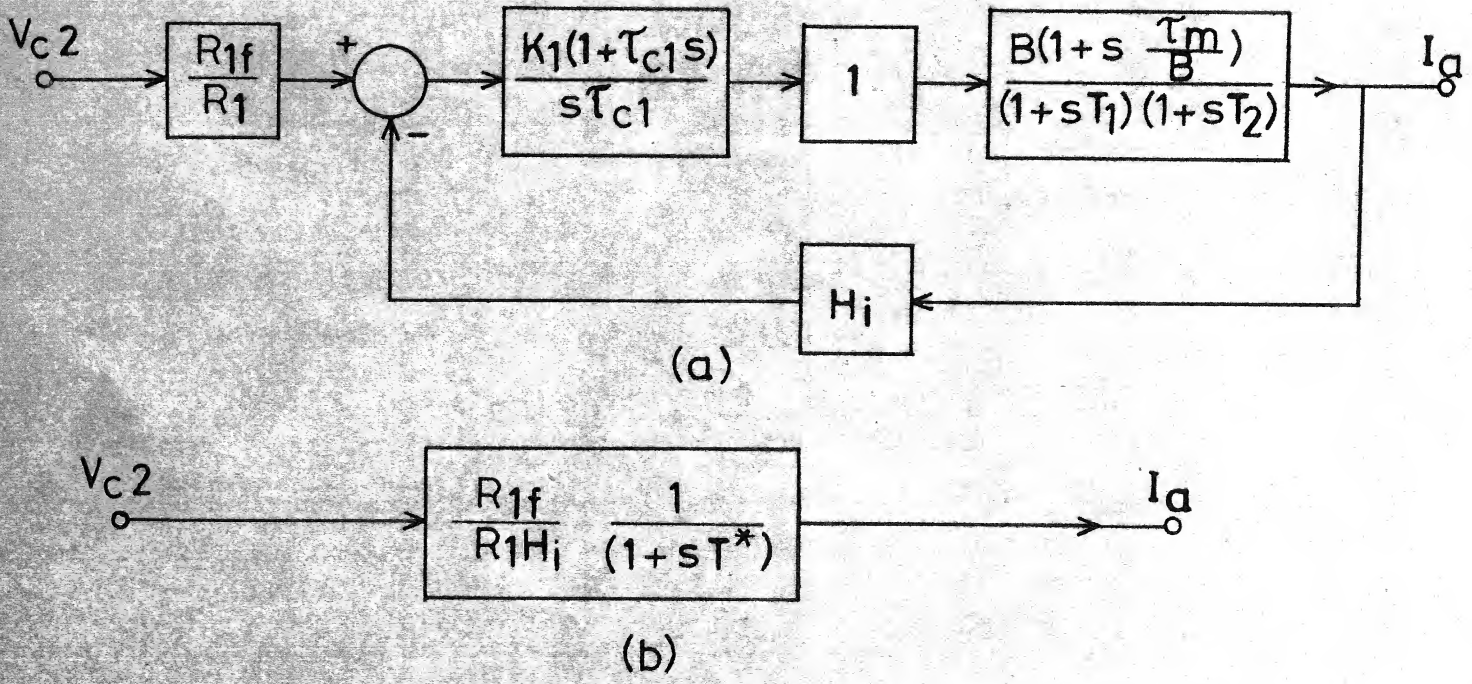

Fig. 4.11 (a) Actual block diagram of current control loop.
(b) Approximated block diagram of (a).

Eqn. (4.17) shows that for e_{ss} to be less than 5%, K_1 should be more than 182. This high value of gain will cause saturation of op-amp. Hence, a PI-controller has been chosen for current control loop as shown in Fig. 4.5. This is a third order system. The loop gain function is

$$GH_i(s) = \frac{K_1 B H_i}{\tau_{c1}} \cdot \frac{(1+\tau_{c1}\, s)(1+s\,\frac{\tau_m}{B})}{s(1+sT_1)(1+sT_2)} \qquad (4.18)$$

Choosing τ_{c1} = 100 ms,

One gets a root locus of current control loop as shown in Fig. 4.7. For different values of K_1, current loop response is plotted in Fig. 4.8. From this, K_1=10 is chosen because it gives fast response. The realization of the current controller is shown in Fig. 4.10. The capacitance in the feedback circuit of the operational amplifier is chosen as c_i = 1 μf, and from the values of K_1 and τ_{c1},

R_i = 100 K Ω R_{1f} 10 K Ω

For a maximum armature current of 1.3A, the input resistance R_1 is chosen from the relation

$$\frac{v_{c2}\ \text{sat}/V_{cm}}{R_1} = \frac{(1.3/I_{st}) \times H_i}{R_{1f}} \qquad (4.19)$$

where v_{c2} sat = 10V is the saturation voltage of the speed controller. Substituting for the other parameters in (4.19)

$$R_1 = 68\ K\Omega$$

The proportional gain of the controller of Fig. 4.10 for the feedback signal v_i is R_i/R_{1f}, which is denoted by K_1. Since $R_1 \neq R_{1f}$, the gain for the signal v_{c2} of the feedforward path is different and is equal to R_i/R_1. Hence, with the controller of Fig. 4.10, the block diagram representation of Fig. 4.5 should include a gain of R_{1f}/R_1 in the path of V_{c2} only, to correspond to the physical situation. This block of gain R_{1f}/R_1 is shown in Fig. 4.11(a).

B. Speed Controller:

A PI controller is used for the speed loop. The current loop is approximated by a first order block of equivalent time constant T^* as shown in Fig. 4.11(b). This time constant is found to be approximately equal to 11.4 ms. The output of the tachogenerator used for sensing the speed signal has a low frequency signal of 25 Hz near the rated speed. Hence an RC filter with a time constant T_f= 50 ms was used in the feedback path. The overall block diagram of the speed control loop for design purpose is shown in Fig. 4.13(a). The loop gain function is given by

$$GH_w(s) = \frac{K_2(1+\tau_{c2}s)}{\tau_{c2}\,s} \cdot \frac{R_{1f}}{R_1 H_i} \frac{1}{(1+sT^*)}$$

$$\frac{1/B}{(1+s\frac{\tau_m}{B})} \cdot \frac{H_w}{(1+sT_f)} \qquad (4.20)$$

From stability considerations, the controller time constant τ_{c2} is to be chosen such that gain crossover occurs at -1 slope, and $\frac{1}{\tau_{c2}} < w_c < \frac{1}{T_f}$ where w_c is the gain crossover frequency. Also the dynamic performance of the loop is largely dependent on the behaviour of the loop gain function in the vicinity of w_c. Based on the numerical time constants involved here, the following approximations can be made in the vicinity of w_c. The term $\frac{1}{1+ s\frac{\tau_m}{B}}$ can be taken as $\frac{1}{s\frac{\tau_m}{B}}$. The time constant T^* can be neglected [2]. With these approximations, the loop gain function of the speed loop can be simplified as

$$GH_w(s) = \frac{K_2(\frac{1}{\tau_{c2}}+s)}{0.355\, s^2 (\frac{1}{T_f}+s)} \qquad (4.21)$$

(i) Choosing $\tau_{c2} = 5\, T_f = 250$ ms, the root locus for $GH_w(s)$ is shown in Fig. 4.12(a). Drawing a line at $\epsilon = 0.707$, one gets closed loop poles at $s = -3.3 \pm j2.3$, then the corresponding value of K_2 is found to be 40.4.

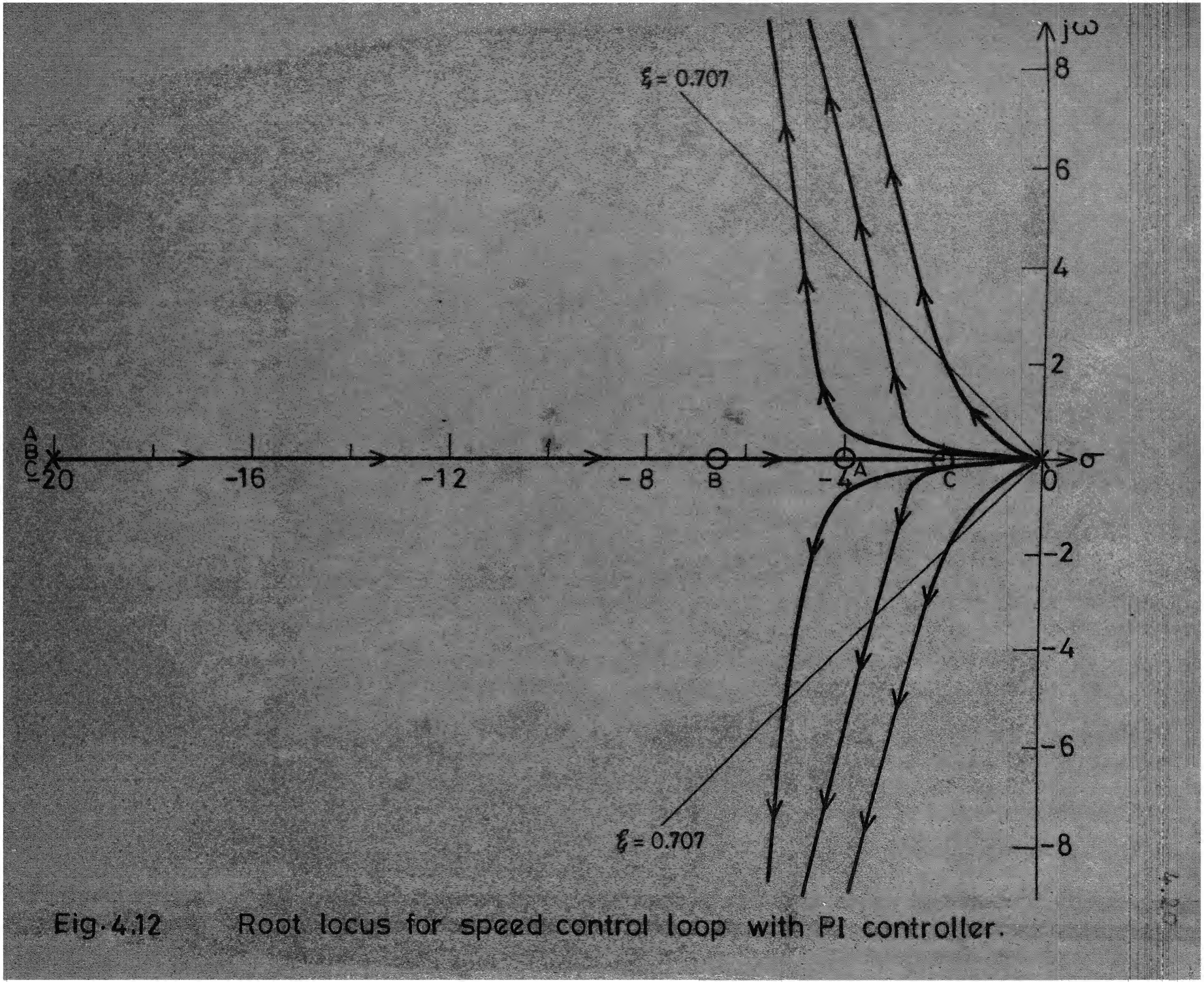

Eig·4.12 Root locus for speed control loop with PI controller.

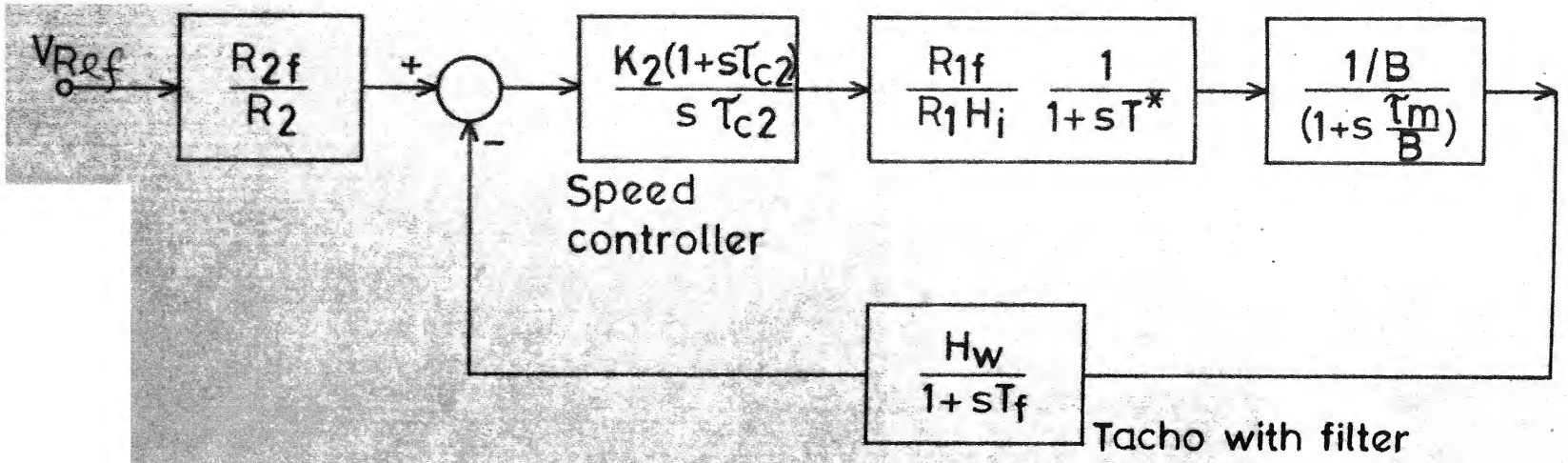

Fig. 4.13 (a) Speed control loop.

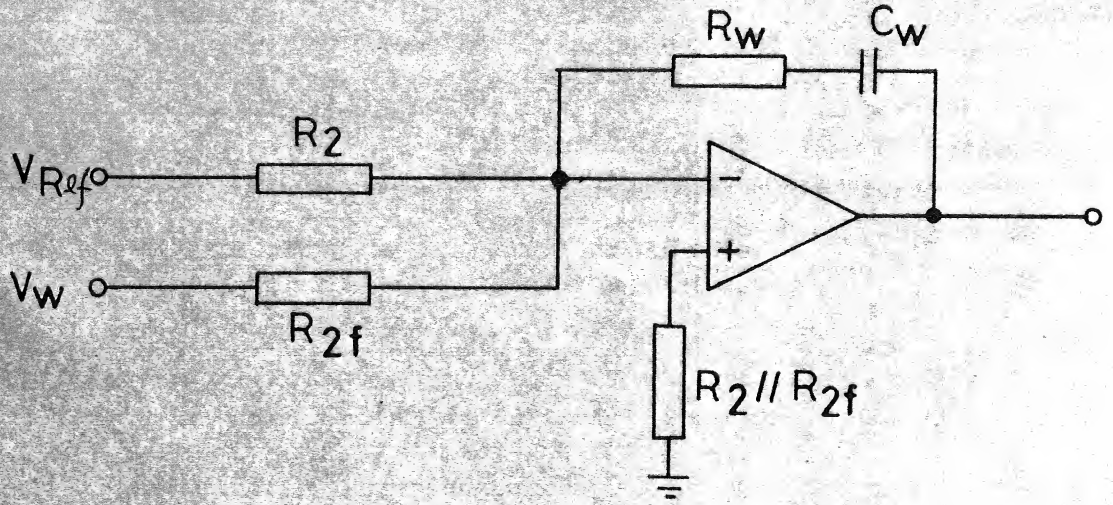

Fig. 4.13 (b) Speed controller.

(ii) Choosing $\tau_{c2} = 3\ T_f = 150$ ms, the root locus for $GH_w(s)$ is shown in Fig. 4.12(b). For $\varepsilon = 0.707$, the value of K_2 is 56.4.

(iii) Choosing $\tau_{c2} = 10\ T_f = 500$ ms, the root locus for $GH_w(s)$ takes the form as shown in Fig. 4.12(c). For $\varepsilon = 0.707$, K_2 comes out to be 27.5.

Case (iii) is chosen to avoid the possibility of saturation of op-amp. The realization of the controller is shown in Fig. 4.13(b). The value of the capacitor in the feedback path of the operational amplifier is chosen to be $C_w = 1\ \mu f$. From the values of K_2 and τ_{c2}, R_w and R_{2f} are found to be

$$R_w = 500\ K\Omega \quad R_{2f} = 18.2\ K\ \Omega$$

The rated speed of the motor is 1200 rpm and the ideal no load speed w_o works out to be 1500 rpm. The maximum motor speed has been chosen 1500 rpm, and this should correspond to 12V, the maximum speed reference voltage. The value of R_2 is correspondingly given by

$$\frac{12/V_{cm}}{R_2} = \frac{(w_m/w_o)H_w}{R_{2f}}$$

or $$R_2 = 18.2\ K\Omega$$

The overall transfer function of the speed loop is given by

$$\frac{W(S)}{V_R(S)} = \frac{G(S)}{1+G(S)\,H(S)} \qquad (4.22)$$

where

$$G(S) = \frac{K_2(1+s\,\tau_{c2})}{s\,\tau_{c2}} \cdot \frac{R_{1f}}{R_1 H_i} \cdot \frac{1/B}{(1+ s\,\frac{\tau_m}{B})} \qquad (4.23)$$

and

$$H(S) = \frac{H_w}{1+ sT_f} \qquad (4.24)$$

Substituting the numerical values and simplifying

$$\frac{W(S)}{V_R(S)} = \frac{3.85(s+2)(s+20)}{(s+15.69)(s^2+4.41s+9.807)} \qquad (4.25)$$

For step input i.e. $V_R(S) = \frac{1}{S}$, w(t) is plotted in Fig. 4.9.

4.5 EXPERIMENTAL RESULTS:

The complete circuit diagram of closed loop speed control system is shown in Fig. 4.14. The steady state speed torque characteristics for single quadrant chopper with closed loop speed control system is shown in Fig. 4.15. A closeness between theoretical results and

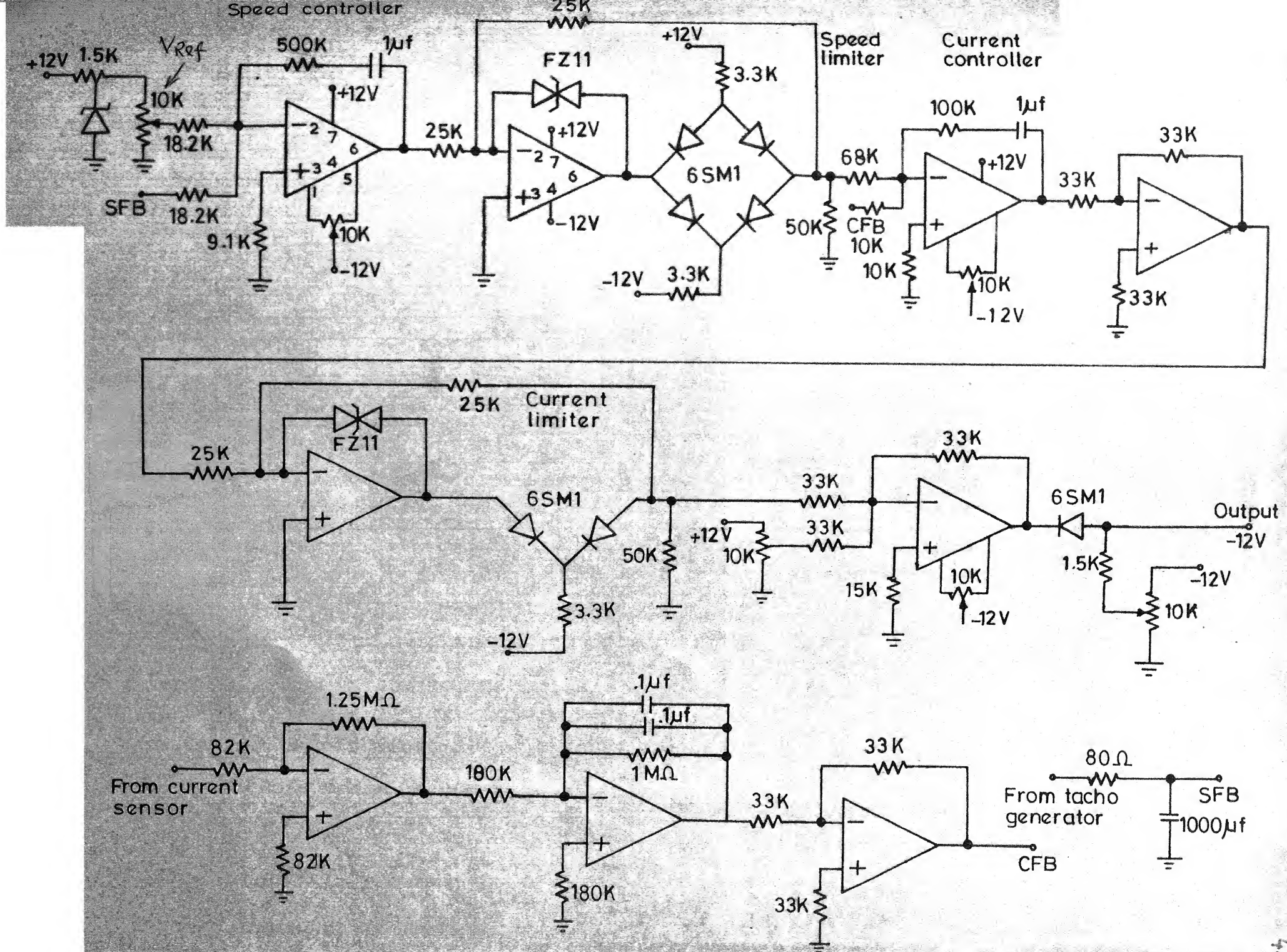

Fig. 4.14 Circuit for closed loop system.

4.24

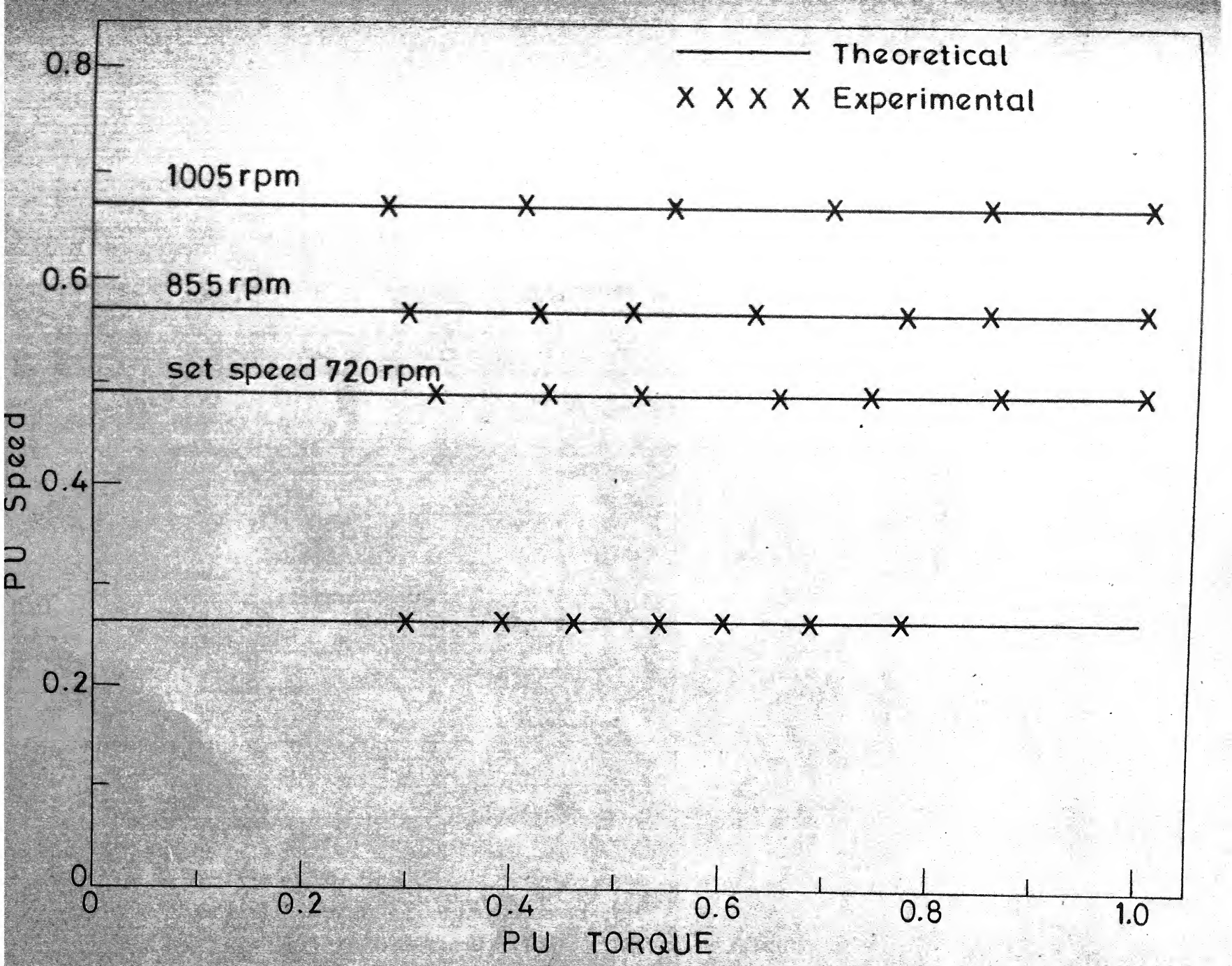

Fig. 4.15 Speed-torque characteristics for chopper A with closed loop system.

experimental results can be clearly seen from the Fig. 4.15. A speed regulation of 2% was observed.

Speed transient responses for closed loop system were found oscillatory for designed values of controller parameters. Therefore the various parameters were experimentally adjusted to get the desired response. The new values of the parameters were as follows:

$$K_1 = 10, \quad \tau_{c1} = 200 \text{ ms}$$

$$K_2 = 15, \quad \tau_{c2} = 350 \text{ ms}$$

The transient responses of speed have been recorded for small perturbation in speed reference and load torque. They are shown in Figs. 4.16 to 4.18.

4.6 CONCLUSION:

In this chapter, a closed loop speed control system for single quadrant chopper has been designed using root locus technique. For simplicity, high order systems are approximated by their low order models. It has been shown that P controller for current control loop can not be used because a high value of gain is required for getting small value of steady state error which may

cause saturation of op-amp. Current limiters are used to limit the current which flows through the thyristors. Inner current control loop is chosen to have fast response against disturbances such as variations in supply voltage. The steady-state and transient response of speed control system of chopper fed dc separately excited motor were found satisfactory. From no load to full-load, the closed loop system offered a speed regulation of 2%.

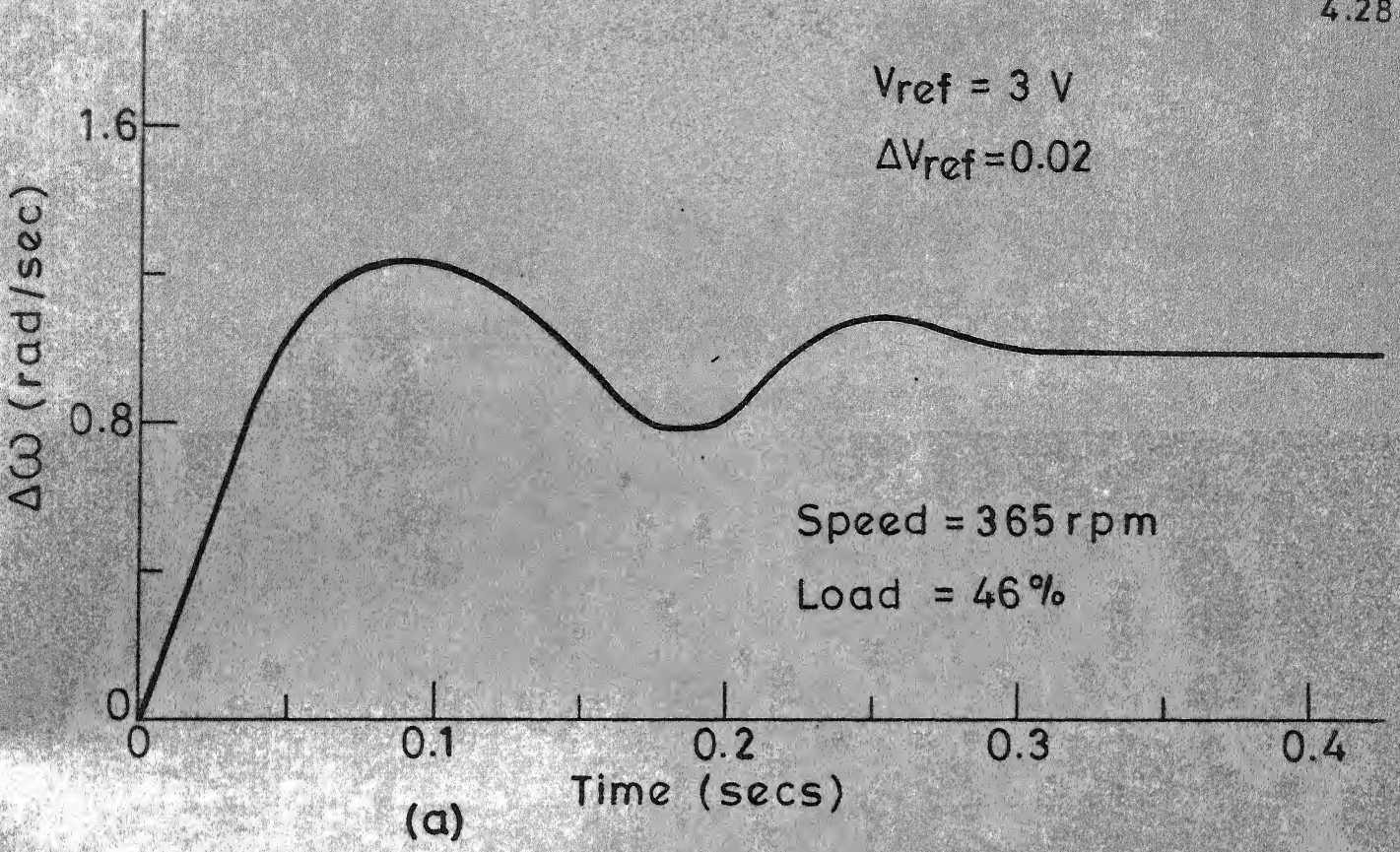

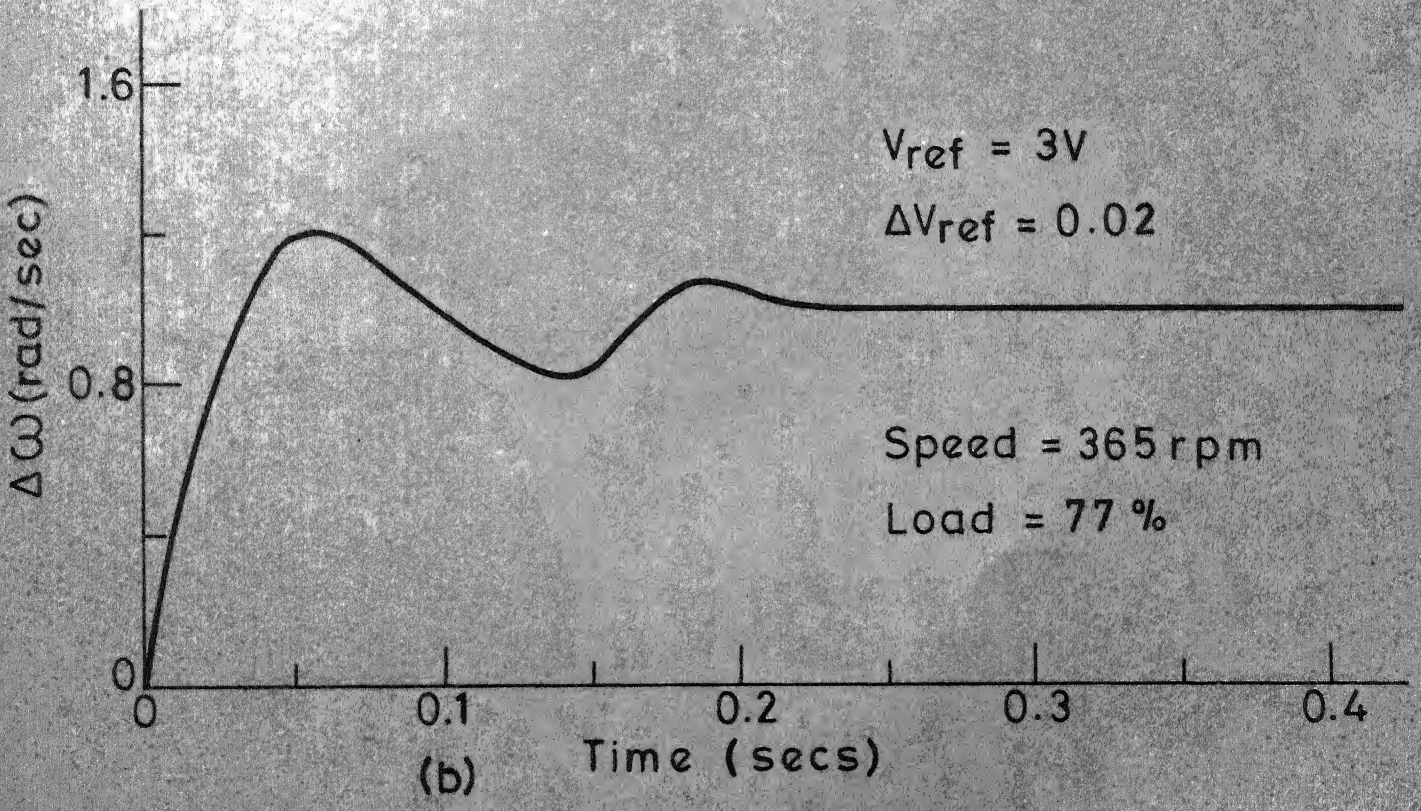

FIG. 4.16 CLOSED LOOP SPEED TRANSIENT RESPONSE FOR PERTURBATION IN SPEED REFERENCE.

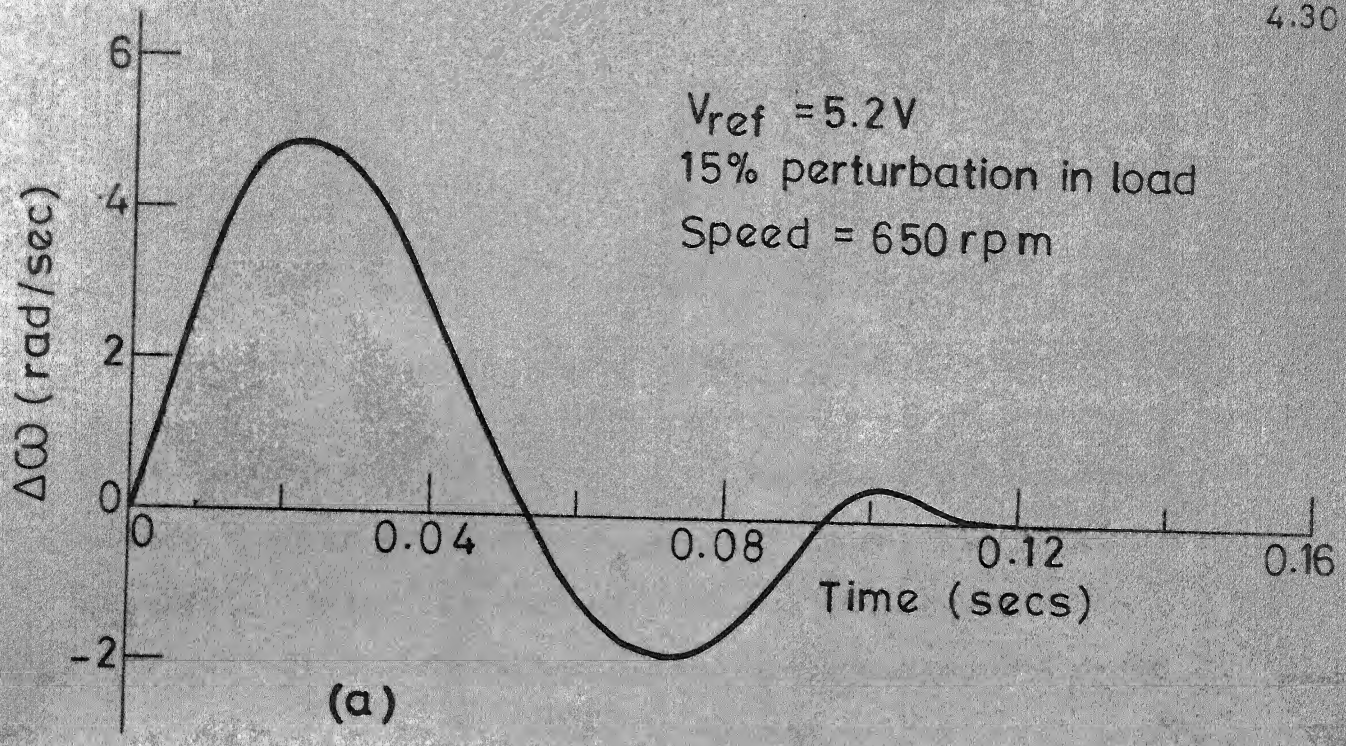

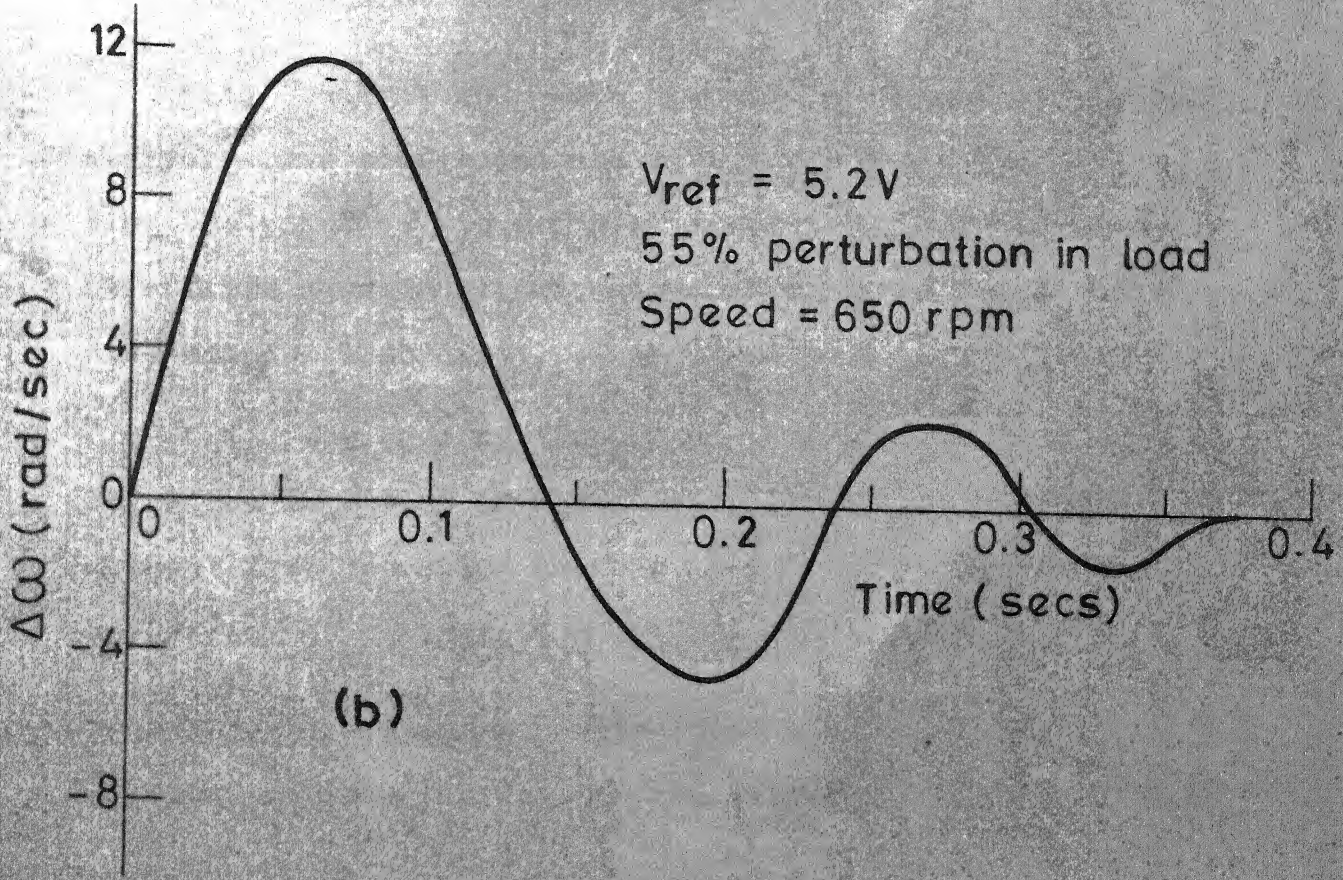

FIG. 4.18 CLOSED LOOP SPEED TRANSIENT RESPONSE FOR LOAD PERTURBATION.

CHAPTER V

CONCLUSION

The thesis is concerned with the chopper control of dc separately excited motor. A comparison has been done between various kinds of two quadrant choppers. This comparative study has been carried out with respect to motor performance characteristics, motor armature current ripple factor, supply current harmonics, regenerated power, efficiency of regeneration and transfer characteristics. From this study, the following important conclusions can be drawn.

(i) Dual chopper with circulating current operation always offers continuous conduction which is beneficial from the point of view of good speed regulation, though it suffers from the disadvantage of high CRF compared to dual chopper with circulating current free operation.

(ii) For regeneration, dual chopper with circulating operation is better than dual chopper with circulating current free operation because it offers higher values of efficiency of regeneration for all values of δ.

Two different circuits of dual chopper with current commutation were fabricated and tested. A digital firing

scheme has been developed for the control of dual chopper. Circuit with type 2 current commutation failed to work because of commutation problems. Since it had common commutation circuitry for choppers of both the quadrants i.e. motoring and regeneration, a decision was taken to go for a simple circuit i.e. dual chopper with type 1 current commutation. This circuit worked upto $\delta = 0.5$ and, afterwards, it also suffered from commutation failures. All efforts to rectify the cause went fruitless and it was felt that commutation circuitry of dual chopper should be designed with more care to avoid the possibility of short-circuiting caused by malfunctioning of commutation circuits.

Because of above mentioned problems, an investigation of single quadrant chopper fed dc separately excited motor has been carried out for the purpose of speed control of dc drive. The steady state and transient performance of motor in open loop fed by this chopper were found theoretically and, further, they have been verified experimentally. A close resemblance between theoretical and practical results was observed.

Since continuous conduction was observed from no-load to full load, a suitable model of dc drive was chosen for the closed loop operation. The inner current control loop

scheme was chosen because of its added advantages over current limit control scheme. It has been presented here that PI - controller rather than P controller should be used for current controller since if P controller is to be used, then, to have a steady state error less than 5%, it should possess a gain of value greater than 200 which may result in saturation of subsequent op-amp. The steady state performance of dc motor with closed loop was found satisfactory. A speed regulation of 2% was noted down. With the designed values of controller parameters, the transient response of system was found oscillatory. Hence, parameters were further adjusted experimentally to achieve the satisfactory speed transient responses of the dc drive system during small perturbation in δ and load torque.

APPENDIX A

Details of dc separately excited motor used

Rated voltage	220 V
Rated current	1.3 A
Rated speed	1500 RPM
Armature resistance	31 ohms
Armature inductance	0.33 H
Back emf constant K_v	1.46
Torque constant K_T	1.46
Moment of inertia J	0.002941
Viscous friction coefficient	0.001948
Normalized viscous friction coefficient B	0.15

APPENDIX B

Details of components used in dual chopper with type 2 current commutation:

Thyristors	SS5101, 8A, 600V (converter grade)
Diodes	EC 1006, 6A, 1000V
C	0.6 μf
L_1	1 mH
R_1	150 ohms
T	0.002 sec.

APPENDIX C

Details of components used for dual chopper with type 1 current commutation:

Thyristors	R36TB6, 42A, 600V (inverter grade), turn-off time 25 micro sec.
Diodes	12S140, 40A, 1200V
L_1, L_2	1.4 mH
C_1, C_2	3 μ F
R_1, R_2	200 ohms
T	5 ms

REFERENCES

1. S.B. Diwan, A. Straughen, 'Power Semiconductor Circuits', John-Wiley and Sons, 1975, pp. 282-353.

2. T. Krishnan and B. Ramaswami, 'A fast response dc motor speed control system', Trans. on Industry Applications, vol. IA-10, No. 5, 1974, pp. 643-651.

3. G.K. Dubey and W. Shepherd, 'Analysis and performance of dc motor controlled by power pulses, Research Report 204, Univ. of Bradford, England, 1975.

4. T.H. Barton, 'The steady state transfer function of a chopper drive', IEEE IAS Annual Meeting 1979, pp. 716-721.

5. G.K. Dubey and W. Shepherd, 'Transient analysis of dc motor controlled by power pulses', Proc. IEE, vol. 124, No. 3, March,1977, pp. 228-230.

6. J.G. Graeme, G.E. Tobey,L.P. Huelsman, 'Operational Amplifiers Design and Application', McGraw Hill (Burr - Brown), 1971, pp. 245-250.

7. H. Satpathi, G.K. Dubey and L.P. Singh, 'Performance and Analysis of Chopper-fed dc Separately Excited Motor under Regenerative Braking', Jr. of Electrical Machines and Electromechanics (to be published in vol. 5, No. 4).

A 66840

Date Slip

This book is to be returned on the date last stamped.

		date
.....	.....	.....
.....	.....	.....
.....	.....	.....
.....	.....	.....
.....	.....	.....
.....	.....	.....
.....	.....	....
.....	.....	....
.....	.....	....
.....	.....	....
.....	.....	...

CD 6.72.9